FACULTY OF SCIENCES

Renormalising the Entanglement Island in the Information Paradox

De Vuyst Julian

Promotor: Dr. Mertens Thomas
Copromotor: Prof. Dr. Verschelde Henri

A thesis submitted to Ghent University in partial fulfillment of the requirements for the degree of *Master of Science in Physics & Astronomy*

2020-2021

Department of Physics & Astronomy
Ghent University, Krijgslaan S9, 9000 Ghent, Belgium

GHENT UNIVERSITY

Abstract

This thesis fits into the conceptual framework of black holes and the information paradox. More specifically, it entails the search for entanglement islands within the context of two-dimensional Jackiw–Teitelboim gravity. The starting point is to acquire the knowledge to make inquiries within this area of study. As such, we begin by a precursory literature study to introduce tools as entanglement entropy, black hole physics, holographic entanglement entropy, and semiclassical Jackiw–Teitelboim gravity. Thereafter, we compute islands in our setup. Unlike in literature, we consider a model for an evaporating black hole originating from a classical energy pulse. We make no assumptions about a potential heat bath, gravitating or not, but we are able to relate our setup to a situation as if a heat bath were glued to the boundary of our spacetime. As the resulting systems are nonlinear in the parameters, we rely on numerical results to extract meaningful information. Prototypical calculations involve the entropy in which the cutoffs, necessary to regulate divergences, are effectively 'ignored'. This approach is followed first. However, these cutoffs can be related to the boundary coordinates and potentially affect the location of possible islands. To take this into account, we define a renormalised entropy which gives a more natural measure from the viewpoint we will present – a boundary observer who collects the outgoing radiation. In both cases we numerically obtain a Page curve; the observer collected all the outgoing radiation and can reconstruct the black hole interior by acting on it – there is no information loss. Intriguingly, we discover that the latter model can exist in two phases depending on the sole dimensionless parameter – a phase with and a phase without islands.

Samenvatting

Deze thesis past binnen het conceptuele kader van zwarte gaten en de informatieparadox. Meer specifiek, het bevat de zoektocht naar verstrengelingseilanden [1] binnen de context van twee-dimensionele Jackiw–Teitelboim-zwaartekracht. Het beginpunt is het verwerven van de nodige kennis om onderzoek te kunnen doen binnen dit domein. Hiertoe beginnen we met een voorafgaande literatuurstudie om begrippen zoals verstrengelingsentropie [2], de fysica van zwarte gaten, holografische verstrengelingsentropie en semiklassieke Jackiw–Teitelboim-zwaartekracht te introduceren. Daarna wagen we ons aan berekeningen omtrent zulke eilanden in ons model. In tegenstelling tot de literatuur beschouwen we een model voor een verdampend zwart gat afkomstig van een klassieke energiepuls. We maken geen assumpties over een potentieel warmtebad, al dan niet met zwaartekracht, maar we kunnen ons model wel relateren aan een situatie waarin een warmtebad is toegevoegd aan de grens van onze ruimtetijd. Omdat de resulterende vergelijkingen niet-linear zijn in de parameters moeten we beroep doen op numerieke technieken om zinvolle informatie te extraheren. Prototypische berekeningen berusten op een entropie waarin de cutoffs, nodig om de divergenties te reguleren, worden 'genegeerd'. Deze aanpak wordt eerst gevolgd. Desalniettemin kunnen deze cutoffs gerelateerd worden aan de coördinaten van een grenswaarnemer en kunnen dus mogelijks de ligging van de potentiële eilanden aanpassen. Om dit in rekening te brengen definiëren we een gerenormaliseerde entropie die bovendien een natuurlijkere maat geeft vanuit het standpunt dat we zullen beschouwen – een grenswaarnemer die de uitgaande straling detecteert. In beide gevallen bekomen we numeriek de Page curve; de waarnemer absorbeerde alle uitgaande straling en kan de binnenkant van het zwart gat reconstrueren door dit te manipuleren – er is geen verlies van informatie. Daarbovenop ontdekken we nog een intrigerend fenomeen in het laatstgenoemde model, het kan zich namelijk in twee fasen bevinden afhankelijk van de enige dimensieloze parameter – een fase met en een fase zonder eilanden.

[1] Van het Engelse begrip 'entanglement island'.
[2] Van het Engelse begrip 'entanglement entropy'.

Acknowledgements

Humans are temporal beings.

Martin Heidegger

The end of this academic year marks a moment in my life where one door closes and another opens. This thesis does not only represent the epitome of my studies in physics, it is also a stepping stone towards the future I am striving for. There is no doubt in the fact that many of the skills I learnt in the past five years will prove critical in my future career. Moreover, the experiences I had and the bonds I made will leave an everlasting mark on my worldline.

To show my gratitude, I would like to take the time to thank a few people without whom my studies would have been quite dull.

First, I owe a debt of gratitude to my promotor Thomas Mertens and copromotor Henri Verschelde for allowing me to conduct research within their group. Especially Thomas Mertens deserves special praise. Our many discussions and his many remarks were constantly able to shed a new light on this topic. Besides, thanks to him I was able to formulate a concrete objective – the result being this thesis.

The past years would not have been a wonderful journey had I not met my group of friends, bearing the same name is our favourite black hole metric. I would like to thank each and every one of them. Particularly, I would like to thank Lukas De Greve, Bram Vancraeynest-De Cuiper and Yarrik Vanwalleghem for the many evenings and nights we spent online. The times we spent talking or playing extended games of *Civilization VI* were certainly a highlight during the week in these dire circumstances. Even more so, I express my utmost gratitude towards Lukas De Greve. The many conversations we had – whether about our hobbies, interests, or on a deeper level – will forever be engraved in my memory. どうもありがとうございます!

I had a great time within the student society for physics – the VVN. It is where I met Simon De Kock and Nicolas Dewolf, both great friends of mine. Whether it was for cracking a joke or conversing about philosophical topics, they also deserve a word of praise. Especially Nicolas Dewolf who helped me a lot with physics and math deserves some extra praise to top it off.

Additionally, I also thank my friends from the University of Amsterdam I met during my Erasmus+ exchange. Their viewpoints were insightful and their hospitality by inviting me to their Master's thesis group did not go unnoticed. The pinnacle was to hold a seminar at the Universidad de Concepción.

Last but not least, I want to thank my family for their constant support throughout my academic journey, my mother in particular. I am sure they will continue to encourage me in my future endeavours and remain a pillar of strength in my life.

— De Vuyst Julian, June 2021

Contents

Abstract ii

Samenvatting iii

Acknowledgements iv

1 Introduction 1
- 1.I Preliminary: Holography . . . 2
  - 1.I.a Plato's Cave and RG Scales (SD) . . . 4

2 Entanglement Entropy and the Replica Trick 6
- 2.I The Art of Quantum Entanglement . . . 6
  - 2.I.a Entanglement in Quantum Systems . . . 6
  - 2.I.b Entanglement in Field Theories . . . 10
  - 2.I.c UV Divergences . . . 11
  - 2.I.d EE Inequalities . . . 12
  - 2.I.e Monogamy of EE . . . 13
- 2.II The Replica Trick . . . 14
  - 2.II.a Twist Fields . . . 17
- 2.III Entanglement and the Taj Mahal Theorem (SD) . . . 18

3 Black Holes and the Information Puzzle 21
- 3.I BH Thermodynamics . . . 21
  - 3.I.a Hawking Temperature . . . 21
  - 3.I.b The Unruh Effect . . . 23
  - 3.I.c The Bekenstein–Hawking Entropy and the BH Laws . . . 25
- 3.II The Information Puzzle . . . 27
  - 3.II.a Central Dogma and the Page Curve . . . 27
  - 3.II.b The End is neigh . . . 28
  - 3.II.c How to get rid of Diaries . . . 30
  - 3.II.d AMPS Paradox . . . 31
  - 3.II.e Possible Resolutions . . . 32

4 Holographic Entanglement Entropy 33
- 4.I Back to the Roots: the Ryu–Takayanagi Formula . . . 33
  - 4.I.a Homology is not Homotopy . . . 35
  - 4.I.b An Example: Vacuum State of CFT_2 on $\mathbb{R}^{1,1}$ . . . 36
- 4.II Navigating towards the Island . . . 38
  - 4.II.a The Quantum Extremal Surface . . . 38
  - 4.II.b The Entanglement Island . . . 39
- 4.III From Island to Page Curve . . . 41
  - 4.III.a The Entanglement Wedge . . . 41

4.IV Ryu–Takayanagi as a Streaming Protocol (SD) . . . 43

5 JT Gravity **45**
5.I Dimensional Reduction of Charged Black Holes . . . 45
5.II The JT Action . . . 48
5.II.a The Conformal Anomaly . . . 49
5.III The Boundary Particle . . . 49
5.III.a Energy from the Boundary . . . 51
5.IV Solving the eom . . . 53
5.IV.a The Static Black Hole Solution . . . 53
5.IV.b A General Solution . . . 56
5.V The Evaporating Black Hole . . . 56
5.V.a Forgetting the Memory Integrals . . . 60
5.VI The Semiclassical Entanglement Entropy . . . 61
5.VI.a Twist Fields Derivation . . . 63

6 An Archipelago from the Boundary **64**
6.I The Boundary Observer Perspective . . . 64
6.I.a Poincaré vs Boundary Coordinates . . . 68
6.II The Radiation and Bekenstein–Hawking Entropy . . . 68
6.III The Generalised Entropy . . . 71
6.IV The Pre-Pulse Island . . . 72
6.IV.a Finding the Island . . . 72
6.IV.b Existency Conditions . . . 73
6.V The Post-Pulse Island . . . 76
6.V.a Finding the Island . . . 76
6.V.b The Initial Island . . . 78
6.V.c Using the Approximation . . . 80
6.VI Results & the Page Curve . . . 81

7 Renormalised Islands **85**
7.I The Generalised Entropy . . . 85
7.I.a Ambiguity for the Pre-Pulse Island . . . 85
7.II The Pre-Pulse Island: Horizon geometry . . . 86
7.II.a Back to the Past . . . 87
7.II.b On the Horizon . . . 87
7.II.c Chasing the new Bifurcate Horizon . . . 88
7.II.d An Archipelago . . . 89
7.III The Pre-Pulse Island: Poincaré geometry . . . 90
7.IV The Post-Pulse Island . . . 92
7.IV.a The Initial Island & a Phase Transition . . . 92
7.V Results & the Page Curve . . . 93

8 Summary & Outlook **97**
8.I Summary & Conclusion . . . 97
8.II Other Developments & Outlook . . . 99

A The Holographic Dual: SYK **101**

B The Time Reparametrisation **102**
B.I Properties of the Modified Bessel Functions 102
B.II Taking Derivatives 103
B.III An Approximation for the Reparametrisation 104
B.IV Early Time Approximation 105

C Mathematica Code **107**

D Acronyms **108**

Bibliography **121**

Chapter 1

Introduction

Black Holes are where God divided by zero.

Albert Einstein

In the '70s, J. Bekenstein made it apparent that a black hole (BH) could be seen as a thermodynamical system as one can write down laws which are of a similar form to the four laws we all love and cherish [1, 2], initiating the age of BH physics.[1] Not long thereafter, S. Hawking introduced the important concept of Hawking radiation through semiclassical calculations; BHs are not that 'black' after all and radiate approximately as a blackbody at the Hawking temperature [3]. This Hawking temperature beautifully connected quantum mechanics (QM) and general relativity (GR) for the first time, paving the way for the study of quantum information in the regime of quantum gravity (QG). A first major breakthrough was the calculation for the entropy of a BH resulting in the well-known Bekenstein–Hawking formula [4]. This gave rise to the analogy with a piece of burning coal as a proxy for the BH. One could ask in a similar way how many degrees of freedom are required to describe this physical system, the amount being fixed by its thermodynamical entropy. However, if a piece of coal is all burnt up and we collect its ash and radiation we can, in theory, reconstruct the initial wood piece we set on fire. It turns out this is not true for a BH, we cannot recreate the initial state that collapsed to a BH since a pure state gets radiated away in a mixed state; it seems information is inevitably lost. It is not surprising a BH is more complicated than a piece of burning coal: strong gravity near and behind the horizon plays an important role, and to accurately describe it we need a theory of QG. The best tool we have for this is holography. From this viewpoint, the BH is dual to a thermal conformal field theory (CFT). If this is true, then we expect that the information is preserved as time evolution is unitary for CFTs. This apparent contradiction is what physicists called the **BH Information Paradox**. How can this paradox be resolved?

Ever since the renowned AdS/CFT correspondence [2], conjectured by J. Maldacena [5], there has been extensive research in this new holographic view, coined by G. 't Hooft [6–9]. This new mathematical tool – or maybe reality – brought about results compatible with the old ones but also new results and new techniques. One of the most important results was the Ryu–Takayanagi formula [10] which computes the entanglement entropy of a CFT through an area of a certain surface in the bulk spacetime, much like the Bekenstein–Hawking formula.

If we believe the BH evaporation process to happen unitarily, then the entanglement entropy of the radiation follows a specific curve – the Page curve [11, 12]. The entropy first increases because of more entangled quanta escaping the BH. From the Page time onwards, the entropy starts decreasing again until it reaches zero when the BH is completely evaporated; it also has zero Bekenstein–Hawking entropy. Ströminger once said that calculating

[1] A list of acronyms is provided in Appendix D.

[2] AdS stands for anti-de Sitter.

the Page curve amounts to solving the paradox [13]. And so it has been done. Not even two years ago, the authors of [14, 15] managed to obtain the Page curve in the context of 2d Jackiw–Teitelboim (JT) gravity [16, 17], and it won them the New Horizons 2020 prize.

Although we live in a 4d spacetime, making calculations in lower dimensions are often more tractable as QG becomes more renormalisable. Therefore, we analyse such models which, hopefully, still have some relevance to Nature. It is likely that certain features present in these models should also be present in a model for QG in 4d, or at the very least we can try to extrapolate this back to 4d.

Due to the advent of these results, research spearheaded into this new direction and quickly led to new results, e.g. the island formula [18] and the use of replica wormholes [19, 20]. It turns out the island is crucial and possibly gives a resolution to the paradox.

Unfortunately, this also limits our view somewhat as other less developed ideas not immediately thread into the spotlight: the use of soft hair, the unitary gauge construction, etc. [21–24]. Whilst the doctrine of humores, originating from Hippocrates and further developed by Galen, dominated the scene for 1 500 years, it was only after criticism by Paracelsus and Vesalius that this scholastic medicine was replaced with the start of modern medicine. Hence, we should always be critical about the road we took. And just like the Copernican vs Ptolemean model we should not turn a blind eye to new ideas which could have merit on their own. Nevertheless, this philosophical debate may be better held another time.

The Page curve has been computed, but Strömminger's words were said too early. Other paradoxes and problems started to show up [13, 25–34]. The information problem is far from over!

The purpose of this thesis is to introduce the reader to these fascinating results of the last two decades which, unfortunately, retain a high barrier to penetrate. Hopefully after the review set out in the following four chapters, the reader is acquainted with the larger idea and most concepts showing up in this field of study. Thereafter, we turn our eye to a specific calculation in JT gravity, albeit with a setup differing from the original one and its successors [14]. As is apparent from many calculations in literature, the cutoffs introduced in the formulas for the entanglement entropy get largely ignored. Our goal will be to use a renormalised entropy – independent of all the cutoffs – and try to find the Page curve.

This thesis is structured as follows: we begin with a brief preliminary on holography after this section and start with the concept of entanglement entropy in Ch. 2. Subsequently, we introduce some BH thermodynamics and a handful of paradoxes with possible solutions in Ch. 3. In Ch. 4 we introduce the concept of holographic entanglement entropy and make our way towards the island formula. A broad review of semiclassical JT gravity in Ch. 5 concludes the literature study. In the next two chapters, Ch. 6 and 7, we present the calculations in our model using the common tool of 'ignoring the cutoffs' and the renormalised entropy respectively. Finally, in the Summary & Outlook 8 we provide a review of our results, and discuss some other developments.

As a homage to the ancient natural philosophers and inspired by [35], we shed a new light on some concepts in the form of a Socratic dialogue and be denoted by SD, they appear at the end of this chapter, Ch. 2 and Ch. 4. [3]

1.I Preliminary: Holography

The **AdS/CFT correspondence** or **gauge/gravity correspondence** – first written down in the renowned paper [5] – is a remarkable duality in which a nonrelativistic CFT, under certain

[3] The characters used in these Socratic dialogues are based on the works of Hajime Kamoshida.

conditions, can be equivalently described by a quantum gravitational theory in one spatial dimension higher, mostly string theory.

$$\text{CFT in } d \text{ dimensions}$$
$$\longleftrightarrow$$
$$\text{Asymptotic AdS QG in } d+1 \text{ dimensions}$$

Since the CFT lives in one less spacelike dimension, the usual picture is that of a bulk spacetime $\mathcal{M}_d$ where the CFT lives on the **conformal boundary** $\partial\mathcal{M}_{d+1}$ (depicted in Fig. 1.1). However, this picture often leads to confusion as it is important to remember that we do not have both theories at the same time. We only work in either one of them and there are relations and dualities between them, but that does not mean we should take this picture literally; both are separate entities [36].

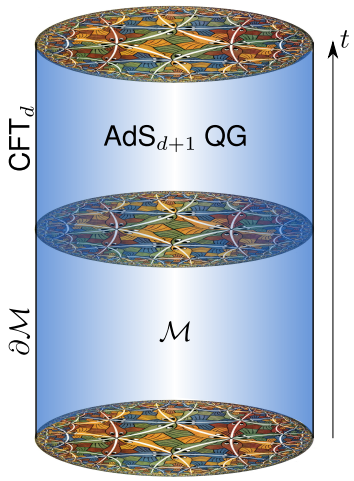

Figure 1.1: AdS$_{d+1}$ QG in the bulk $\mathcal{M}$ is dual to a CFT$_d$ on its boundary $\partial\mathcal{M}$. Time is running upwards and three equal time slices are shown, the geometry of such a slice is equivalent to the hyperbolic metric.

The duality is further enhanced by the fact that

$$\text{Symmetry generators of the conformal symmetry SO}(d,2) \text{ of the CFT}$$
$$\longleftrightarrow$$
$$\text{Bulk symmetry generators of the isometries in the asymptotically AdS spacetime}$$

and correlation functions can be calculated via the **GKPW rule/extrapolate dictionary**

$$\left\langle e^{\int d^d x\ J(x)\mathcal{O}(x)} \right\rangle_{\text{CFT}} = \int \mathcal{D}\phi\ e^{-S_{\text{AdS}}} \Big|_{\phi(\partial\mathcal{M})=J(x)} \tag{1.1}$$

named after Gubser, Klebanov & Polyakov [37], and Witten [38].

By oversimplification, the CFT can be described by two parameters [39]

- λ: a coupling constant measuring the interaction strength between its constituents;
- c_{eff}: a measure for the effective number of degrees of freedom.

according to their values, and by taking different limits one obtains a different bulk picture. The most general being that of an interacting string theory.

- **Planar limit** $c_{\text{eff}} \to \infty$: string interactions become weak and we can truncate them to tree level, a classical string limit. From the path integral (PI) perspective, it localises around a nontrivial saddle point described by a master field configuration equivalent to an expansion in $1/c_{\text{eff}}$;

- **Semiclassical limit** $\lambda \to \infty$: the CFT is strongly coupled and massive string states decouple due to becoming heavy such that we are left with semiclassical gravity. It can be thought of as a thermodynamic limit.

When taking both limits simultaneously we end up in a semiclassical theory: the gravity sector is described by Einstein–Hilbert gravity and the quantum fields can be treated semiclassically on this fixed background due to the negligible contributions of the gravitons (dual to the CFT stress tensor). Theories which have a holographic map in this limit are said to be an element of the **code subspace**.

Ultimately, we end up with relations between these two parameters and the gravitational constant $G_{\mathsf{N}}^{(d+1)}$, the AdS scale l_{AdS}, and the string scale l_s

$$c_{\mathsf{eff}} = \frac{l_{\mathsf{AdS}}^{d-1}}{16\pi G_{\mathsf{N}}^{(d+1)}}, \qquad \lambda = \left(\frac{l_{\mathsf{AdS}}}{l_s}\right)^{\gamma} \tag{1.2}$$

with $\gamma > 0$ and dependent on the CFT.

1.I.a Plato's Cave and RG Scales (SD)

As usual during lunch break, the science room was occupied by only two high school students: the sole science club member, Futaba, and a close friend, Sakuta. Ever since the strange occurrences, Sakuta had been reading books about quantum physics and the foundations, and wanted to work towards entanglement. Futaba was already way ahead of him, currently reading something related to string theory. The room was quiet, only filled by the sound of the wind blowing through the single open window and the Bunsen burner with which Futaba warmed their coffee. It would give anyone who enters a feeling of serenity. One would usually find other means for a Bunsen burner... Meanwhile, Sakuta was reading a book about holography as a preliminary for his follow-up on entanglement as advised by Futaba. The difference in level was palpable; while Futaba was soaking up information, Sakuta was struggling with his content and could not wrap his head around it. [4]

"I really don't get this", Sakuta said followed by a deep sigh. "How can some physics be the same as gravity with an extra dimension? What is this extra dimension even supposed to be?"

"What is it this time?", Futaba asked with an annoyed look on her face. Not too surprising, someone suddenly broke her out of her concentration. "Oh, you're reading the book I gave you about holography. Good choice."

"Yeah, but I don't understand any of it", he replied while taking a sip of his coffee. "What are these holograms even? A theory living on a boundary? I get no intuition whatsoever." He knew Futaba could explain it in simpler terms, he was hoping for this. After all, she was the best student of their class and already grasped the concepts of Schrödinger's cat and quantum teleportation quite well. He hoped that by showing his struggles, she would step in and give him a condescending lecture, like always.

"You really are hopeless sometimes, you know", Futaba replied in exasperation. "Well, let's go back to something you might understand. Ever heard of Plato's cave?"

"Plato...", Sakuta mumbled confusingly. He heard the name before in some of his classes, but was probably not paying attention anyway. "I feel like you are going to scold me."

"You are right about that. You should know one of the most important Greek philosophers", Futaba said without a sign of surprise on her face. "Anyway, Plato's cave is a certain view on reality. According to him, we live in a cave without direct access to the outside, ergo reality. At the entrance there is a fire, and objects passing by cast a shadow on the wall inside the cave for the people to see. Basically, it says that what we see are inaccurate representations

[4] The content is based on [39–41].

of reality."

"Okay, I see", Sakuta nodded agreeingly. "So why are you bringing this up?"

"Well, there is more to it, but let's stick to the simplified version for now. Can you make the link between those shadows and the holograms?"

"Uhm, hmmmm..." He was contemplating about what she meant until he reached an epiphany. "They are the same thing! These shadows are equivalent to the holograms living on the boundary of our spacetime."

"Exactly! You sometimes surprise me how quickly you can catch up", she said with a slight smile of pride. "These shadows in the allegory are the same as the holograms of our theory. Plato stated that these shadows are inaccurate or don't fully describe reality. However, the AdS/CFT correspondence says that these shadows are enough: all the information about the higher theory is contained in these objects. So we might as well study one of them to learn about the other."

"Okay, I think I kind of get the gist of it. But still, we are talking about a field theory versus a theory of quantum gravity. What exactly is this extra dimension?" Meanwhile, he was staring at Futaba's shadow on the blackboard behind her, caused by the Bunsen burner. She seemed to be making another cup of coffee.

"I assume you know a bit about energy scales and renormalisation?"

"Well, yeah, a bit. Like how the parameters of a theory depend on the energy scale at which you probe them."

"Indeed, that's already enough", she replied quite pleased. "This extra dimension is just that: a length/energy scale which tells us in what regime we probe the boundary theory."

"That seems rather arbitrary. How is this exactly realized?" He seemed to not believe her. Well, it is rather unconvincing at first.

"We know the boundary theory is scale invariant, so scale transformations $z \to \lambda z$ leave our state invariant", she explained while writing it down on the blackboard. "It also leaves the metric of the gravitational system intact, but we seem to be zooming in or out. In other words, we are looking close to the boundary or close to the centre of the bulk. From this perspective, close to the boundary is related to UV scales in the boundary theory. Likewise, deep in the bulk represents IR scales. Hence, this extra dimension can be seen as the energy scale at which we probe the theory. It is most easily seen by looking at the metric: it diverges near the boundary, indicating a high energy divergence."

"That's quite an interesting perspective."

"Indeed, and one which turns out to be useful for other concepts."

"As always, you have a knack for explaining things to a commoner like me", Sakuta said looking impressed. They both took a large sip from their coffee – as if they both calmed down a little – and Futaba returned to her book. In the meantime, Sakuta was staring out the window reflecting about this interpretation. The room became quiet once more as the wind died down.

Figure 1.2: Plato's Cave Allegory. Reality (the bird) gets projected on a wall (shadow) which the observer (right) then sees. In AdS/CFT these shadows contain all the information about reality.

Chapter 2

Entanglement Entropy and the Replica Trick

We begin our journey with the central theme of this research area: entanglement. Entanglement remains a bizarre phenomenon but nevertheless lies at the heart of QM. Mainly because it is a concept which has no classical analogue, it is purely a quantum phenomenon. Even so, entanglement often raises a lot of confusion due to its counterintuitive nature like the Reeh-Schlieder theorem: local measurements instantaneously affect local measurements far away and is often quoted as 'spooky action at a distance'.

While its importance in BH physics was discovered early, it mainly remained a tool in the condensed matter physics community. At the advent of the Ryu–Takayanagi formula to calculate entropies in holographic theories, a collaboration between a condensed matter physicist and a string physicist, it made its way into high energy physics research. Even today, entropy and entanglement remain well-established concepts within the high energy community and has inspired a lot of new ideas and research. One of them, for instance, proposing spacetime is the result of many entangled qubits – 'It from Qubit'.

In this chapter we explore the basics of entanglement, starting in quantum systems with a finite dimensional Hilbert space, e.g. a lattice system. After introducing some concepts like density matrices and von Neumann entropies, we discuss these concepts in a continuum setting. Of great importance will be the monogamy of entanglement entropy which leads to the specific paradox discussed in Ch. 3. At the end we introduce a mathematical tool to calculate entropies in field theories: the replica trick and twist fields.

2.I The Art of Quantum Entanglement

2.I.a Entanglement in Quantum Systems

We begin by discussing the entanglement in a given lattice system with lattice spacing ε and a finite-dimensional Hilbert space $\mathcal{H}_\alpha$ at each lattice site α [39, 42]. A pure quantum state is then an element of the full tensor product Hilbert space $|\Psi\rangle \in \bigotimes_\alpha \mathcal{H}_\alpha$. This wavefunction represents the exact state of the system from which we can construct a **state/density matrix** ρ representing the actual knowledge we have of the system

$$\rho^\dagger = \rho, \qquad \rho \geq 0, \qquad \operatorname{Tr} \rho = 1 \tag{2.1}$$

Any operator satisfying the above three criteria is in fact a density matrix.

The easiest density matrix is that of a **pure** state which is just the projector onto the quantum state

$$\rho = |\Psi\rangle\langle\Psi| \tag{2.2}$$

States which are not pure are called **mixed**.

Because of its properties, there exists a basis in which this density matrix takes a diagonal form such that the eigenvalues p_i form a classical probability distribution

$$\rho = \sum_i p_i \left|i\right\rangle \left\langle i\right| \tag{2.3}$$

Moreover, via these density matrices we can calculate the expectation value associated to some physical observable $\mathcal{O}$ as

$$\left\langle \mathcal{O} \right\rangle_\rho = \mathrm{Tr}(\mathcal{O}\rho) \tag{2.4}$$

Let us now bipartition our system into a spatial region $\mathcal{A}$ and $\mathcal{A}^c = \mathcal{B}$ which has a fictitious boundary $\partial\mathcal{A} = \partial\mathcal{B}$ called the **entangling surface**, a representation is given in Fig. 2.1. This naturally leads to a bipartite factorisation of the full Hilbert space $\mathcal{H} = \mathcal{H}_\mathcal{A} \otimes \mathcal{H}_\mathcal{B}$. If our full quantum system is in a pure quantum state $|\Psi\rangle$ with density matrix $\rho = |\Psi\rangle\langle\Psi|$, we can construct an operator which only acts on subsystem $\mathcal{A}$ and captures our knowledge about that subsystem by tracing out the degrees of freedom (dof) encompassed by $\mathcal{B}$, i.e. only having access to $\mathcal{A}$ and feigning complete ignorance of $\mathcal{B}$. The operator we obtain is called the **marginal state/reduced density matrix**

$$\rho_\mathcal{A} = \mathrm{Tr}_\mathcal{B}(|\Psi\rangle\langle\Psi|) \tag{2.5}$$

From this definition we can compute the expectation value of operators only acting on this subsystem $\mathcal{O}_\mathcal{A}$ as

$$\langle \mathcal{O}_\mathcal{A} \rangle = \mathrm{Tr}_\mathcal{A}(\mathcal{O}_A \rho_\mathcal{A}) \tag{2.6}$$

This is completely equivalent to computing the expectation value of the operator $\mathcal{O}_\mathcal{A} \otimes \mathbb{1}_\mathcal{B}$ on the full system through (2.4).

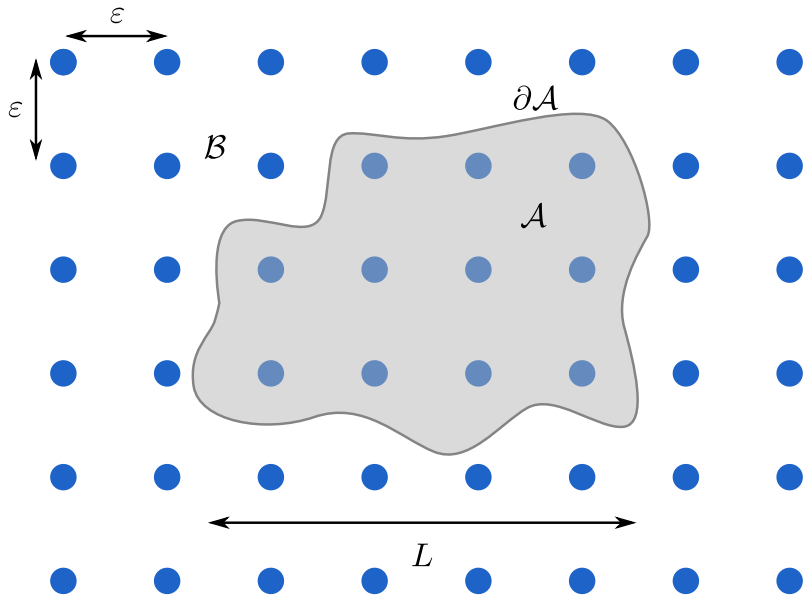

Figure 2.1: Bipartitioning of a lattice system. A cubic, two-dimensional lattice with spacing ε is divided in subsystems $\mathcal{A}$ and $\mathcal{B}$ by the entangling surface $\partial\mathcal{A}$. Subsystem $\mathcal{A}$ encompasses all lattice sites within.

Successively, we want to know the amount of entanglement across the entangling surface as a result of our decomposition in two subsystems. A quantitative measure is introduced through the **von Neumann (vN) entropy/entanglement entropy (EE)** of the reduced density matrix

$$S(\mathcal{A}) = -\,\mathrm{Tr}_\mathcal{A}(\rho_\mathcal{A} \ln \rho_\mathcal{A}) \geq 0 \tag{2.7}$$

which quantifies the amount of ignorance just like the classical Shannon entropy. Or, it is the logarithm of the amount of states of the inaccessible part of our system which are consistent with all measurements restricted to the accessible part, assuming the total system is in a pure state [43]. Therefore, it is also a measure for the dimension of the Hilbert space $\mathcal{H}_\mathcal{A}$.

For a finite system we can diagonalise the reduced density matrix giving us an entanglement spectrum p_i such that the logarithm can be safely taken. Notice that a pure state only has one nonzero eigenvalue which must be equal to 1 according to the definition (2.1); hence it has zero entropy, signalling complete knowledge.

Moreover, the EE is invariant under unitary transformations $\rho \to U\rho U^\dagger$ precisely because of the cyclicity of the trace. Specifically, it is invariant under unitary time evolution.

Clearly, this quantity and others derived from it are dependent on the division into subsystems.

There is another set of entropies which are useful when discussing the replica trick – the **Rényi entropies**

$$S^{(n)}(\mathcal{A}) = \frac{1}{1-n} \ln \mathrm{Tr}_\mathcal{A}(\rho_\mathcal{A}^n) \tag{2.8}$$

for $n \in \mathbb{N}$.

Besides their use in the replica trick, the $n = 2$ case can be used to measure the **purity** $\mathrm{Tr}(\rho^2)$ of a state, which is equal to unity for a properly normalised density matrix in a pure state. But for a mixed state $\mathrm{Tr}(\rho^2) < 0$, and this can be probed via the second Rényi entropy.

In the limit $n \to 1$ we retrieve the EE, but this requires moving away from integer n by analytically continuing to $n \in \mathbb{R}_+$ which is well-defined due to Carlson's theorem: since $\mathrm{Tr}\,\rho^n = \sum_i p_i^n$ is a uniformly convergent sum of analytic functions, $\mathrm{Tr}\,\rho^n$ is itself an analytic function for $\mathrm{Re}\{z\} \geq 1$. Because of normalisation, it is bounded and satisfies the requirements of this theorem. However, it is not immediately apparent how this can be proven in field theories where the local Hilbert space becomes infinite-dimensional.

Due to our bipartitioning, a general state of the full system can be represented as a linear combination of tensor products between $\mathcal{A}$ and $\mathcal{B}$

$$|\Psi\rangle = \sum_{i,j} \psi_{ij} |\alpha_i\rangle |\beta_j\rangle \tag{2.9}$$

with $|\alpha_i\rangle \in \mathcal{H}_\mathcal{A}$ and $|\beta_j\rangle \in \mathcal{H}_\mathcal{B}$.

A state $|\Psi\rangle$ is then called **entangled** if it can not be written as a product state

$$|\Psi\rangle \neq |\alpha_i\rangle |\beta_j\rangle \tag{2.10}$$

The famous example of such an entangled state is one of the four Bell states between two qubits

$$\left|\Phi^+\right\rangle = \frac{|00\rangle + |11\rangle}{\sqrt{2}} \tag{2.11}$$

Additionally, this state is also **maximally entangled** because its density matrix is proportional to the identity – $\rho_\mathcal{A} = \mathbb{1}_\mathcal{A}/2$ – and thus has only equal eigenvalues, classically analogous to maximum randomness. Such states have maximum entropy equal to $\ln \dim \mathcal{H}_\mathcal{A}$.

If the total density matrix is pure, we can look at the Schmidt decomposition

$$|\Psi\rangle = \sum_i \sqrt{p_i} |\alpha_i\rangle_\mathcal{A} |\beta_i\rangle_\mathcal{B} \tag{2.12}$$

Clearly, the eigenvalues of $\rho_\mathcal{A}$ and $\rho_\mathcal{B}$ are the same, leading to similar reduced density matrices, and so they have equal Rényi entropies

$$S^{(n)}(\mathcal{A}) = S^{(n)}(\mathcal{B}) \tag{2.13}$$

Whilst for the full system the EE is zero, this is not the case for the subsystems, denoting entanglement between the two. The vN entropy does not necessarily reflect entanglement but does detect it. By averting our attention to one of the subsystems we inevitably lost information stored in the correlations between the two when we traced out the other one; a reduced density matrix represents what we know about one subsystem without knowing anything about the other.

This process can also be reverse-engineered to **purification**. We start with a diagonal reduced density matrix (2.3) and adjoin it to another system such that the state on this larger system becomes pure. The density matrix on this larger system is then simply the Schmidt decomposition (2.12). This is impossible to do classically.

Originally, the EE represented a quantitative measure for how mixed a state is. Nevertheless, the above process shows that mixedness, however it came to be, is indistinguishable from that arising from entanglement. This important insight led to both concepts – entanglement and entropy – being interchangeable. It is not solely a measure for ignorance [42].

Given the purification, the notion of EE can be rephrased: the quantity $e^{S(\mathcal{A})}$ is the minimal amount of auxiliaries needed to entangle with $\mathcal{A}$ such that we obtain $\rho_{\mathcal{A}}$ from a purification [36].

We heavily relied on the assumption that the total state is pure, but it might be mixed as well. In the most general sense, from a quantum information perspective, a mixed state is **entangled** if it is not **separable/classically correlated**

$$\rho \neq \sum_i p_i \rho^i_{\mathcal{A}} \otimes \rho^i_{\mathcal{B}} \tag{2.14}$$

For a pure state this reduces to being not a product state.

The EE does not prove useful for such mixed states, and we need to introduce another measure which we will see later on – the mutual information.

For all reduced density matrices, there exists a formal Hamiltonian called the **modular Hamiltonian** $K_{\mathcal{A}}$ turning the reduced density matrix into a Gibbs state

$$\rho_{\mathcal{A}} = \frac{1}{\mathcal{Z}} e^{-K_{\mathcal{A}}} \tag{2.15}$$

From this perspective, the Rényi entropies can be seen as modular free energies

$$S^{(n)}(\mathcal{A}) = \frac{1}{1-n} \ln \mathrm{Tr}_{\mathcal{A}}\, e^{-nK_{\mathcal{A}}} \tag{2.16}$$

at inverse temperature n.

Besides, these Rényi entropies are not thermodynamical quantities. For this purpose, consider a canonical ensemble at inverse temperature β

$$\rho = \frac{1}{\mathcal{Z}_\beta} e^{-\beta H} \tag{2.17}$$

then

$$S^{(n)} = \frac{n\beta}{1-n}(F_\beta - F_{n\beta}) \tag{2.18}$$

while for the microcanonical ensemble

$$\rho = \frac{1}{n(E)} \sum_{E \leq E_a \leq E + \Delta E} |a\rangle\langle a| \tag{2.19}$$

the Rényi entropy would be $\ln n(E)$ [42]. In the thermodynamic limit $N \to \infty$ for N dof, extensive quantities like the Rényi entropies are to leading order in $1/N$ proportional to N. Leading

contributions which are also independent of the chosen ensemble are thermodynamic quantities, something which we do not see in the example above. Notice how (2.18) also depends on the free energy at inverse temperature $n\beta$.

In contrast, the **coarse-grained entropy** is a thermodynamical entropy via the following procedure: consider a set of coarse-grained observables $\mathcal{O}_i$, now consider all density matrices $\tilde{\rho}$ leading to the same result for the expectation values for the given system ρ – $\mathrm{Tr}(\mathcal{O}_i\tilde{\rho}) = \mathrm{Tr}(\mathcal{O}_i\rho)$. Next, compute the vN entropy $S(\tilde{\rho})$ and maximise over all possible $\tilde{\rho}$. It turns out this entropy obeys the second law, increases under unitary time evolution, and is larger than S_{vN}. Hence, it sets an upper bound on how entangled a system can be with something else; an upper bound on the vN entropy itself. To distinguish this from the vN entropy, the latter is also called the **fine-grained entropy** [44].

It is clear from the Schrödinger picture that when a state evolves in time, so does its EE. But how can we see this from the Heisenberg picture where the states do not evolve but the operators do? In this picture, the factorisation itself evolves in time

$$\mathcal{H} \cong \mathcal{H}_{\mathcal{A}} \otimes \mathcal{H}_{\mathcal{B}} \tag{2.20}$$

and the time dependence is hidden inside the isomorphism because the unitary map $U : \mathcal{H}_{\mathcal{A}} \otimes \mathcal{H}_{\mathcal{B}} \to \mathcal{H}$ evolves according to

$$U^\dagger \frac{\mathrm{d}U}{\mathrm{d}t} = iH \tag{2.21}$$

with H the Hamiltonian of the full system [42].

2.I.b Entanglement in Field Theories

In the continuum limit, when the lattice spacing goes to zero $\varepsilon \to 0$, we arrive at relativistic quantum field theories (QFTs) where we have wavefunctionals $\Psi[\Phi(x)]$ associated to a field configuration $\Phi(x)$. We can repeat the definitions above, but instead of tracing over dof in a certain region, we integrate over all possible field configurations within that region.

To calculate entropies, we pick a Cauchy slice Σ to define a moment of simultaneity on which we are able to define a state of the system represented by ρ_Σ (remember that we need to specify a time from the Heisenberg picture point of view). It is possible to spatially bipartition this slice into two subsystems $\Sigma = \mathcal{A} \cup \mathcal{B}$ with entangling surface $\partial\mathcal{A}$. If our QFT is not a gauge theory, this leads to a factorisation of the total Hilbert space. However, when facing gauge symmetries, this factorisation should be taken in a gauge-invariant way leading to link variables. We assume a particular choice has been made [39, 45]. From this state we can consider the reduced density matrix $\rho_{\mathcal{A}} = \mathrm{Tr}_{\mathcal{B}}\,\rho_\Sigma$ and calculate the EE. As always, we expect UV divergences in a continuum system, so we should specify a regulator ε for the short distance entanglement present.

It is worth noting that in a relativistic QFT, the EE is robust against deformations of the subsystem $\mathcal{A}$ within its causal diamond. For this purpose, we define the **domain of dependence/causal diamond** $D[\mathcal{A}]$ to be the region where the reduced density matrix can be uniquely evolved once the Hamiltonian is known. More intuitively, it is the set of points which must be causally influenced by or influence events in that region [46]. Since the eigenvalues of $\rho_{\mathcal{A}}$ are invariant under unitary evolution of $\rho_{\mathcal{A}}$ supported only in $\mathcal{H}_{\mathcal{A}}$ or $\mathcal{H}_{\mathcal{B}}$, the entropies remain unaffected. Moreover, any deformation to a region $\mathcal{A}'$ such that $D[\mathcal{A}] = D[\mathcal{A}']$ results in the same Rényi entropies precisely because the two reduced density matrices are related by a unitary transformation. We can think of $\mathcal{A}$ and $\mathcal{A}'$ constituting the same 'subsystem' as their Hilbert spaces are isomorphic to each other [42]. This process is illustrated in Fig. 2.2.

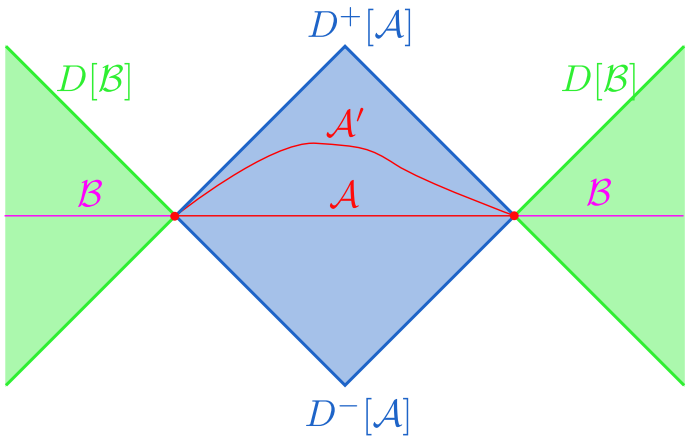

Figure 2.2: The domain of dependence. A Cauchy slice is divided in $\mathcal{A}$ and $\mathcal{B}$, and their causal diamonds are indicated. This can be further divided into the future $D^+[\mathcal{A}]$ and past $D^-[\mathcal{A}]$ domain of dependence. A deformation of $\mathcal{A} \to \mathcal{A}'$ is also shown, leading to the same causal diamond $D[\mathcal{A}] = D[\mathcal{A}']$.

2.I.c UV Divergences

As is usual in field theories, our quantities are UV divergent and so is the EE. These divergences arise from the short range correlations across the entangling surface, because field theories usually retain some notion of locality. Therefore, we expect that the entangled modes across this surface have the largest contribution, leading to the divergence [39, 42]. In another sense, the entanglement can only depend on a quantity which is common to both subsystems – the entangling surface [47].

Consider a lattice again with spacing ε, the full Hilbert space of our system is the tensor product of the Hilbert space at each lattice site: $\bigotimes_\alpha \mathcal{H}_\alpha$. Let us divide our subsystem in two regions $\mathcal{A}, \mathcal{B}$ again. The Hilbert space associated to region $\mathcal{A}$ is the same tensor product of the individual Hilbert spaces but now with the restriction $\alpha \in \mathcal{A}$, similar for $\mathcal{H}_\mathcal{B}$

$$\mathcal{H}_\mathcal{A} = \bigotimes_{\alpha\in\mathcal{A}} \mathcal{H}_\alpha, \qquad \mathcal{H}_\mathcal{B} = \bigotimes_{\alpha\in\mathcal{B}} \mathcal{H}_\alpha \tag{2.22}$$

leading to the factorisation

$$\mathcal{H} = \bigotimes_{\alpha} \mathcal{H}_\alpha = \mathcal{H}_\mathcal{A} \otimes \mathcal{H}_\mathcal{B} \tag{2.23}$$

If our subregion $\mathcal{A}$ has a size of $L \gg \varepsilon$ and consists of $N_\mathcal{A}$ lattice sites, the entropy can be as large as $N_\mathcal{A} \ln \dim \mathcal{H}_\alpha$ which is approximately the logarithm of the dimension of $\mathcal{H}_\mathcal{A}$. In this case, when a random state is picked we get

$$S(\mathcal{A}) \propto N_\mathcal{A} \propto \left(\frac{L}{\epsilon}\right)^{d-1} \tag{2.24}$$

which is called a **volume law** growth since $d-1$ is the number of spatial dimensions. The ratio stems from considering how many lattice hypercubes with side ε fit into the big hypercube with side L.

Physical states which retain a notion of locality have an entropy dominated by the entanglement across the entangling surface

$$S(\mathcal{A}) \propto \left(\frac{L}{\epsilon}\right)^{d-2} \tag{2.25}$$

which is an **area law** growth and is given by the amount of bonds cut by the entangling surface [47].

Obviously, for most d these diverge in the continuum limit $\varepsilon \to 0$. Again, this is not that surprising as in a QFT the local Hilbert space becomes infinite-dimensional. The amount of fields at either side of the entangling surface grows when ε decreases, leading to an amount of correlations proportional to the area of this surface.

Taking the limit $\varepsilon \to 0$ involves subtleties – especially when gauge symmetries are present – and care should be taken. Due to microcausality, the subregions can still be interpreted as having independent dof.

Remarkably, these leading order contributions scale as the area of the entangling surface rather than the volume as what would be expected from an extensive quantity; it was this result that led [48] to link this with the Bekenstein–Hawking entropy. The subleading terms generally depend on the geometry of the entangling surface. For even d there is an additional logarithmic divergence present, called the universal term but is absent for odd d. In the special case of $d = 2$, this is the only divergent contribution and is the result of the entangled surface consisting of a set of disconnected points. The significance of these universal terms is related to the renormalisation group [49].

2.I.d EE Inequalities

There is a useful set of entropy inequalities mainly employed in the context of quantum information theory but can also be proven within the context of holography [50–52]. For this purpose, we often need multiple partitions of our full system which we denote as $\mathcal{A}_i$. In a continuum system they become subregions of a certain Cauchy slice [39, 42].

The first inequality is that of **subadditivity** for a bipartite system:

$$S(\mathcal{A}_1) + S(\mathcal{A}_2) \geq S(\mathcal{A}_1\mathcal{A}_2) \tag{2.26}$$

and is often abbreviated to the statement 'the whole is more than the sum of its parts'. It naturally leads to the notion of **mutual information**

$$\begin{aligned} I(\mathcal{A}_1 : \mathcal{A}_2) &= S(\mathcal{A}_1) + S(\mathcal{A}_2) - S(\mathcal{A}_1\mathcal{A}_2) \\ &= S(\mathcal{A}_1) - H(\mathcal{A}_1|\mathcal{A}_2) \geq 0 \end{aligned} \tag{2.27}$$

which is symmetric in $\mathcal{A}_1$ and $\mathcal{A}_2$, and vanishes if these two subsystems are independent; a nonzero value means that they are correlated, so it encodes the amount of correlation. This quantity represents the amount of information we gain about $\mathcal{A}_1$ if we learn what the state of $\mathcal{A}_2$ is and vice versa, or what we lose when we describe the system as the sum of its parts. It is a better probe for correlations of thermal states – mixed density matrices – in many body physics, because some correlations stem from a classical origin [42, 53].

On the second line, we rewrote this quantity making use of the **conditional entropy**

$$H(\mathcal{A}_1|\mathcal{A}_2) = S(\mathcal{A}_1\mathcal{A}_2) - S(\mathcal{A}_2) \geq 0 \tag{2.28}$$

denoting how much we do not know about $\mathcal{A}_1$ even if $\mathcal{A}_2$ is known, and is zero for a perfectly correlated system: there is nothing left to learn $I(\mathcal{A}_1 : \mathcal{A}_2) = S(\mathcal{A}_1)$. Notice that for an entangled pure state $H(\mathcal{A}_1|\mathcal{A}_2) = -S(\mathcal{A}_2) < 0$. Although negativity of the conditional entropy is a probe for entanglement, the converse does not always hold.

Since the mutual information is nondecreasing when adjoining systems, i.e. $I(\mathcal{A}_1 : \mathcal{A}_2\mathcal{A}_3) \geq I(\mathcal{A}_1 : \mathcal{A}_2)$, we acquire **strong subadditivity**

$$S(\mathcal{A}_1\mathcal{A}_2) + S(\mathcal{A}_2\mathcal{A}_3) \geq S(\mathcal{A}_2) + S(\mathcal{A}_1\mathcal{A}_2\mathcal{A}_3) \tag{2.29}$$

Besides those, we also have the **Araki–Lieb inequality**

$$S(\mathcal{A}_1\mathcal{A}_2) \geq |S(\mathcal{A}_1) - S(\mathcal{A}_2)| \tag{2.30}$$

leading to $S(\mathcal{A}_1) = S(\mathcal{A}_2)$ if the state is pure on $\mathcal{A}_1\mathcal{A}_2$, and the **second form of strong subadditivity/weak monotonicity**

$$S(\mathcal{A}_1\mathcal{A}_2) + S(\mathcal{A}_2\mathcal{A}_3) \geq S(\mathcal{A}_1) + S(\mathcal{A}_3) \tag{2.31}$$

Combination of Eqs. (2.27, 2.30) results in classical monotonicity $S(\mathcal{A}_1\mathcal{A}_2) \geq \max[S(\mathcal{A}_1), S(\mathcal{A}_2)]$.

The quantities we defined can also be used in the context of the Rényi entropies, e.g. the Rényi mutual information. Due to the Rényi entropies not satisfying subadditivity – except for $n = 1$ of course – the Rényi mutual information can even be negative.

The last quantity we mention is the **relative entropy**, providing a measure for the distinguishability between two density matrices ρ, σ [54]

$$S(\rho||\sigma) = \mathrm{Tr}(\rho \ln \rho) - \mathrm{Tr}(\rho \ln \sigma) \geq 0 \tag{2.32}$$

which is zero if $\rho = \sigma$ and satisfies monotonicity, decreasing under inclusion

$$S(\rho_{\mathcal{A}}||\sigma_{\mathcal{A}}) \leq S(\rho||\sigma) \tag{2.33}$$

after tracing out the same dof.

Furthermore, using the modular Hamiltonian (2.15) we can define the **modular free energy** as

$$F(\rho) = \mathrm{Tr}(\rho K_\sigma) - S(\rho) \tag{2.34}$$

such that $S(\rho||\sigma) = F(\rho) - F(\sigma)$.

It defines a metric on the manifold of density matrices and leads to the notion of Bures distance [55]. When considering $\rho = \sigma + \varepsilon\rho_1 + \dots$ around $\rho_0 = \sigma$, to first order we obtain the **first law of entanglement entropy**

$$\delta S = -\mathrm{Tr}(\delta\rho \ln \rho) = \delta \langle K_{\rho_0} \rangle \tag{2.35}$$

since $S(\rho||\sigma) = \Delta \langle K_\sigma \rangle - \Delta \langle S \rangle \geq 0$ is at least of order $\mathcal{O}(\varepsilon^2)$.

To second order in ε, we can define a positive definite inner product called the **quantum Fisher information**, a constraint on achievable precision in parameter estimation [55].

$$\begin{aligned} \varepsilon^2 \langle \rho_1, \rho_1 \rangle_{\rho_0} &= S(\rho_0 + \varepsilon\rho_1||\rho_0) \\ &= \frac{1}{2}\varepsilon^2 \,\mathrm{Tr}\left(\rho_1 \frac{\mathrm{d}}{\mathrm{d}\varepsilon} \ln(\rho_0 + \varepsilon\rho_1)\right) \end{aligned} \tag{2.36}$$

2.I.e Monogamy of EE

In Ch. 3 we will talk about one of the paradoxes involving BHs making use of a property known as **monogamy of EE**: two maximally entangled systems with each other cannot be entangled with a third system, they only show up in pairs. Since this property generally stems from quantum information theory, we treat it here [24, 56].

If two systems have observables whose correlations exceed that of possible classical correlations, the systems are said to be entangled [57]. Now consider a pair of observables A_1, A_2 and B_1, B_2 each from a separate system. The **Clauser-Horne-Shimony-Holt (CHSH) operator** is defined as [58]

$$C_{AB} = A_1(B_1 + B_2) + A_2(B_1 - B_2) \tag{2.37}$$

In the classical regime, when all operators can be diagonalised simultaneously and assuming their eigenvalues are in the range $[-1,1]$, we get $|C_{AB}| \leq 2$. If both systems are part of a larger system, these observables should commute within the larger Hilbert space.

Nevertheless, [59] showed that in a QM system the classical bound enlarges to **Tsirelson's bound** for any state $|\Psi\rangle$

$$|\langle C_{AB}\rangle_\Psi| \leq 2\sqrt{2} \tag{2.38}$$

Forasmuch as our definition of entangled being the classical value to be exceeded, there is entanglement if

$$2 < |\langle C_{AB}\rangle_\Psi| \leq 2\sqrt{2} \tag{2.39}$$

For the sake of showing monogamy, let us consider a third system with a third set of operators C_1, C_2 with eigenvalues also in $[-1,1]$ and which commute with the other observables with respect to a larger Hilbert space. The authors of [60, 61] proved that

$$\langle C_{AB}\rangle_\Psi^2 + \langle C_{AC}\rangle_\Psi^2 \leq 8 \tag{2.40}$$

Subsequently, let A and B be entangled. The inequality (2.39) implies $|\langle C_{AB}\rangle_\Psi| > 2$ such that $\langle C_{AB}\rangle_\Psi^2 > 4$. In contrast, the expression above tells us $\langle C_{AC}\rangle_\Psi^2 < 4$ or $|\langle C_{AC}\rangle_\Psi| < 2$ from which follows that A and C cannot be entangled with each other; A cannot be entangled with both B and C simultaneously.

There is another way of showing monogamy, i.e. by making use of the second form of strong subadditivity (2.31) and the conditional entropy (2.28) [42]:

$$H(A|B) + H(C|B) \geq 0 \tag{2.41}$$

Probing entanglement via the negativity of the conditional entropy, this inequality tells us that at most one of the two can be negative: either A is entangled with B or either B is entangled with C, but not both.

While it is not entirely clear whether this also holds for field theories with infinite-dimensional local Hilbert spaces, it turns out that when using the holographic formula in Ch. 4, it also obeys all of the aforementioned inequalities. From the holographic picture, one would thus believe this to hold in a theory of QG.

2.II The Replica Trick

To compute the EE in field theories, one mainly makes use of a tool called the **replica trick**: the basic idea is to take n identical copies of a system/field configuration and cyclically sew them together where the last copy gets sewn back to the first one. In this way, it is possible to obtain an expression for the Rényi entropies which after analytical continuation to $n \in \mathbb{R}_+$ leads to the EE in the limit $n \to 1$.

Consider a static state or a moment of time-reflection symmetry, e.g. define $\rho_\mathcal{A}$ on a Cauchy slice Σ with trivial time evolution. For such states, it is easier to work in the Euclidean setting. If we bipartition our Cauchy slice Σ, we can divide our set of field configurations $\Phi(x)$ in those only having support on $\mathcal{A}$ and those only having support on its complement. Since the density matrix acts as an operator, it can be represented by a PI having two open cuts. These cuts represent the boundary conditions (BC), the bra and ket, when computing an expectation value $\langle\Phi_1|\rho|\Phi_2\rangle$. Open cuts are represented by leaving these BC unspecified [36].

The reduced density matrix can then be represented by introducing the following BC

$$\Phi_\mathcal{A}|_{t=0^\pm} = \Phi_\pm \tag{2.42}$$

such that [39, 62]

$$(\rho_{\mathcal{A}})_{-+} = \int \mathcal{D}\Phi e^{-S[\Phi]} \delta[\Phi_{\mathcal{A}}(t=0^-) - \Phi_-] \delta[\Phi_{\mathcal{A}}(t=0^+) - \Phi_+] \tag{2.43}$$

Note that tracing over the dof encompassed in $\mathcal{B}$ is equivalent to gluing the cuts lying in this subregion together and integrating over all field configurations along this sewn cut. An example is drawn in Fig. 2.3a.

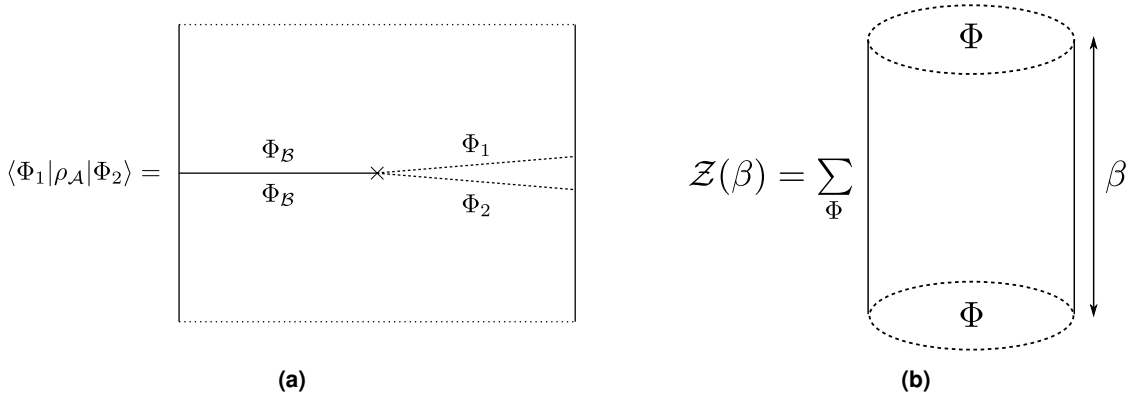

Figure 2.3: (a) Visual representation of a matrix element via the reduced density matrix. We divided our Cauchy slice in two subsystems and traced one subsystem out by integrating over all possible field configurations, i.e. by setting $\Phi_{\mathcal{B}}$ on both sides along the cut. The matrix element is then represented by setting $\Phi_+ = \Phi_1$ on one side of the remaining cut and $\Phi_- = \Phi_2$ on the other side. **(b)** Visual representation of a thermal partition function. We glue both ends together and sum over all possible field configurations Φ. The resulting surface would be a torus.

For instance, the thermal density matrix $\rho = e^{-\beta H}$ in which we glue the BC together and sum over all such BC field configurations results in the Euclidean partition function (see Fig. 2.3b)

$$\mathcal{Z}(\beta) = \operatorname{Tr} e^{-\beta H} = \sum_{\Phi} \langle \Phi | e^{-\beta H} | \Phi \rangle \tag{2.44}$$

For systems with nontrivial time dependence, the definition should be modified to take causality into account; we should not prepare our density matrix by making use of field configurations at $t' > t$. The usual framework is the **Schwinger–Keldysh/closed time–path/in–in formalism**: we basically evolve the initial state, let it interact, and evolve it back to the initial state. This leads to a complex time contour representation and a natural doubling of the microscopic fields and BC – one copy for forwards and one for backwards evolution. A special case of this formalism is the thermofield double state [63–66].

Since the Rényi entropies involve powers of the reduced density matrix (2.8), we want to find a PI representation which directly computes this n'th power. To reach this goal, we take n identical copies of the original setup and sew the cuts in a cyclical way:

$$\Phi_+^{(j)} = \Phi_-^{(j+1)} \tag{2.45}$$

resulting in

$$\begin{aligned}(\rho_{\mathcal{A}})^n_{-+} = &\int \prod_{j=1}^{n-1} d\Phi_+^{(j)} \delta(\Phi_+^{(j)} - \Phi_-^{(j+1)}) \\ &\int \prod_{i=1}^{n} \mathcal{D}\Phi^{(i)} e^{-\sum_{i=1}^n S[\Phi^{(i)}]} \delta[\Phi_{\mathcal{A}}^{(i)}(0^-) - \Phi_-] \delta[\Phi_{\mathcal{A}}^{(i)}(0^+) - \Phi_+]\end{aligned} \tag{2.46}$$

To compute the Rényi entropy, we ultimately identify $\Phi_+^{(n)}$ with $\Phi_-^{(1)}$. Again, for a time-dependent setup we should resort to the Schwinger–Keldysh formalism.

What does this manifold look like? We started with taking n copies of the original manifold $\mathcal{M}$ on which we introduced two cuts. Subsequently, we sew those cuts cyclically along the manifolds where the second cut of the last manifold gets sewn with the first cut of the first manifold. The result is a n-fold branched cover $\mathcal{M}_n$ over $\mathcal{M}$ as depicted in Fig. 2.4. The cyclicity of the trace is now transferred to the cyclicity of the n copies such that our manifold enjoys a cyclic permutation symmetry $\mathbb{Z}_n$, called the **replica symmetry**. On top of this, for a system which has time-reflection symmetry $\mathbb{Z}_2$, the replica symmetry gets enhanced to the dihedral group $\mathbb{D}_{2d}$.

This replica construction can lead to quite complicated Riemannian manifolds. For instance, take a single manifold with m disconnected regions. Using the replica construction for n copies introduces a handle for every two copies such that we obtain a Riemannian manifold with genus $\chi = (n-1)(m-1)$. Notice how the amount of copies creeps into the genus and renders it highly nontrivial to analytically continue. Another example would be by having a torus as base manifold, leading to a manifold of genus n.

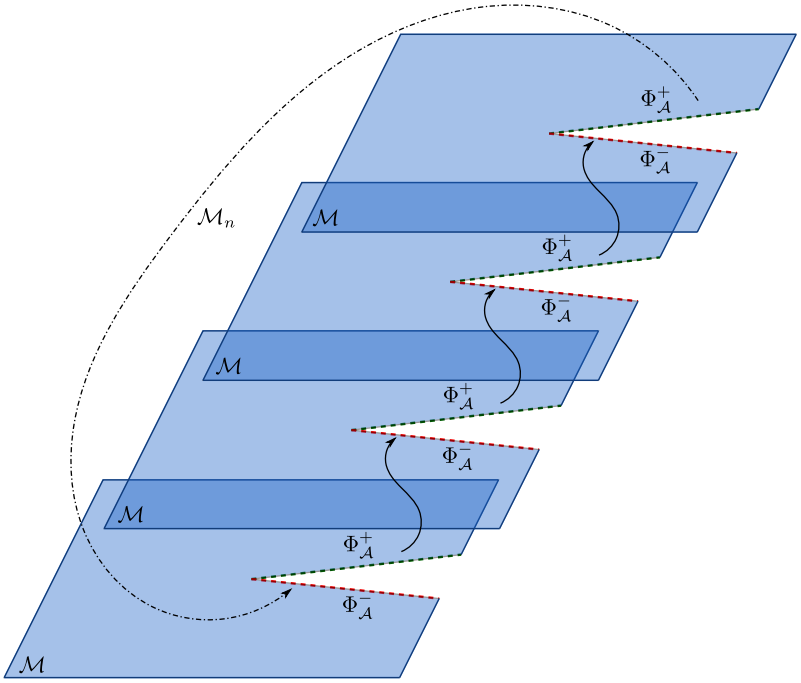

Figure 2.4: Visual representation of the replica manifold $\mathcal{M}_n$. The base manifold $\mathcal{M}$ is a single reduced density matrix. Cuts which are sewn together are indicated by the arrows.

Assuming we can use Carlson's theorem/the Phragmén–Lindelöf principle, we can analytically continue from the integer n to real, positive values of n. The PI (2.46) constructed above computes such powers of the density matrix, in particular the partition function on this branched cover

$$\mathcal{Z}_{\mathcal{A}}^{(n)} = \operatorname{Tr} \rho_{\mathcal{A}}^n = \mathcal{Z}[\mathcal{M}_n] \tag{2.47}$$

such that with proper normalisation (2.1, 2.8)

$$\begin{aligned} S^{(n)}(\mathcal{A}) &= \frac{1}{1-n} \ln \frac{\mathcal{Z}_{\mathcal{A}}^{(n)}}{[\mathcal{Z}_{\mathcal{A}}^{(1)}]^n} \\ &= \frac{1}{1-n} \ln \frac{\mathcal{Z}[\mathcal{M}_n]}{\mathcal{Z}[\mathcal{M}]^n} \end{aligned} \tag{2.48}$$

Taking the $n \to 1$ limit and using l'Hôpital's rule results in the EE (2.8)

$$\begin{aligned} S(\mathcal{A}) &\overset{H}{=} -\lim_{n\to 1} \frac{\mathrm{d}}{\mathrm{d}n} \operatorname{Tr} \rho_{\mathcal{A}}^n \\ &\overset{H}{=} -\lim_{n\to 1} \frac{\mathrm{d}}{\mathrm{d}n} \left[\ln \mathcal{Z}_{\mathcal{A}}^{(n)} - n \ln \mathcal{Z}_{\mathcal{A}}^{(1)}\right] \\ &= \lim_{n\to 1} \left(1 - n\frac{\mathrm{d}}{\mathrm{d}n}\right) \ln \mathcal{Z}_{\mathcal{A}}^{(n)} \end{aligned} \tag{2.49}$$

Observe how the last line looks similar to the thermodynamical expression $(1 - \beta\partial_\beta) \ln \mathcal{Z}$.

2.II.a Twist Fields

For computational purposes, it is often easier to work with the orbifold theory $\mathcal{M}^n/\mathbb{Z}_n$ by taking the quotient of our replicated geometry $\mathcal{M}^n$ with the cyclic permutation symmetry $\mathbb{Z}_n$. By moving the topology from the total worldsheet to the target space, where our fields live, we obtain local fields $\mathcal{T}, \tilde{\mathcal{T}}$ implementing the BC of our replicated manifold, called **twist fields** [62]. Instead of fields living on a single copy, we obtain fields living on all copies and subsequently turn them into a composite field on a single manifold obeying twisted BC. The partition function of such a manifold is through this procedure proportional to the correlation function of these twist fields.

Such fields exist whenever there is a global internal symmetry σ. For the replica construction, this is the cyclic exchange symmetry of the copies $\mathbb{Z}_n$. There are two such permutation symmetries: $i \to i+1$ and $i+1 \to i$ leading to

$$\mathcal{T}_n \equiv \mathcal{T}_\sigma \qquad \sigma : i \to i+1 \mod n \tag{2.50a}$$

$$\tilde{\mathcal{T}}_n \equiv \mathcal{T}_{\sigma^{-1}} \qquad \sigma^{-1} : i+1 \to i \mod n \tag{2.50b}$$

with the additional identification $\tilde{\mathcal{T}}_n = \mathcal{T}_{-n}$.

Now take a CFT with multiple disconnected intervals, then $\operatorname{Tr} \rho_{\mathcal{A}}^n$ transforms as a conformal two-point function of the twist fields which are primary operators with conformal dimension

$$h_n = \overline{h}_n = \frac{c}{12}\frac{(n-1)(n+1)}{n} \tag{2.51}$$

With this fact, it becomes easier to calculate the EE: for k endpoints we need to calculate the k-point function of our twist fields inserted at the endpoints/branch points of these intervals and subsequently transform to coordinates where this correlator is explicitly known.

Under a Weyl transformation $g \to \Omega^{-2} g$, we have

$$\left\langle \mathcal{T}_1 \tilde{\mathcal{T}}_2 \right\rangle_{e^{2\omega} g} = \Omega_1^{h_n} \Omega_2^{h_n} \left\langle \mathcal{T}_1 \tilde{\mathcal{T}}_2 \right\rangle_g \tag{2.52}$$

with the expectation values normalised according to the partition function. For a single interval

$$S^{(n)} = -\frac{1}{n-1} \ln \left\langle \mathcal{T}_1 \tilde{\mathcal{T}}_2 \right\rangle_{\mathcal{M}^n/\mathbb{Z}_n} \tag{2.53}$$

Combine this with (2.52), and take the limit $n \to 1$ through

$$\lim_{n\to 1} -\frac{1}{n-1} h_n \overset{H}{=} -\frac{c}{6} \tag{2.54}$$

results into the well-known formula

$$S_{\Omega^{-2} g} = S_g - \frac{c}{6} \sum_{\text{endpoints}} \ln \Omega \tag{2.55}$$

which generally holds for multiple intervals as well.

To end this subsection, we give an example for a single interval in a CFT_2 and consider a static vacuum state on $\mathbb{R}^{1,1}$ which through time independence can be mapped to the complex plane $\mathbb{C} = \mathbb{R}^2$ [39]. For our region $\mathcal{A}$, we choose $\mathcal{A} = \{x \in [-a, a]\}$ with the entangling surface being the two endpoints of the interval. After constructing our replica manifold by cyclically gluing these intervals, we end up with a genus-0 surface containing a function which is multi-branched. The partition function can now be written in terms of the two-point function

$$\mathcal{Z}[\mathcal{M}_n] = \prod_{i=0}^{n-1} \left\langle \mathcal{T}_n(-a,0)\tilde{\mathcal{T}}_n(a,0) \right\rangle_{\mathcal{M}} \tag{2.56}$$

which, after the introduction of a UV regulator ε, leads to

$$\mathcal{Z}[\mathcal{M}_n] = \left(\frac{2a}{\varepsilon}\right)^{-\frac{c}{6}\left(n-\frac{1}{n}\right)} \tag{2.57}$$

Finally, through (2.49)

$$\begin{aligned} S(\mathcal{A}) &= \lim_{n\to 1} \frac{c}{3n} \ln \frac{2a}{\varepsilon} \\ &= \frac{c}{3} \ln \frac{2a}{\varepsilon} \end{aligned} \tag{2.58}$$

This is the logarithmic scaling mentioned in Sect. 2.I.c. For the whole computation in more detail, see [62].

2.III Entanglement and the Taj Mahal Theorem (SD)

"'If you think you understand quantum mechanics, you don't understand quantum mechanics.' Now these are words I can relate to", Sakuta mumbled. [1]

This quote from Richard Feynman left him pondering for a while. He had been reading *Quantum for Dummies* and has gotten to chapter 2 about entanglement and entropy. To nobody's surprise, it left him puzzled. Even during his biology classes like right now, he seemed to be more invested in his book than what is written on the blackboard. Finally, at the end of his class he took his bag and went straight to the science room on the other side of the building. On his way through the halls, he met up with Futaba.

"Huh, Feynman's quote isn't it?", she responded when Sakuta repeated it. "Don't think too highly of me now. He didn't say that quote for nothing. Even I don't understand everything about quantum mechanics..."

"And here I thought you would be humble for once..."

"I'll take that as a compliment", she replied with a smile on her face. "Ever heard of the Taj Mahal theorem?"

"Taj Mah– You mean like that world wonder in India? So it has its own theorem now, that's nice."

"I suppose you don't. Well that's no problem, it is rather remarkable and strange. But let's discuss it when we get to the science room."

The room was quite dark and only some sunlight was flickering through the blue curtains. There was also some leftover smell from the experiments which is not so pleasant... It became suddenly more lively as the curtains were opened and the room was lit by golden sun rays. Meanwhile, it seemed the club activities just started; the track team was busy with their

[1] The contents are based on [35].

usual warm up routine.

"Coffee?"

"Yeah, sure. I was getting tired in biology class anyway."

She was already taking the usual stuff from the cabinet. As the sole club member, she doesn't regularly set up any experiments but rather enjoys the quiet environment while being lost in some book.

"So, entanglement was it? Quite a confusing topic", Futaba remarked.
"Yup, I was reading through chapter 2, trying to understand this concept and stuff like von Neumann entropy."

"I can see where you're coming from. Let's take a step back first. You have read the part about EPR [2] pairs and how we can't communicate faster than the speed of light, even with entanglement, right? For instance, let's assume you and Mai prepare an aligned electron pair and put you on the moon. Th–"

"If I measure my electron's spin to be up, then instantaneously the other spin will also be in the up state", he interrupted her and went on. "But Mai can't know this without measuring her spin along the same axis, or without me sending her that information through a classical channel. In this way, causality is preserved."

"... Huh, didn't know you had it in you."

She seemed impressed by his continuation of the story. Sakuta was gloating, he appeared to be proud for once. In the meantime, the Bunsen burner was slowly heating their water.

"Well, if you know all that. What if you beforehand compose a message: if you find water, then you'll make your electron to be up. Surely, Mai can then receive this message instantaneously if she does a measurement, right?"

"No, that would break causality again. But I don't know the answer to this one", he replied. His moment of glory was short-lived.

"The answer is pretty easy actually. You can never force it to be in the up state. There is an equal probability of it being up or down. So even if it were in the up state, there is no way for Mai to be completely sure you found water on the moon. Also, how would she know you did a measurement?"

"That makes sense. And here I thought I was starting to get it... But what is this theorem now exactly?"

"The Taj Mahal theorem states that by acting here on this table, there is a probability for the Taj Mahal to be constructed on the moon."

"... Well, that's it; you officially lost me. We didn't even went over entropy yet", he replied with a disappointed look on his face.

"Okay, let's explain it like this. Suppose our Universe consists of just two boxes and we consider the total wavefunction. There is only one wavefunction containing all the information we need. The boxes don't separately have a wavefunction, only the total system does. However, sometimes we do like to work as if there were separate wavefunctions. But if we do, we lose information about the total wavefunction. There is seemingly a state of ignorance about the second box if we only look at one box. Much like when you do a measurement, you know the total system collapsed to a definite state. Yet, Mai doesn't know this. In this sense, the total system can be said to be entangled; the von Neumann entropy gives a measure for this entanglement. It's nonzero because we lose information by only looking at one box."

"... huh", Sakuta was listening carefully while Futaba was drawing on the blackboard. She seemed to be in 'the zone' and continued here mini-lecture. The water was still boiling, nobody was paying any attention to this subsystem.

"Instead of two boxes, let's divide the Universe, empty space, in a bunch of boxes. We have one smoothly varying wavefunction. Now look at box A and B. To have a smooth transition on the boundary we require information of its behaviour in both boxes, right? A discontinuous

[2] Einstein–Podolsky–Rosen

jump would require an infinite amount of energy. But this does not happen in empty space, so both boxes are enta–" She suddenly realised the water was still boiling and quickly turned off the Bunsen burner. "Couldn't you have said something?", she asked sharply.

"Sorry, I was a bit lost in your lecturing. In a good way that is", he replied.

"I hope that's the case... Anyway, we can continue this throughout all boxes. All boxes are entangled with each other, it doesn't matter how far they are. But the amount of entanglement decreases between them if they are further away."

"Okay, I can see that. So what does this mean?"

"It means that if we act on one box we change the state in all other boxes simultaneously since they are entangled. So by acting locally, we make a change globally. By acting on this table, we can create a Taj Mahal on the moon. Of course, it's very improbable and we can't force it, but it's true nonetheless."

"Hmmm, this all seems rather strange... But I somehow believe you're right."

"It is quite remarkable. I still don't fully understand it."

"For you to not understand something is quite remarkable indeed", Sakuta remarked, laughing aloud.

After exchanging some laughs, they went on to talk about other topics; less about physics for once. At the end, the water was back to being cold again. It seemed that mini-lecture took some time to finish as the track team was on its way to the locker room.

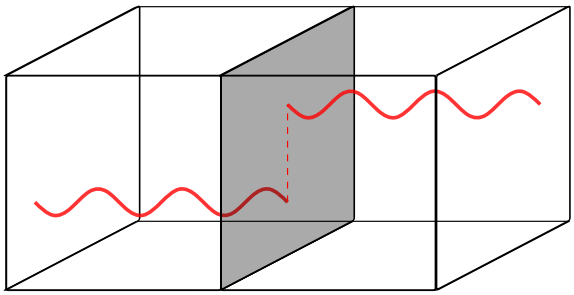

Figure 2.5: Entanglement between two boxes. To have a smooth transition, one requires information about the wavefunction in both boxes. Equivalently, we need information about the wavefunction on the region common to both boxes – the entangling surface (shaded in gray).

Chapter 3

Black Holes and the Information Puzzle

Many physicists dispute the actual reasons and its many possible resolutions, but everyone acknowledges that there is a problem when considering BHs from a quantum information viewpoint. The different views and opinions many physicists hold have led to many debates, and it has become hard to grasp what exactly the information paradox entails. It has left many physicists puzzled for over more than four decades.

In this chapter, we discuss some of these questions after an introduction to some BH physics. We try to be as complete as possible, but there will certainly be some concepts we omitted for the sake of brevity. There are many great resources on this problem, and we definitely use some of them in this chapter [13, 24, 44, 67].

3.I BH Thermodynamics

3.I.a Hawking Temperature

In 1975, S. Hawking showed in his landmark paper that a BH actually emits radiation at a temperature related to its surface gravity – the **Hawking temperature** [3, 68]. There is a much shorter derivation than the original one, making use of the 'periodicity trick' for the Euclidean BH, i.e. with Wick rotated Euclidean time $t_E = it$, albeit it resulting in less physical intuition [36, 44, 69, 70].

Consider the general Schwarzschild metric in d dimensions

$$ds^2 = -f(r, M)dt^2 + \frac{dr^2}{f(r, M)} + r^2 d\Omega_{d-2}^2 \tag{3.1}$$

where the horizon r_h is found through $f(r_h, M) = 0$

$$f(r, M) = 1 - k\frac{r^2}{L^2} - \frac{16\pi G_{\mathsf{N}} M}{(d-2)A(\Omega_{d-2})r^{d-3}} \tag{3.2}$$

with $A(\Omega_{d-2})$ the area of the transverse sphere and k the sign of the cosmological constant with curvature $1/L^2$. Near the horizon, we expand the redshift factor as

$$\begin{aligned} f(r, M) &= f(r_h, M) + (r - r_h)f'(r_h, M) + \mathcal{O}[(r - r_h)^2] \\ &\approx \frac{4\pi}{\beta}(r - r_h) \end{aligned} \tag{3.3}$$

In the last line we rewrote our redshift factor by introducing a constant β. Plugging this into the metric (3.1) and Wick rotating to Euclidean time $t_E = it$ results in the near-horizon metric

$$ds^2 \approx \frac{4\pi}{\beta}(r - r_h)dt_E^2 + \frac{\beta}{4\pi}\frac{dr^2}{r - r_h} \tag{3.4}$$

after ignoring the angular directions. We can successively introduce new coordinates

$$\rho = \sqrt{\frac{\beta}{\pi}(r - r_h)}, \qquad \theta = \frac{2\pi}{\beta}t_E \tag{3.5}$$

such that the near-horizon metric looks like that of a flat space in polar coordinates

$$ds^2 \approx d\rho^2 + \rho^2 d\theta^2 \tag{3.6}$$

Wick rotating back through $\eta = i\theta$ and transforming to Minkowski space gives us the Rindler coordinate system

$$x = \rho\cosh\eta, \qquad t = \rho\sinh\eta \tag{3.7}$$

Hence, the near-horizon metric is equivalent to the Rindler metric.

Of course, for an observer nothing special happens at the horizon because it is just a coordinate singularity. This implies that in the (ρ, θ) coordinates at $\rho = 0$ we must remove the conical singularity by assuming periodic BC in the θ-coordinate: $\theta \sim \theta + 2\pi$, which is equivalent to $t_E \sim t_E + \beta$ or $t \sim t + i\beta$ (see Fig. 3.1). It is well-known that a periodicity in Euclidean time with period β represents a thermal state at inverse temperature β [71]. Therefore, we obtain the general Hawking temperature

$$T_H = \frac{f'(r_h, M)}{4\pi} \tag{3.8}$$

For the Schwarzschild BH in a flat Universe $f(r) = 1 - \frac{r_s}{r}$ this is

$$T_H = \frac{1}{4\pi r_s} \tag{3.9}$$

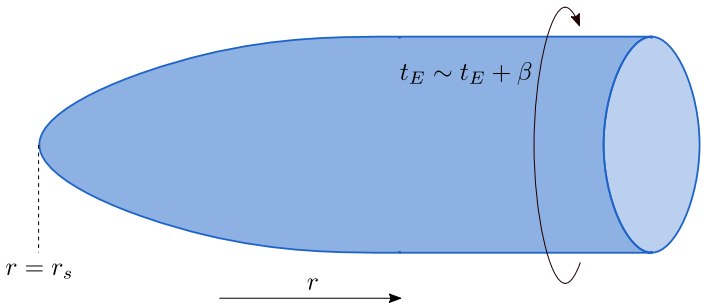

Figure 3.1: The Euclidean BH. After Wick rotating the Schwarzschild metric, we obtain a cigar-like geometry with the horizon located at the tip. The Euclidean time turns out to be periodic in the inverse Hawking temperature in order to get rid of the conical singularity.

The actual temperature an observer measures is the **Unruh temperature**, found through the Tolman relation [72]

$$T_U(r) = \frac{1}{\sqrt{g_{\theta\theta}(r)}}T_\theta = \frac{a(r)}{2\pi} \tag{3.10}$$

for an observer close to the horizon with constant proper acceleration $a = 1/\rho$ and diverges on the horizon. From this perspective, the Hawking temperature is what an observer at infinity

would measure; this can be seen by going back to the original BH coordinates and using the redshift relation $T_U(r)\sqrt{-g_{tt}(r)} = T_U(r')\sqrt{-g_{tt}(r')}$ with $r(\rho) \approx r_s$ and $r' \to \infty$ such that $-g_{tt}(r') \to 1$.

Restoring units – multiply with $\hbar/(ck_B)$ – one should be accelerating at $2.5 \cdot 10^{20}\ m/s^2$ to observe a temperature of $1\ K$ [36].

3.I.b The Unruh Effect

Let us look at the **Unruh effect** next: an accelerating observer detects a particle bath at a temperature equal to the Unruh temperature with respect to the Minkowski vacuum.

This effect was independently discovered by P. Davies and W. Unruh via general quantum field theoretical calculations on a fixed, curved background spacetime making use of machinery like the Bogoliubov transformations [73, 74].

From the previous subsection we found that $\theta \sim \theta + 2\pi$, which in Rindler time $\eta = i\theta$ becomes $\eta \sim \eta + 2\pi i$ and looks like a temperature $\frac{1}{2\pi}$ associated to Rindler time translations ∂_η. Hence, if H_η is the Hamiltonian generating these translations, we find a density matrix

$$\rho_{\text{Rindler}} = \frac{1}{\mathcal{Z}} e^{-2\pi H_\eta} \tag{3.11}$$

After identification with (2.15, 2.17) it defines a thermal Gibbs state at this temperature [36]!

The modular Hamiltonian in this case is $K = 2\pi H_\eta$ and generates rotations over 2π in the Euclidean plane or equivalently, Lorentz boosts $\partial_\eta = x\partial_t + t\partial_x$. Of course, the Tolman relation associates an accelerating observer to a thermal heat bath at the Unruh temperature (3.10).

The same conclusion can be obtained by starting from 2d Minkowski space (t, x), looking at the region $\mathcal{A} = \{t = 0, x \geq 0\}$, and tracing over the fields in its complement. The causal domain of $\mathcal{A}$ is the right Rindler wedge (Fig. 3.2) and preserves the boost subgroup of the Poincaré group [42]. While the overall state may be in the Minkowski vacuum, an accelerating observer causally restricted to the right Rindler wedge only sees a mixed state. The Minkowski vacuum is highly entangled!

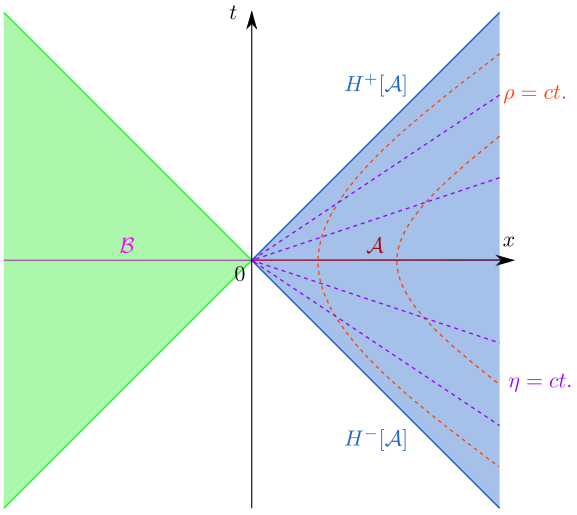

Figure 3.2: The Rindler wedge. Two-dimensional Minkowski space is subdivided in regions $\mathcal{A}$ and $\mathcal{B}$. We avert our attention to the right Rindler wedge – the domain of dependence associated to $\mathcal{A}$. Lines of constant Rindler coordinates ρ and η are also shown, along with the future and past Rindler horizons $H^{\pm}[\mathcal{A}]$.

So, a stationary observer in the Minkowski vacuum does not detect any particles with his detector, but an accelerating observer with a detector calibrated to the Minkowski vacuum does.

The essence of this phenomenon is the definition of what a particle is: a localised clump of energy on top of the vacuum/a distinguishable wobbling of the underlying quantum field. These particles are generally associated to positive frequency modes which are itself defined with respect to a preferred time coordinate – the proper time of the observer. This effect occurs because both observers, the accelerating and the free-falling one, each have a different preferred time coordinate. Hence, what their detector would interpret as a particle (positive frequency mode) differs [36]

$$\text{time} \longleftrightarrow \text{energy} \longleftrightarrow \text{particle} \longleftrightarrow \text{vacuum}$$

The Minkowski vacuum is annihilated by the annihilation operators with respect to the free-falling time coordinate; therefore, this state looks thermally occupied by an accelerating observer. Vice versa, the Rindler vacuum looks thermally occupied when seen by a free-falling observer [36].

The usual picture of Hawking radiation is that of vacuum excitations localised near the horizon where one particle escapes to radial infinity, and the other gets captured behind the horizon (see Fig. 3.3). Whilst this is certainly a good pedagogical way of explaining this phenomenon, it is inherently wrong as shown by S. Giddings [75] and which Hawking himself already knew. If all those excitations are truly localised near the horizon, then there must be an enormous energy density at that location.[1] The equivalence principle, however, dictates that nothing special happens at that location. What is exactly going on? Giddings used the Stefan–Boltzmann law and some manipulations with the stress tensor to show that the outgoing Hawking flux originates from an atmosphere up to a few Schwarzschild radii; the stress tensor only takes a small value near the horizon. The width of the wavepackets of the radiation is even considerably larger than its distance to the horizon. Moreover, it explains why outgoing modes do not separate from their partners inside the BH until well outside the BH's vicinity [76]. The resemblance with the Unruh effect is not far off: different observers have a different notion of what a particle is. For an observer at spatial infinity this looks like a thermal bath at the Hawking temperature – an infinitely redshifted Unruh temperature [77].

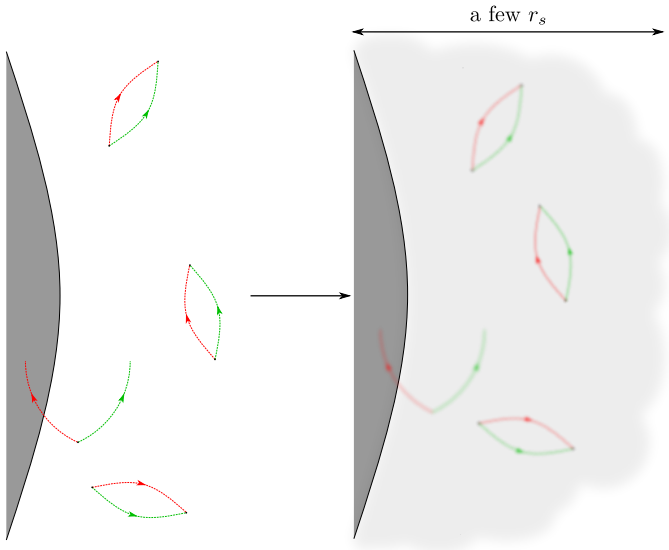

Figure 3.3: Hawking Radiation. In the left picture we see the pedagogical way of introducing Hawking radiation: particle-antiparticle pairs pop in and out of existence. Close to the horizon, one can get trapped behind it whilst the other escapes. On the right is the actual blurred picture of this phenomenon. It is delocalised and stretches to a few Schwarzschild radii.

[1] While also called a firewall, it is different from the one in the information paradox.

3.I.c The Bekenstein–Hawking Entropy and the BH Laws

The usual derivation of the Bekenstein–Hawking entropy is by making a saddle point approximation in the gravitational PI (GPI) and subsequently make use of thermodynamical relations [13, 36, 78]. There is an alternative approach related to the replica trick and the appearance of conical defects [70, 79], but we will follow the first one.

The full GPI includes both the contribution of the quantum fields and all possible geometries/metrics. To leading order, we can restrict ourselves to integration over the geometries only

$$\mathcal{Z}(\beta) = \int_{\mathcal{M}} \mathcal{D}g\, e^{-I_G[g]} \tag{3.12}$$

with the gravitational action being the Einstein–Hilbert action, taking into account boundary terms and regularisation [80].

In this GPI we integrate over the metrics on an Euclidean manifold which asymptotically has periodicity β and $g_{t_E t_E} \to 1$ analogous to a thermal partition function. To leading order, we approximate the GPI by its saddle point $\tilde{g}$ which we take to be the Euclidean Schwarzschild BH.

To evaluate the action, we put a cutoff on our spacetime at large, fixed r_0. Since this adds a boundary to our manifold, we need to add the Gibbons–Hawking–York term

$$I_G[g] = -\frac{1}{16\pi G_{\mathsf{N}}} \int_{\mathcal{M}} \sqrt{g} R - \frac{1}{8\pi G_{\mathsf{N}}} \int_{\partial\mathcal{M}} \sqrt{\gamma} K \tag{3.13}$$

with boundary metric γ and extrinsic curvature K. This term is required in order to eliminate the boundary term when varying the action, leading to [2]

$$\delta I_G[g] = \int_{\mathcal{M}} (eom)\delta g + \frac{1}{2} \int_{\partial\mathcal{M}} \sqrt{\gamma} T^{\mu\nu} \delta g_{\mu\nu} \tag{3.14}$$

For the Euclidean Schwarzschild BH we found a period $t_E \sim t_E + 4\pi r_s$ with $r_s = 2G_{\mathsf{N}}M$, it has $R = 0$ due to the Einstein equations. Hence, the boundary term at $r = r_0$ reduces to

$$\int_{\partial\mathcal{M}} \sqrt{\gamma} K = \beta(8\pi r_0 - 6\pi r_s) \tag{3.15}$$

Clearly, this diverges for $r_0 \to \infty$, and we are therefore required to add a counterterm

$$\mathsf{CT} = \frac{1}{8\pi G_{\mathsf{N}}} \int_{\partial\mathcal{M}} \sqrt{\gamma} K_0 \tag{3.16}$$

with K_0 the extrinsic curvature of $\partial\mathcal{M}$ embedded in flat spacetime, resulting in

$$\int_{\partial\mathcal{M}} \sqrt{\gamma} K_0 = \beta[8\pi r_0 - 4\pi r_s + \mathcal{O}(r_0^{-1})] \tag{3.17}$$

This could also be obtained by setting $r_s = 0$ in K, but this is not true in general.
Putting the pieces together (3.15, 3.17) we end up with

$$I_G[g] = \frac{\beta r_s}{4G_{\mathsf{N}}} = \frac{\beta^2}{16\pi G_{\mathsf{N}}} \tag{3.18}$$

such that the partition function becomes (3.12)

$$\mathcal{Z}(\beta) = e^{-\frac{\beta^2}{16\pi G_{\mathsf{N}}}} \tag{3.19}$$

[2] eom stands for equation(s) of motion.

and ultimately

$$S = (1 - \beta\partial_\beta) \ln \mathcal{Z}(\beta) = \frac{4\pi r_s^2}{4G_\mathsf{N}} \tag{3.20a}$$

$$E = -\partial_\beta \ln \mathcal{Z}(\beta) = M \tag{3.20b}$$

The first expression contains the area of the horizon such that we finally acquire the **Bekenstein–Hawking (BH) entropy** [2, 4]

$$S_\mathsf{BH} = \frac{A}{4G_\mathsf{N}} \tag{3.21}$$

As a matter of fact, we subtracted the flat piece from the Schwarzschild action $I_G[g_S] = I_G[g_\mathsf{flat}] + \frac{\beta^2}{16\pi G_\mathsf{N}}$. By doing so, we removed the contribution stemming from thermally exciting the gravitons far away from the BH. Additionally, the flat piece $I_G[g_\mathsf{flat}]$ is on itself another saddle point associated to a gas of radiation in flat space. Since a BH in asymptotically flat space evaporates, the latter dominates our ensemble. We are solely interested in the contribution from the BH itself; accordingly, we removed these two pieces and looked at the subleading contribution with respect to the flat solution [13, 78].

One can choose to include a scalar field with saddle point $\phi = 0$. Calculation of the one-loop determinant conspires together with a similar contribution from the gravitons to a renormalisation of the coupling constant G_N whilst preserving the form of the BH entropy. A rather remarkable result [81, 82].

It has been argued that this is the maximum entropy a certain spatial region can have, and is therefore called the **Bekenstein bound** [83]. [3]

Rewriting the entropy as $S = 4\pi G_\mathsf{N} M^2$ such that $dS = 8\pi G_\mathsf{N} M dM$ with $r_s = 2G_\mathsf{N} M$, Hawking temperature (3.9), and $dE = dM$ leads to the **first law** of thermodynamics

$$TdS = dE \tag{3.22}$$

This can be further rewritten making use of the Hawking temperature (3.9) in terms of the surface gravity $\kappa = \frac{1}{2r_s}$ [1, 44]

$$\frac{\kappa}{8\pi G_\mathsf{N}} dA = dM - \Omega dJ - V dQ \tag{3.23}$$

in which we added a rotational velocity Ω, angular momentum J, electric potential V, and electric charge Q.

This surface gravity is related to the force on a massless string as observed from infinity: the product of an infinite acceleration near the horizon and a redshift factor going to zero. It is constant everywhere on the surface of the horizon for a stationary BH, equivalent to the **zeroth law** [36].

The above equation governs the response of the area when one of the BH properties is changed according to the **no-hair theorem**; this states that a BH is uniquely defined by $(M,\ J,\ Q)$. It was shown that the area always increases, through the BH formula this mimics the **second law** [4, 84]. When including quantum fields outside the BH, it was proven that the entropy of the BH increases more than the exterior entropy decreases – the **generalised second law** [48, 85].

Finally, the **third law** simply states that $T_H \geq 0$, or the surface gravity cannot be reduced to 0 in a finite amount of operations.

[3] This was later reformulated to the Bousso bound and the equivalent with the generalised entropy.

3.II The Information Puzzle

3.II.a Central Dogma and the Page Curve

It was proposed by J. Bekenstein [2, 4] that we should interpret the BH entropy as a statistical entropy counting microstates. This also gained support from calculations within the framework of string theory, e.g. [86]. With this assumption, the interpretation of the BH as a lump of burning coal comes full circle. Much like how molecular biology has a **Central Dogma**, there was also one proposed for BHs: from the outside, a BH can be described as a unitarily evolving quantum system with the amount of dof set by the BH entropy [44]. Therefore, the Hilbert space has a finite dimension. The 'quantum system' in question comprises the BH itself and an area around it of a few Schwarzschild radii.

By evolving a certain state backwards in time, we should be able to find the initial state. However, taking the no-hair theorem into account, the BH destroys most of this information; hence, a macrostate is the result of different initial states. So the BH entropy indeed naturally counts microstates. But this assumption is not sufficient to avoid information destruction for evaporating BHs (EBHs).

In classical physics and QM, the time evolution of a system is governed by a Hamiltonian which can be reversed to evolve backwards in time. Moreover, it is a unitary process. This principle to preserve information holds only in isolated systems and even works when taking the adjoining system into account when doing a measurement in the QM framework. However, Hawking showed that the outgoing radiation is completely independent of the initial state of the photons: a pure state gets radiated into a mixed state. So from semiclassical QG one would obtain information loss. Nevertheless, if one believes in holography, then the process of BH evaporation is dual to some time evolution of the CFT which is necessarily unitary. We arrive at a contradiction.

If we start with a pure, collapsing state which eventually radiates; then initially due to the entanglement between the ingoing and outgoing quanta, the radiation entropy $S_{\mathcal{R}}$ rises. Meanwhile, the area shrinks and so does the BH entropy. Since the BH is a coarse-grained entropy, the fine-grained entropy cannot become larger than the latter. Ergo, if the BH and radiation were initially in a pure state: $S_{\mathcal{R}} = S_{\mathcal{BH}} \leq S_{\text{BH}}$. The entropy of radiation logically cannot increase to arbitrarily large values. D. Page suggested that after some point – the **Page time** when the two become equal – the entropy of the radiation should decrease, even when taking backreaction into account. If BH evaporation really is unitary, it is believed that the radiation entropy should follow this **Page Curve** [11, 12]. This evolution is depicted in Fig. 3.4.

Alternatively, one can consider the entanglement as arising from between 'early' radiation – the quanta which already escaped to spatial infinity $S_{\mathcal{R}}$ – and 'late' radiation – that which has yet to escape $S_{\mathcal{BH}}$. It naturally leads to a tensor product decomposition in $\mathcal{H}_{\mathcal{R}} \otimes \mathcal{H}_{\mathcal{BH}}$ [13].

Moreover, the paradox holds to all orders in perturbation theory, so any resolution would likely come from a nonperturbative effect.

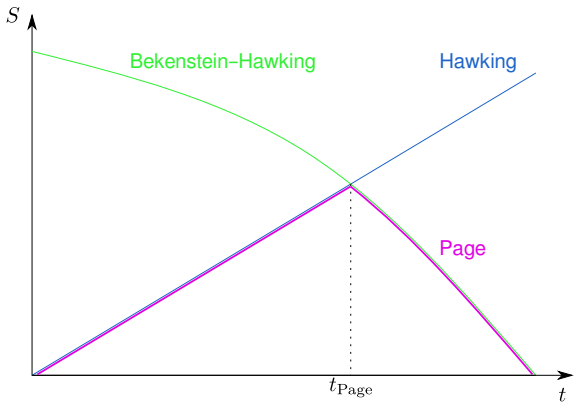

Figure 3.4: The Page curve. Initially, the entropy rises due to the increasing entanglement between Hawking quanta. After the Page time, it decreases again and follows the coarse-grained BH entropy instead. Eventually, the BH is fully evaporated and all the information is released.

3.II.b The End is neigh

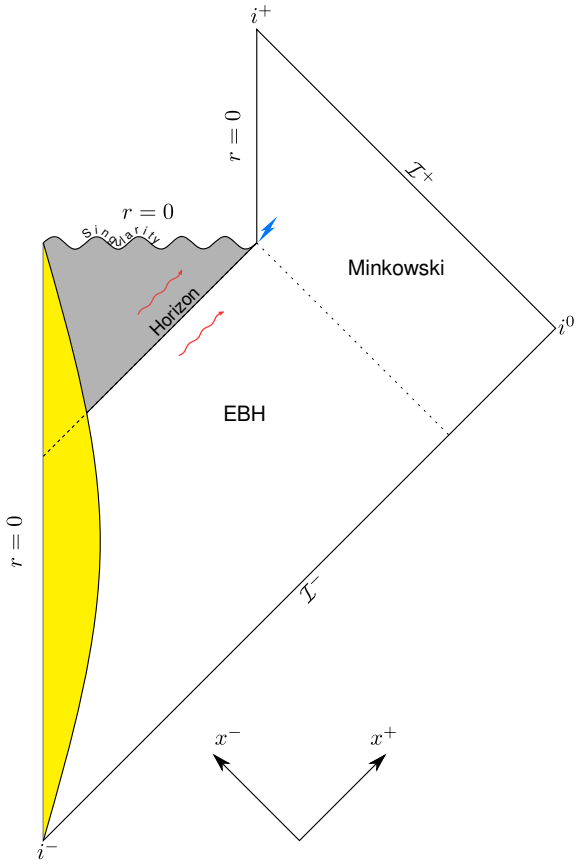

Figure 3.5: Penrose diagram for an EBH. After complete evaporation we obtain Minkowski again. The thunderbolt denotes the point when the semiclassical breakdown happens.

In order to understand what happens, let us start with a collapsing shell in a pure quantum state (the Penrose diagram is shown in Fig. 3.5). After collapse, the BH starts to evaporate and the radiation becomes more and more mixed as more Hawking quanta are escaping into the exterior – its entropy is rising. Meanwhile, the BH is shrinking which we can track up until the point the BH becomes of Planckian size. We do not know exactly what happens beyond this point without a full theory of QG but we can make some suggestions [13] (see Fig. 3.6).

- **Remnants**: evaporation stops, we are left with a remnant. It stores a high amount of entropy if the initial collapsing shell was a pure quantum state and the evaporation process is unitary. This large value would exceed the BH entropy; therefore, counting microstates is not reconcilable with this scenario [26–29];
- **Information Loss**: complete evaporation leaves us with a mixed state of the radiation field consisting of photons and gravitons. Energy conservation prevents a final burst/'thunderbolt' from completely purifying the radiation, and we are left with an entropy of the order of the initial BH entropy. This is a non-unitary process, so we have information loss;
- **No Information Loss**: the radiation is not in a mixed state, but the information is carried by the correlations between the interior and exterior quanta – a pure final state of the radiation field is achieved. However, we see a mixed state because we only have access to the exterior modes.

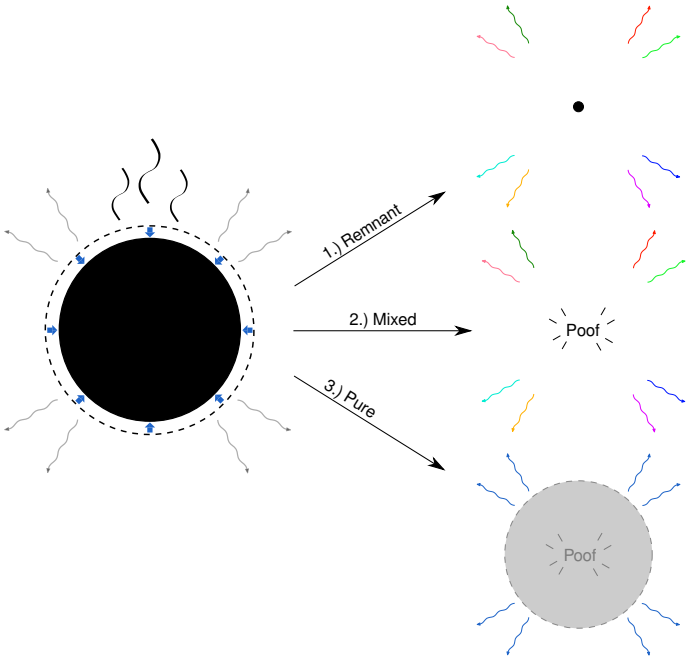

Figure 3.6: The end of an EBH. The three possible scenarios are illustrated as in the text respectively. The different colours for the radiation on the right denotes a mixed state, the same colour represents a pure state. In principle, we can reconstruct the BH in the third scenario (denoted by its transparency).

As a side note, by using the Stefan–Boltzmann law we can estimate how long it takes for a BH to evaporate [13]. More exact calculations incorporate greybody factors and the mode expansion for a free scalar in the Schwarzschild geometry [87].

The Stefan–Boltzmann law tells us the following

$$\frac{\mathrm{d}E}{\mathrm{d}t} = -\sigma_{\mathrm{SB}} T^4 A \tag{3.24}$$

Combining this expression with Eqs. (3.20a, 3.20b) for a Schwarzschild BH $r_s = 2G_{\mathrm{N}}M$ leads to

$$\frac{\mathrm{d}M}{\mathrm{d}t} \propto -\frac{1}{(G_{\mathrm{N}}M)^2} \tag{3.25}$$

Therefore, the evaporation rate for a BH initially at mass M is approximately

$$t_{\mathrm{evap}} \approx G_{\mathrm{N}}^2 M^3 \tag{3.26}$$

For a BH with a mass equal to one solar mass this would be about 10^{66} years. To put this in perspective, the age of our Universe is 'only' $13.8 \cdot 10^{10}$ years. Unfortunately, astrophysical BHs are not feasible to use in experiments related to the information paradox. We require BHs of a much lower mass; consequently, a lower temperature.

3.II.c How to get rid of Diaries

What if instead information comes out before the breakdown? And if the information is preserved in its radiation, how can it be transferred from the inside to the outside? To address these questions we consider a Gedankenexperiment.

Let us say the main protagonist of our Socratic dialogues has a diary he would not want anyone to read. Needless to say, Mai is curious about what exactly is in Sakuta's diary and would like to take a peek. To prevent this from happening, Sakuta travels to Sagittarius A* and throws it into the BH. Meanwhile, the BH is slowly radiating and Mai wonders if she can catch this radiation to reconstruct the diary. Is this scenario feasible?

Obviously, if BHs destroy information she will never be able to discover the contents of the diary. If information does slowly leak out, then how does this happen? The following two scenarios would be nonsensical [35]

- **FTL Communication**: the diary eventually plunges into the singularity. Right at that moment, its contents are instantaneously transferred to the outgoing radiation. This seems unreasonable; for something to escape a BH it should be travelling at a speed greater than the speed of light. So, this would require faster-than-light (FTL) communication/dynamical nonlocality. This is in contradiction with ordinary QFT, or perhaps it should be revised;

- **Quantum Xeroxing/Bleaching**: as the diary is falling towards the singularity, it is copied onto the outgoing radiation. Unfortunately, this violates the **no-cloning theorem**: having a copy of the same quantum state $|\Psi\rangle \to |\Psi\rangle \otimes |\Psi\rangle$ violates the superposition principle

$$\begin{aligned} |\Psi\rangle + |\Psi\rangle &\to |\Psi\rangle \otimes |\Psi\rangle + |\Phi\rangle \otimes |\Phi\rangle \\ &\neq (|\Psi\rangle + |\Phi\rangle) \otimes (|\Psi\rangle + |\Phi\rangle) \end{aligned} \tag{3.27}$$

  The original has to be destroyed in such a process [27].

These scenarios inherently fail. However, the BH entropy formula tells us that the entropy of a BH is given by its surface area. In other words, the information of everything inside the BH – including the diary – can be re-interpreted as being encoded into a lower-dimensional hologram on its horizon. From this perspective, the first scenario is already solved; the information was on the horizon all along and no FTL communication is needed to transfer it to the radiation. This is basically the essence of the **Holographic Principle** [6–9] built on the observation in [88].

Wait, does this mean we have two diaries – one on the horizon and one in the interior? This seems to violate the no-cloning principle. To prevent this, the authors of [89] argued that we should take the causality of the observer into account – **BH Complementarity**. No single observer can see both copies simultaneously. QM should only describe what individual observers, restricted by causality, would see. Heuristically, an observer would never see an infalling diary crossing the horizon; the diary would become dimmer and stationary as it approaches the horizon when seen from outside a BH. But the diary itself would just fall through the horizon without anything special happening. This idea of not seeing/measuring both copies is reminiscent of the Heisenberg uncertainty principle, both are different ways of describing the same scenario.

Although this seems like a plausible idea, is it possible for Mai to collect the radiation and then jump into the BH, effectively obtaining two copies of the diary? The idea of BH complementarity was later refined to the **Hayden–Preskill Protocol**; information only comes out after the **scrambling time** t_{scr} [90, 91]

$$t_{\text{scr}} = \frac{\beta}{2\pi} \ln(S - S_0) \tag{3.28}$$

In addition, this is also the time it takes for the diary to reach the singularity after horizon crossing.

In conclusion, Mai is able to decode the contents of the diary but never has two copies at once. The diary will already have ended its life at the singularity before she can even reach it.

3.II.d AMPS Paradox

If we go back to the Minkowski vacuum and look at the left and right Rindler wedges, the entanglement between these two is essential to have a smooth crossing (recall Fig. 2.5). If there were no entanglement between the two wedges, fluctuations near the boundary are of the order $\mathcal{O}(\varepsilon^{-2})$ with ε a UV regulator. Without entanglement we would have an immense energy density sitting right at the horizon – a **firewall**. This would also be the result if Hawking radiation was truly localised around the event horizon but stemming from a different origin [13]. Being entangled is not sufficient, but is necessary to obtain a smooth infalling experience.

The argument set out in [34] commonly known as the **AMPS paradox** [4] goes as follows; to have a smooth horizon after the Page time there needs to be maximum entanglement between the interior modes and the outgoing modes close to the horizon (late radiation). However, from the Page argument we saw that the early radiation needs to be maximally entangled with the late radiation to preserve unitarity. The late radiation appears to be both maximally entangled with the early radiation and the interior modes – a clear violation of the monogamy of EE!

It seems that reconciliation of unitarity and a smooth horizon is impossible. Preserving unitarity requires giving up on a smooth horizon, resulting in a firewall. Vice versa, a smooth horizon inevitably destroys unitarity. The authors recast this argument to the following three statements to not be true at the same time

1. The horizon is nothing unusual;
2. Hawking radiation is in a pure state;
3. The information is emitted from a region near the horizon (holographic principle).

Rephrased in [32, 33], any endeavour to describe the interior and exterior as a single QM system results in a violation of one of the three following principles

1. **Equivalence Principle**: freely falling observers experience nothing special at the horizon;
2. **Unitarity**: BHs evolve unitarily just like an ordinary quantum system and information is preserved;
3. **No Quantum Xeroxing**: information falling through the horizon is not copied to the radiation while still being maintained in the interior – there is no duplication.

If standard quantum rules are indeed not sufficient to describe the geometry from a global picture with horizons, we need something entirely different.

[4] After its authors Almheiri–Marolf–Polchinski–Sully.

3.II.e Possible Resolutions

Finally, we give a handful of possible resolutions physicists have come up with throughout the decades [13]

- **Firewall**: discard the entanglement between the outgoing modes and the modes behind the horizon, leading to a huge energy density near the horizon;
- **Superselection Sectors**: A. Ströminger argued that the paradox can be resolved by making use of superselection sectors. He compared this with doing quantum electrodynamics experiments without knowing the value for α. We would not be able to predict the out-state of a single experiment; but if we have access to this value, this information is not lost. So the information paradox stems from ignorance about the coupling constants of which there are many – of the order $e^{4\pi M^2}$ [27];
- **ER = EPR**: basically, an ER-bridge[5] is created [92] between two BHs through EPR-like correlations [93] and can possibly resolve the paradox [94]. The main idea is that through acting on the radiation, we can create a thermofield double state with a smooth horizon resulting in a BH interior looking like an ER-bridge constructed from these dof. More generally, 'entanglement generates geometry' or 'It from Qubit' [35, 95, 96];
- **Fuzzballs**: such solutions look like ordinary BHs from afar, but near the horizon we enter the domain of higher dimensions. The interior is akin to a ball of strings [97];
- **Shut Up and Calculate in the UV**: this quote, without the UV part, is attributed to David Mermin and is often used to mock physicists who blindly follow the Copenhagen interpretation and ridicule those who pursue research in the foundations of QM [35]. However, its context is different here: we already have models of QG, string theory for instance, so we can calculate exactly what happens there and accept its outcome. Nevertheless, we do not understand the depths of those theories well enough to make the final decision whether to believe its predictions or not.

[5] After the authors Einstein–Rosen.

Chapter 4

Holographic Entanglement Entropy

One of the most basic building blocks of the developments of the past 15 years is the Ryu–Takayanagi formula. It computes the EE of a CFT from the dual bulk perspective through the area of the minimal surface. This way, the formula is very reminiscent of the Bekenstein–Hawking formula where the minimal surface is the BH horizon itself. Even so, it also works in more general bulk spacetimes without a BH and can be seen as a generalisation of this principle. Besides, it gives a realisation of the 'entanglement builds geometry' view.

Since this formula stirred the recent developments up until the island formula and beyond, much emphasis will be placed upon the understanding of this expression. After the Ryu–Takayanagi formula itself, we start to navigate towards the entanglement island by succinctly describing the developments and thought patterns which ultimately led to this concept. At the end, we extract the Page curve and try to resolve the information paradox from this novel perspective.

4.I Back to the Roots: the Ryu–Takayanagi Formula

We start by turning our attention towards the celebrated Ryu–Takayanagi formula in its full glory. First conjectured in [39], it is a formula which computes the entropy of region $\mathcal{A}$ in a CFT – with holographic dual – across the entangling surface $\partial\mathcal{A}$ via a minimal surface $\gamma_{\mathcal{A}}$ which begins at the conformal boundary and extends into the bulk (as illustrated in Fig. 4.1). Since the entropy is just given by the area, the problem reduces to the minimisation of a classical area functional; a pure geometrical problem. It is believed this statement is more profound than just a computational contraption to easily calculate EEs. It has been suggested this relation lies at the heart of the idea that the bulk spacetime emerges from entanglement [96, 98, 99].

Ryu–Takayanagi (RT) Formula: consider a foliation of the static bulk spacetime $\mathcal{M} = \prod_t \mathcal{N}_t \times R_t$ with conformal boundary $\partial\mathcal{M} = \prod_t \partial\mathcal{N}_t \times R_t$ and divide the leaf in a bipartite way $\partial\mathcal{N}_t = \mathcal{A} \cup \mathcal{B}$. The holographic EE (HEE) across this entangling surface $\partial\mathcal{A}$ is given by

$$S(\mathcal{A}) = \min_{\gamma_{\mathcal{A}}} \frac{A(\gamma_{\mathcal{A}})}{4G_N} \tag{4.1}$$

where $\gamma_{\mathcal{A}}$ is the codimension-2 **minimal surface** in the bulk satisfying the following constraints

- It ends on $\partial\mathcal{A}$: $\partial\gamma_{\mathcal{A}} = \gamma_{\mathcal{A}}\big|_{\partial\mathcal{M}} = \partial\mathcal{A}$;
- It is homologous to $\mathcal{A}$: $\exists\mathcal{R} \subset \mathcal{M} : \partial\mathcal{R} = \gamma_{\mathcal{A}} \cup \mathcal{A}$ with $\mathcal{R}$ a smooth, interpolating codimension-1 surface (homology constraint).

If there is more than one minimal surface with these constraints possible, we pick the one with the smallest area.

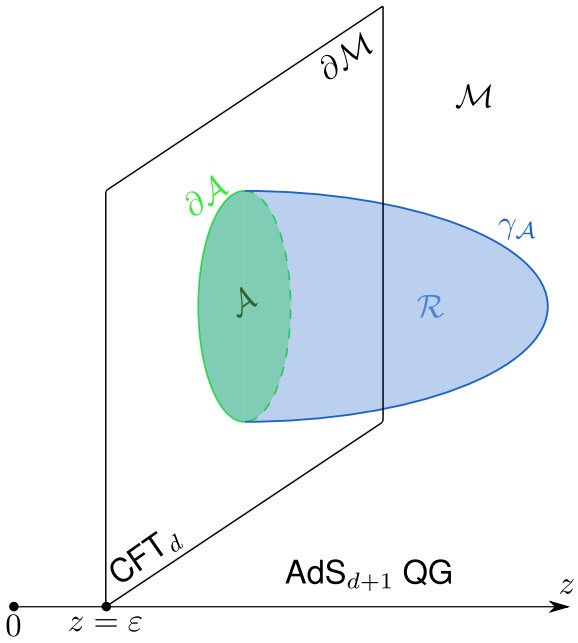

Figure 4.1: The RT formula. The HEE of the subregion $\mathcal{A}$ on the boundary CFT can be computed through the area of the minimal surface $\gamma_{\mathcal{A}}$ extending into the bulk.

This statement has similarities to how one would define the BH entropy by computing the area of the bifurcate horizon found as, e.g. the locus of the fixed points of a Killing vector [42]. Basically, it comes down to treating the density matrix $\rho_{\mathcal{A}}$ as being described by a BH with horizon $\gamma_{\mathcal{A}}$. Nevertheless, the bulk spacetime does not need to have a BH with a Killing horizon, so this statement is much more general. The minimal surface $\gamma_{\mathcal{A}}$ can be seen as a holographic screen obscuring the region an observer has no access to – a manifestation of the holographic principle and a clear analogy with the EE from a reduced density matrix.

Since the area is computed in a spacetime obeying the Einstein–Hilbert action, corrections can be taken into account by adding higher derivative terms contributing to the area functional [100, 101].

The formula we discussed above holds for static spacetimes in which there is a natural time coordinate; due to symmetry reasons, the minimal surface lies in a fixed time slice [36, 42]. One can relax this condition to allow dynamical spacetimes leading to the **Hubeny–Rangamani–Takayanagi (HRT) formula**: instead of finding a minimal surface, we look for an **extremal surface** $\mathcal{W}_{\mathcal{A}}$ obeying the same constraints as the minimal surface but extremise the area functional instead – much like how geodesics extremise the length of curve [102]. This is the HEE associated to a region $\mathcal{A}$ lying on a Cauchy slice $\Sigma = \mathcal{A} \cup \mathcal{B} \subset \partial\mathcal{M}$. Besides, a Cauchy surface in the bulk is not uniquely defined by a Cauchy slice on the conformal boundary. One is free to pick any bulk Cauchy surface as long as each point remains spacelike separated from the boundary Cauchy slice; the region defined by this procedure is the **FRW wedge** encompassing the extremal surface [39, 103].

The area law divergence in Ch. 2 stems from the diverging metric near the boundary. To regulate it, we need to put a cutoff on the radial coordinate $z = \varepsilon$. The metric of the minimal surface inherits this divergence, and thus has its largest contribution at the cutoff itself. Its bulk extension tends to end perpendicular to the boundary to get as quickly away as possible from this diverging piece, resulting in the area law divergence.

Another construction was given by the authors of [104] – the **maximin construction**: one first minimises the area on a complete achronal slice Σ and then maximises this area with

respect to Σ. It turns out this is equivalent to the HRT construction for spacetimes obeying the null curvature condition.

The RT/HRT formula gives the leading order contribution to the EE $\mathcal{O}(G_{\mathsf{N}}^{-1})$, quantum corrections can be taken into account by adding the EE contribution of the bulk quantum fields. We will discuss this in Sect. 4.II.

This framework turns out to be very robust: it satisfies many of the nontrivial EE inequalities back in Chapter 2 [105–107] and is consistent with EE calculations carried out via the replica trick [79, 108, 109], dubbed the **Lewkowycz–Maldacena (LM) formalism**. For a more topological approach, see [110].

4.I.a Homology is not Homotopy

There is often some confusion on the homology constraint: it is generally true that homotopy implies homology but not the converse. For this purpose, we juxtapose two possible minimal surfaces to elucidate this difference: we consider the HEE of a thermal state in CFT_2 on S^1 [39, 46, 111].

The dual bulk geometry is the Bañados–Teitelboim–Zanelli (BTZ) BH ($l_{\mathsf{AdS}} = 1$)

$$ds^2 = -(r^2 - r_+^2)dt^2 + \frac{dr^2}{r^2 - r_+^2} + r^2 d\varphi^2 \tag{4.2}$$

with region of interest $\mathcal{A} = \{(t, \varphi) | t = 0, \varphi \in (-\varphi_0, \varphi_0)\}$. Computing the minimal surface yields two possible solutions both satisfying the homology constraint: a spacelike geodesic anchored at the boundary points $\gamma_{\mathcal{A}}$, and the union of the spacelike geodesic associated to the complement of $\mathcal{A}$ and the BH horizon $\gamma_{\mathcal{A}^c} \cup \mathsf{S}_{\mathsf{BH}}$. These two solutions are shown in Fig. 4.2

$$S(\mathcal{A}) = \frac{c}{3} \ln \left[\frac{\beta}{\pi\varepsilon} \sinh\left(\frac{R}{\beta} \varphi_0 \right) \right], \qquad \varphi_0 < \varphi^*$$

$$S(\gamma_{\mathcal{A}^c} \cup \mathsf{S}_{\mathsf{BH}}) = \frac{c}{\pi} \pi r_+ + \frac{c}{3} \ln \left[\frac{\beta}{\pi\varepsilon} \sinh\left(\frac{R}{\beta} (\pi - \varphi_0) \right) \right], \qquad \varphi_0 \geq \varphi^*$$

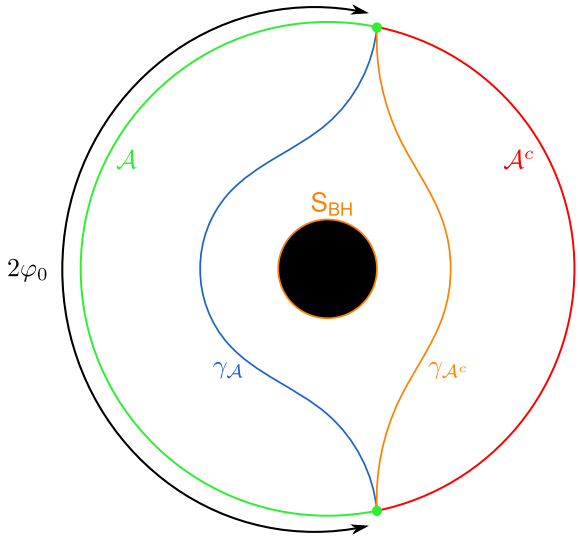

Figure 4.2: The RT construction for the BTZ BH. We show the compactified BTZ BH geometry with the two minimal surfaces as discussed in the text. The second minimal surface consists of the geodesic associated to the complement of $\mathcal{A}$ and the BH horizon.

The RT formula requires us to take the minimum of the two, there is hence a turning point at φ^*. Notice how the second minimal surface is a good example of a disconnected one.

Regarding the homology constraint, the first minimal surface $\gamma_{\mathcal{A}}$ is clearly homotopic to $\mathcal{A}$ because it can be smoothly contracted to this boundary region. However, this is not true for the second geodesic $\gamma_{\mathcal{A}^c}$ because the BH acts as a 'defect' hindering the homology of this geodesic. To satisfy the homology constraint, we need to add the BH horizon S_{BH} such that there indeed exists an interpolating region $\mathcal{R}$ with the desired properties.

Furthermore, when the boundary region exceeds a critical value related to the fraction the boundary region $\mathcal{A}$ encompasses with respect to the total conformal boundary $\mathrm{Vol}(\mathcal{A})/\mathrm{Vol}(\mathsf{S}^1)$, the entropy saturates the Araki–Lieb inequality (2.30)

$$S(\mathcal{A}) = S(\mathcal{A}^c) + S(\mathsf{S}_{\mathsf{BH}}) \tag{4.4}$$

which the authors called the **entanglement plateau** [111].

To end this discussion, we further emphasise that the orientation of our boundary region also plays an important role in the search for a minimal surface [42]. For example, take the case of two disconnected intervals with associated orientation from left to right. The orientation of the minimal surface gets inherited by the boundary region itself and must be consistent with each other; each geodesic must begin on the left endpoint of an interval and end on the right endpoint of an interval. On these grounds, the configuration where two geodesics intersect each other is excluded as a possible minimal surface candidate (see Fig. 4.3). Also note that the point of intersection would have two orientations assigned to it.

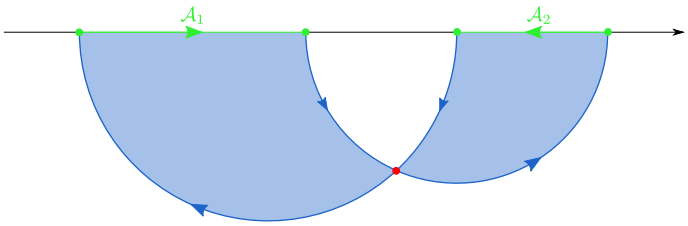

Figure 4.3: The importance of orientation in making use of the RT formula. Here we show how the two intervals inherit the orientation from the bulk minimal surface leading to a contradiction. Moreover, the intersection would have two orientations associated to it.

4.I.b An Example: Vacuum State of CFT$_2$ on $\mathbb{R}^{1,1}$

As an example of the RT formula 4.1, we calculate the entropy associated to the vacuum state of a CFT$_2$ on $\mathbb{R}^{1,1}$ dual to a Poincaré-AdS$_3$ spacetime [39].

The RT/HRT formula requires us to find a minimal/extremal surface of the area functional. To find this saddle point, we start from the bulk metric $g_{\mu\nu}(x)$ and parametrise our surface by intrinsic parameters ξ^i. Next, we embed them in our bulk through $X^{\mathcal{A}}(\xi^i)$. From this embedding we can find the induced metric h_{ij} as the pullback of our bulk metric to the surface

$$ds^2_{\mathcal{W}_{\mathcal{A}}} = h_{ij} d\xi^i d\xi^j = \frac{\partial x^\mu}{\partial \xi^i} \frac{\partial x^\nu}{\partial \xi^j} g_{\mu\nu} \tag{4.5}$$

This geometrical problem then turns into a variational problem of the action

$$S = \frac{l_{\mathsf{AdS}}^{d-2}}{4G_N^{(d)}} \int d^{d-2}\xi \sqrt{\det h_{ij}} \tag{4.6}$$

under the BC $\mathcal{W}_\mathcal{A}\big|_{z\to 0} = \partial\mathcal{A}$.

We want to calculate the EE associated to the region $\mathcal{A} = \{x \in [-a, a]\}$, an interval of length $2a$ on a constant time slice centred around the origin. The dual geometry is that of Poincaré-AdS$_3$ spacetime ($d = 3$)

$$ds^2 = \frac{l_{\text{AdS}}^2}{z^2}\left(dz^2 + dx^2 - dt^2\right) \tag{4.7}$$

where we introduce an UV regulator by cutting the spacetime off at $z = \varepsilon$ near the boundary.

For the static case $dt^2 = 0$, we parametrise our surface according to $(x(\xi), z(\xi))$ resulting in the induced metric (4.5)

$$ds^2_{\gamma_\mathcal{A}} = \frac{l_{\text{AdS}}^2}{z^2}\left(x'(\xi)^2 + z'(\xi)^2\right)d\xi^2 \tag{4.8}$$

with the determinant just being the prefactor. Plugging this into the area functional (4.6) brings about

$$A = l_{\text{AdS}}\int d\xi \frac{\sqrt{x'(\xi)^2 + z'(\xi)^2}}{z} \tag{4.9}$$

To obtain the eom we can vary to the coordinates $x(\xi)$ and $z(\xi)$ separately or use the Euler–Lagrange equations

$$\partial_\xi \frac{x'}{z\sqrt{x'^2 + z'^2}} = 0 \tag{4.10a}$$

$$\partial_\xi \frac{z'}{z\sqrt{x'^2 + z'^2}} + \frac{\sqrt{x'^2 + z'^2}}{z^2} = 0 \tag{4.10b}$$

The solution is the parametrisation of a semicircle

$$x(\xi) = a\cos\xi, \qquad z(\xi) = a\sin\xi \tag{4.11}$$

with the additional constraint $\frac{\varepsilon}{a} \le \xi \le \pi - \frac{\varepsilon}{a}$ after implementing the BC $\lim_{z\to\varepsilon} x = \pm a$. An illustration is given in Fig. 4.4.

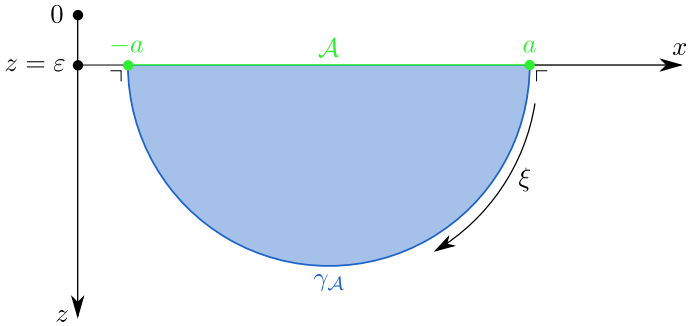

Figure 4.4: The semicircle. We show the associated minimal surface to our setup. Notice how it ends perpendicular on the boundary region as expected.

To find the area, a length in our setup, we plug this back into (4.9) and evaluate it on-shell

$$\begin{aligned} A &= l_{\text{AdS}}\int_{\xi_1}^{\xi_2}\frac{d\xi}{\sin\xi} = l_{\text{AdS}}\left[-\ln\cot\left(\frac{\xi}{2}\right)\right]_{\xi_1}^{\xi_2} \\ &= 2l_{\text{AdS}}\ln\left(\frac{2a}{\varepsilon}\right) \end{aligned} \tag{4.12}$$

in which we approximated for small ε. Finally, we can use the Brown–Henneaux central charge [112]

$$c = \frac{3l_{\text{AdS}}}{2G_{\text{N}}} \tag{4.13}$$

to find the HEE

$$S = \frac{A}{4G_{\text{N}}} = \frac{c}{3}\ln\frac{2a}{\varepsilon} \tag{4.14}$$

In perfect agreement with our calculations in 2.II.a.

4.II Navigating towards the Island

4.II.a The Quantum Extremal Surface

Like previously mentioned, the RT/HRT formulas are the leading order contributions to the HEE of order $\mathcal{O}(G_{\text{N}}^{-1})$. To add one-loop quantum corrections, we need to take the contribution of the bulk fields into account. Luckily, there is a natural bipartition of the bulk due to the RT/HRT construction: we namely have the interpolating region $\mathcal{R}$ and its complement $\mathcal{R}^c$. From this viewpoint, we can see the extremal surface $\mathcal{W}_{\mathcal{A}}$ as a natural entangling surface across which we can compute the entropy of the bulk quantum fields. This bulk entropy can be computed semiclassically by considering the quantum fields to form an effective field theory living on a fixed background geometry.

This approach was first described in [113] and is called the **FLM formalism** after its authors Faulkner–Lewkowycz–Maldacena

$$S(\mathcal{A}) = S_{\text{HRT}}(\mathcal{A}) + S_{\text{QM}}(\mathcal{A}) + \mathcal{O}(G_{\text{N}}) \tag{4.15a}$$
$$S_{\text{QM}}(\mathcal{A}) = S_{\text{bulk}}(\mathcal{R}) + \dots \tag{4.15b}$$

where the ellipsis represent additional terms to cancel UV divergences. Another approach was discussed in [114].

We can also consider both the LM and FLM formalisms through the GPI [79, 113] consisting of the gravitational action and the action of the quantum fields. In the semiclassical theory, we take the gravitational action to be on-shell such that

$$\mathcal{Z}(\beta) = e^{-I_{\text{G}}}\mathcal{Z}_{\text{QM}} \tag{4.16}$$

In the LM formalism, we only take the leading order contribution of the Euclidean action into account and ignore the quantum fields

$$\ln\mathcal{Z}(\beta) = -I_{\text{G,E}} \tag{4.17a}$$
$$S(\mathcal{A}) = (1-\beta\partial_\beta)\ln\mathcal{Z} \tag{4.17b}$$

making use of the replica trick for n copies we obtain

$$S(\mathcal{A}) = -\lim_{n\to1}\frac{\mathrm{d}}{\mathrm{d}n}[\ln\mathcal{Z}_n(\beta) - n\ln\mathcal{Z}(\beta)] = S_{\text{HRT}}(\mathcal{A}) \tag{4.18}$$

The FLM formalism is obtained by adding the QM partition function into the mix

$$S_{\text{QM}} = -\lim_{n\to1}\frac{\mathrm{d}}{\mathrm{d}n}[\ln\mathcal{Z}_{\text{QM},n} - n\ln\mathcal{Z}_{\text{QM},1}] \tag{4.19}$$

To account for even higher order quantum corrections, the authors of [115] had the ingenious idea to include the bulk entropy in the extremisation problem of the RT/HRT proposal.

Its result is a formula sensitive to quantum effects at any order of G_{N}, reproduces FLM at $\mathcal{O}(G_{\mathsf{N}}^0)$ and LM at $\mathcal{O}(G_{\mathsf{N}}^{-1})$.

Quantum Extremal Surface (QES) Formula: the HEE of a region $\mathcal{A}$ in a field theory with a holographic dual can be calculated via the **generalised entropy** at the QES $\mathcal{X}$ obeying the same constraints as the extremal surface

$$S(\mathcal{A}) = \underset{\mathcal{X}}{\mathsf{Min}}\ \underset{\mathcal{X}}{\mathsf{Ext}} \left[\frac{A(\mathcal{X})}{4G_{\mathsf{N}}} + S_{\mathsf{QM}}(\mathcal{X}) \right] \tag{4.20}$$

If there are multiple QESs, we pick the one resulting in the smallest entropy (an example is drawn in 4.5).

This formula was the one employed in [14, 15] to compute the Page curve for the first time and led them to the New Horizons Prize in Physics 2021. Subsequently, this formula can also be constructed through the maximin procedure [116] or through the GPI approach [117].

4.II.b The Entanglement Island

The QES formula computes the fine-grained entropy of the BH, but the paradox talks about the entropy of radiation. So how can this be computed? Furthermore, the BH region $\mathcal{BH}$ stretches from the boundary to the QES itself, so where exactly does the radiation go? What interval should we specify that captures it?

To specify a region capturing the radiation $\mathcal{R}$, one adds an auxiliary **heat bath** to the system, usually taken flat, in which the BH can evaporate. In most scenarios, like JT gravity, this extra spacetime is added to the boundary of the theory. For other cases, the Schwarzschild BH for instance, one can define a cutoff surface along which there exists a natural time coordinate. The region between this cutoff surface and the singularity can be used for the QES formula while the bath region is the part of spacetime between the cutoff surface and the true boundary [44].

Taking only the region collecting the radiation into account, one finds an increasing entropy à la Hawking [118]. Although the QES formula also works for a region without a BH, it is not directly clear how we can get a nonincreasing entropy. To resolve this, we should account for the possibility of disconnected QESs which add extra boundaries but whose semiclassical entropy should counter this. A QES being disconnected should not be that surprising as one can think of the two regions being entangled with each other, just like how Hawking radiation is entangled with the interior modes.

This approach was first used in the setup of a doubly holographic model, one where the conformal matter has itself a holographic map [18]. In such a model we may use the RT/HRT formula for the bulk entropy as well, turning the whole problem in one geometrical problem from the double holographic viewpoint. The authors found the existence of a region disconnected from the radiation region and only making up a part of the BH interior which should be considered in the QES formula as well – the **island** $\mathcal{I}$. From the double holographic model viewpoint, this island is connected to the radiation region through the extra dimension in which the total surface is not disconnected; a manifestation of the ER $=$ EPR idea.

Quantum Extremal Islands: the HEE of the radiation region $\mathcal{R}$, **mainland**, in a field theory with a holographic dual is governed by the **entanglement island** $\mathcal{I}$

$$S(\mathcal{R}) = \underset{\mathcal{I}}{\mathsf{Min}}\ \underset{\mathcal{I}}{\mathsf{Ext}} \left[\frac{A(\partial\mathcal{I})}{4G_{\mathsf{N}}} + S_{\mathsf{QM}}(\mathcal{R}\cup\mathcal{I}) \right] \tag{4.21}$$

The extremisation is with respect to the location and shape of this island.

The matter in this region is entangled with the matter in the radiation region $\mathcal{R}$, effectively countering the increase of entropy due to the extra boundary terms (see 4.5 again for an illustration).

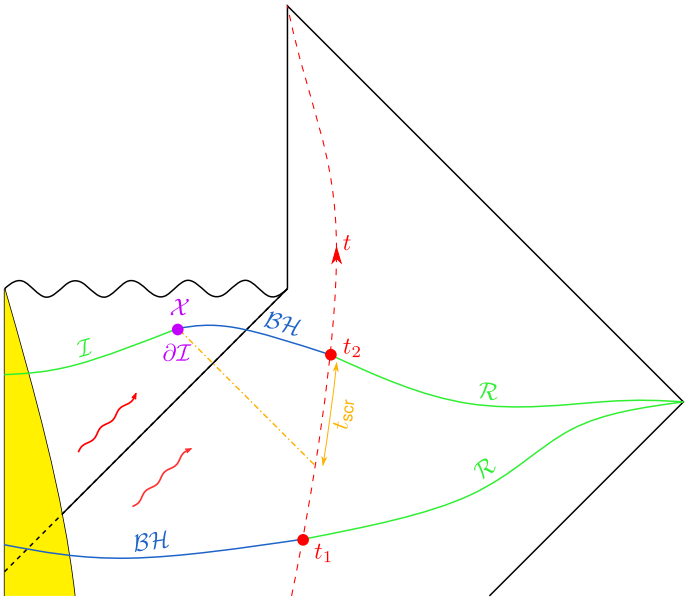

Figure 4.5: The QES and the entanglement island. The geometry is divided in two regions by introducing a surface along which a natural time coordinate flows. The radiation region lies to the right of this surface, to the left we find the BH region and the island region. Two instances of time are shown. At t_1 we have the trivial island extending all the way to the singularity. At t_2 we have a nontrivial island behind the horizon; it lies on an ingoing null ray a scrambling time t_{scr} into the past.

Some comments are in order:

- The left hand side computes the full entropy of the radiation, the radiation region appearing on the right hand side computes it in the semiclassical description;
- The trivial island $\mathcal{I} = \emptyset$ leads to the radiation entropy only $S_{\text{QM}}(\mathcal{R})$;
- If the BH was formed from an initially pure state, we expect $S(\mathcal{X}) = S(\mathcal{R})$. Additionally, if $\mathcal{I} \cup \mathcal{BH} \cup \mathcal{R}$ constitutes a full Cauchy slice of our spacetime and the matter state is pure on this Cauchy slice, then $S_{\text{QM}}(\mathcal{X}) = S_{\text{QM}}(\mathcal{R} \cup \mathcal{I})$ and $\partial\mathcal{I} = \mathcal{X}$. We can call both locations 'the island'; [1]
- The semiclassical entropy of a union of intervals is hard to calculate and there is a general expression for only a few cases, e.g. free fermions [119, 120]. Even when approximating it to $S_{\text{QM}}(\mathcal{I}) + S_{\text{QM}}(\mathcal{R})$ results in a stationary island as the time dependence comes from the radiation region $\mathcal{R}$ having an endpoint on the cutoff surface. For this purpose, many authors make explicit assumptions like the matter state being pure [20, 121] or some extremisation assumption [122] such that the calculation reduces to the QES formula;
- It implies a more general Bekenstein bound incorporating the generalised entropy instead of the leading order contribution only.

[1] Originally, the island is considered to be $\mathcal{I}$ but in literature this tends to differ. Henceforth, we call $\mathcal{I}$ the island region, its boundary is then the island $\partial\mathcal{I}$.

4.III From Island to Page Curve

How can one extract the Page curve from this new island phenomenon? The story goes along these lines [44]

1. $t < t_{\text{scr}}$: before any Hawking quanta escape the BH region into the heat bath, the island is trivial and there is no area term but purely a semiclassical term coming from the matter enclosed by the cutoff surface. This remains invariant under time evolution. If the BH were formed from a pure collapsing shell, this results in a zero entropy;

2. $t_{\text{scr}} < t < t_{\text{Page}}$: evaporation starts and quanta can escape into the heat bath building up entanglement between these escaping modes and the interior modes. The entropy starts to grow due to the increase in mixed interior modes. At this moment, a nontrivial islands starts to form near the horizon. The mixed interior modes now get captured by the island region $\mathcal{I}$ and the region of $\mathcal{BH}$ penetrating the event horizon. Since this purifies the outgoing modes, the semiclassical entropy starts to decrease while the BH horizon is shrinking such that the generalised entropy of this nontrivial island closely mimics this shrinking area. The competition has begun, the winner is currently the rising $S(t) = S_{\text{QM}}[\mathcal{R}(t)]$;

3. $t > t_{\text{Page}}$: after the Page time t_{Page}, the island has become large enough to purify most of the outgoing modes making the semiclassical entropy very small. Meanwhile, the BH has shrunk enough such that it declares a new winner: $S(t) \approx \frac{A_h(t)}{4G_{\text{N}}}$.

In short: the entropy first follows that of the trivial island and after the Page time follows the one stemming from the nontrivial island. When computing the entropy associated to the Hawking radiation, one should take the interior into account!

4.III.a The Entanglement Wedge

Since this new island rule led to the Page curve, how should we interpret the information paradox from this perspective? Do the dof describing the BH as seen from the outside also describe the interior?

If we associate a density matrix to the island formula, we know that the entropy remains robust to deformations of the island region within its causal diamond. Ergo, it seems to be more natural that the dof only describe a part of the BH interior, namely the part associated to the causal diamond of the island region – the **entanglement wedge (EW)** [44, 103, 104, 123].

To each region one can associate such an EW encoding the dof. As time progresses, how these wedges exactly look changes (as seen in Fig. 4.6). Needless to say, the EW associated to the full Cauchy slice is the full spacetime itself. As the island grows, its EW also grows along with it. Eventually at the time of evaporation, the island reaches the endpoint of the singularity and the EW becomes equal to that of the full BH interior: all Hawking quanta have become purified and the interior is described by the dof which are not a part of the central dogma.

To extract the information encoded in this region, one makes use of the **EW Reconstruction Hypothesis**: we can read off the state of the qubits encompassed by the EW by performing operations on the BH or radiation dof [15]. The required operation to consider for this procedure is the Petz map [124, 125]. In a certain way, these islands act as barrier up to which we can construct the bulk spacetime via probing the boundary region [115]. These ideas are closely related to quantum error correction [126, 127].

Moreover, this solves the issue of the so-called 'Wheeler's Bags of Gold' [128].

From the perspective above, the AMPS paradox is resolved exactly by this EW not describing the full BH interior leading to a possible quantum state and a smooth horizon: a part of the

interior is identified with the early radiation now entangled with the late radiation [44]. There are only two states being maximally entangled – the one associated to $\mathcal{BH}$ and the one associated to $\mathcal{R} \cup \mathcal{I}$.

It naturally encodes the Hayden–Preskill protocol of Sect. 3.II.c. Everything in the EW of the island region is entangled with the early radiation and can be decoded by capturing this radiation. But this island only exists after a scrambling time; consequently, information only starts to come out after the same scrambling time.

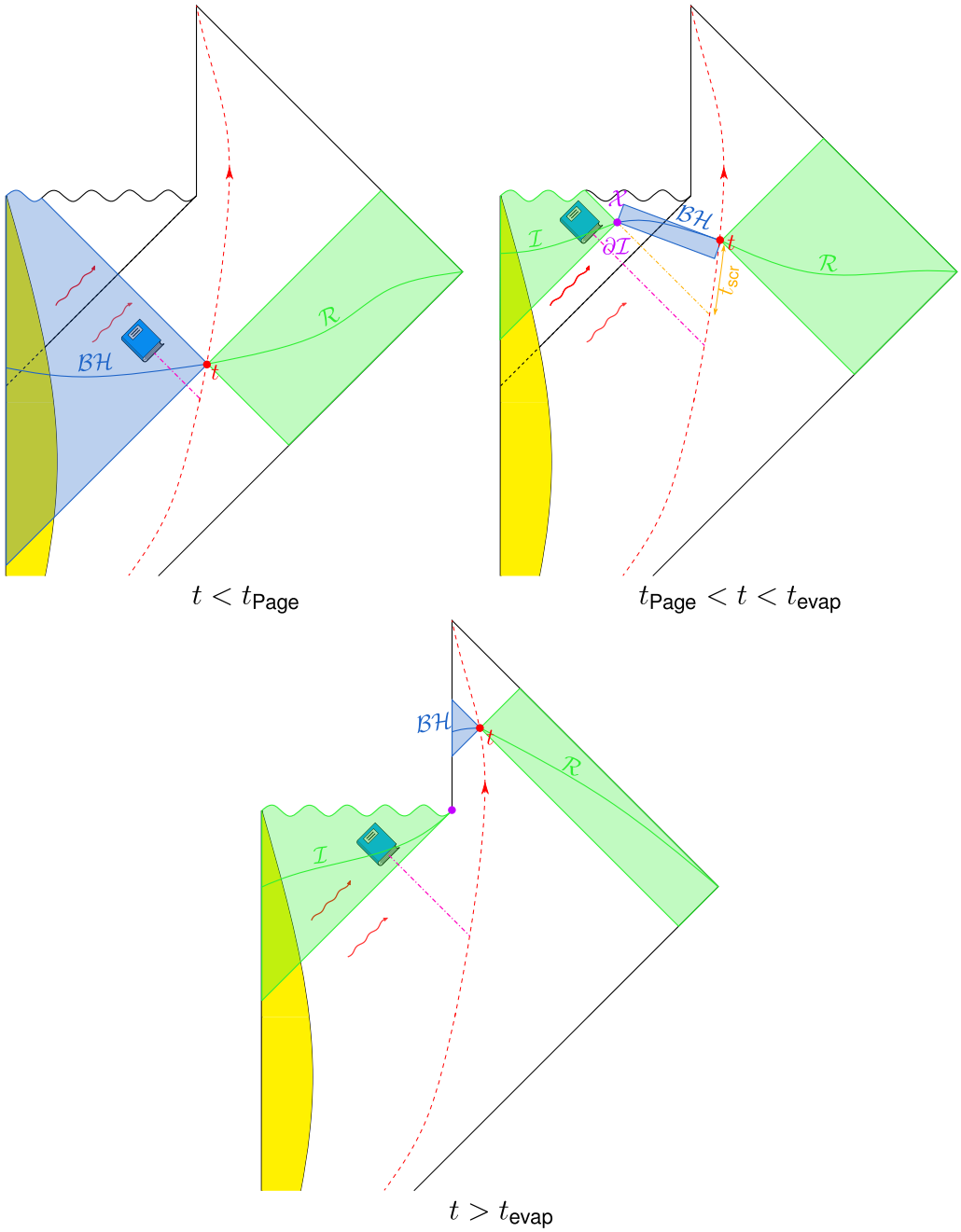

Figure 4.6: Evolution of the EWs. The top depicts the EWs for the trivial island followed by the one for a nontrivial island. The bottom picture shows the EWs when the BH is fully evaporated; the EW associated to the island region is the full interior. It can be reconstructed through the information contained in the EW associated to the radiation. Only a diary in the EW of the island can be reconstructed, this only happens after a scrambling time – the Hayden–Preskill protocol in action.

4.IV Ryu–Takayanagi as a Streaming Protocol (SD)

It was already Friday afternoon, long after class time, when Futaba was making her way to the science room. Much to her surprise – and initial annoyance – Sakuta was sitting there. She could predict what's about to happen. He looked puzzled and was staring out in front of him. It was quite dim in the room as the sky was clouded; two mugs could be discerned in front of him. Obviously, he had been waiting for her. [2]

Futaba sat down, grabbed one of the mugs and cut to the chase: "What is it this time?" However, she was less annoyed than before. She rather started enjoying these conversations about physics.

Sakuta had been making his way through *Holographic Entanglement Entropy* and reached the famed Ryu–Takayanagi formula, but there was something which left him confused.
"So, I have been thinking", he started. "When you look at the RT formula you are searching for a surface with some prescribed conditions, right?"

"Yes, that is correct."

"Then why does this surface extend into the bulk. Wouldn't it be more logical if it stayed close to the boundary to have a minimum surface."

"I am surprised, that's actually a good question", she replied with a genuine look of bewilderment on her face. "Well, there is a reason for this. Remember the conversation we had a couple of days ago about the interpretation of holography?"

"–Ah, you mean about Plato's cave and the energy interpretation?"
Futaba nodded approvingly while she took a piece of chalk. "Indeed, that one. Don't forget that the area is calculated through the metric inherited from the bulk."

"Yes, naturally, and that metric blows up near the– ", he started explaining before realising what she was about to say. "Ah, I think I get it. Since the metric diverges near the boundary, so will the area contribution from that surface. To reach a lower area, it must extend deeper into the bulk."

"That's right! You actually are getting better at this stuff", Futaba said showing signs of relief. She took a sip of her coffee, "Lukewarm... I guess you should leave this to me", she complained while Sakuta was making a smug face. "Anyway, to get quickly away from the boundary, the surface ends perpendicular on it. Since this corresponds to UV physics, it results in the area law divergence of the entropy in the boundary field theory."

"Okay, I am starting to understand."

"There is a nice analogy by Patrick Hayden to understand the formula from that viewpoint", she further elaborated. "If you view the entropy as a way of compressing information and subsequently sending it to Mai, much like streaming a series, the RT formula is the most efficient way to do this."

"...", he didn't know how to respond.

"I am used to it. Nevertheless, when streaming a movie you can choose to watch it directly while downloading it. Well, these represent the UV or short time correlations. Immediately seeing the movie frame per frame while downloading it comes with a high cost. However, some scenes are quite similar to others. For instance, the characters change clothes or expressions but their basic features like hair colour, etc. stay the same. We can only know this if we have access to correlations which are longer in time, in other words, IR correlations. By having access to these IR correlations, the streaming procedure is more efficient as it can reuse something for later times. You see?"

"Of course, a character might be smiling in one scene and crying in another but their build stays the same", he admitted. "He sure has his way of explaining things. I better try to remember this. I need to go now though. I promised Mai to watch a movie together. What a coincidence..."

[2] The coming analogy was given during a talk at the Berkeley Simons institute [129].

Meanwhile, the sky cleared and the sun was getting lower, casting an eerie spectacle of half-light, half-shadow into the science room. It was time to go. Both cleaned up, packed their bags, and started heading home. What remained of their presence was a large drawing of a minimal surface on the blackboard together with some formulas and other drawings like a cave and some boxes.

Chapter 5

JT Gravity

In this chapter, we take a look at a particular model of 2d QG: **Jackiw–Teitelboim (JT) Gravity** [16, 17]. This model is a useful playground for many calculations, especially those regarding the island, owing to a lot of its quantities being analytically computable. Even the classical Einstein equations can be exactly solved for arbitrary mass and energy distributions, and the partition function and correlation functions can explicitly be calculated at the quantum level. Moreover, this model is physically relevant as it can be obtained from the s-wave reduction of a class of near-extremal (charged) BHs.

Its holographic dual describes the low-energy dynamics of the **Sachdev–Ye–Kitaev (SYK) model**: a large amount of all-to-all interacting Majorana fermions in $(0+1)$d with random couplings, first studied in [130–133]. We direct the interested reader to Appendix A.

We begin by taking a look at the dimensional reduction of a magnetically charged BH and make our way to the general action. Then we consider the eom and some of its solutions both in the classical and semiclassical regime, including the boundary particle prescription. Going full quantum will not be necessary for our discussion. Subsequently, we describe the model for an EBH and how we can compute EEs. Of great importance is the renormalised entropy from the boundary angle.

5.I Dimensional Reduction of Charged Black Holes

To obtain the action from a higher-dimensional BH we follow the approach set out in [134, 135] and start with a magnetically charged Reissner–Nordström BH:

$$ds^2 = -f(r,M,p)dt^2 + \frac{dr^2}{f(r,M,p)} + r^2 d\Omega_2^2 \tag{5.1a}$$

$$f(r,M) = 1 - \frac{2G_{\mathsf{N}}M}{r} + \frac{p^2 G_{\mathsf{N}}}{4\pi r^2} \tag{5.1b}$$

$$F = p\sin\theta d\phi \wedge d\theta \tag{5.1c}$$

with magnetic charge p, magnetic gauge field F and mass M. This is the nonrotating BH solution of the Einstein–Maxwell action, coupling gravity with electromagnetism [136]

$$I = \int_{\mathcal{M}} \sqrt{-g}\left[\frac{1}{16\pi G_{\mathsf{N}}}R - \frac{1}{4}F^2\right] \tag{5.2}$$

with eom

$$\partial_\mu \left(\sqrt{-g}F^{\mu\nu}\right) = 0 \tag{5.3a}$$

$$R_{\mu\nu} - \frac{1}{2}g_{\mu\nu}R = 8\pi G_\mathsf{N} T_{\mu\nu} \tag{5.3b}$$

$$T_{\mu\nu} = F_{\mu\rho}F^\rho_\nu - \frac{1}{4}g_{\mu\nu}F^2 \tag{5.3c}$$

The horizons are given by the root of the warp factor $f(r, M, p)$ – an inner and outer horizon

$$r_\pm = G_\mathsf{N}M \pm \sqrt{(G_\mathsf{N}M)^2 - \frac{p^2 G_\mathsf{N}}{4\pi}} \tag{5.4}$$

As a special case, we take it to be the **extremal** BH with $p^2 = 4\pi G_\mathsf{N} M^2$ which has two coinciding horizons $r_+ = r_- = r_h$ and is thermodynamically at zero temperature as (3.8)

$$T \propto \lim_{r\to r_h} f(r, M, p) = 0 \tag{5.5}$$

Moreover, we can define a new coordinate $\nu = r - G_\mathsf{N}M$ such that the metric (5.1a) becomes

$$ds^2 = \frac{-dt^2}{\left(1 + \frac{G_\mathsf{N}M}{\nu}\right)^2} + \left(1 + \frac{G_\mathsf{N}M}{\nu}\right)^2 \left(d\nu^2 + \nu^2 d\Omega_2^2\right) \tag{5.6}$$

and look at the near-horizon limit $\nu \to 0$ after the transformation $z = (G_\mathsf{N}M)^2/\nu$. This is the Robinson–Bertotti metric describing the geometry in the throat

$$ds^2 = (G_\mathsf{N}M)^2 \left(\frac{-dt^2 + dz^2}{z^2} + d\Omega_2^2\right) \tag{5.7}$$

Interestingly enough, this is the line element for the product manifold $\mathsf{AdS}_2 \times S^2$ in Poincaré coordinates with AdS radius l_AdS equal to the radius of the sphere $r_S = l_\mathsf{AdS} = G_\mathsf{N}M$ [40].

Note that the Penrose diagram indeed looks like a part of AdS_2 when zooming in on the horizon, as is shown in Fig. 5.1.

To find the JT action, we go back to the Einstein–Maxwell (5.2) action and make a general static, spherically symmetric ansatz

$$ds^2 = h_{ij}dx^i dx^j + e^{2\psi(r,t)}d\Omega^2 \tag{5.8}$$

It has the form of a warped product space [137]

$$ds^2 = h_{ij}dx^i dx^j + e^{2\psi}g_{\mu\nu}dx^\mu dx^\nu \tag{5.9a}$$

$$R = R_h + e^{-2\psi}R_g - 2k\nabla_h^2\psi - k(k+1)h^{ij}\partial_i\psi\partial_j\psi \tag{5.9b}$$

with R_h the Ricci scalar for the metric h_{ij}, similar for R_g and the metric $g_{\mu\nu}$ with dimensionality k. In our case we have the metric of a 2d sphere such that we obtain the reduction

$$R = R_h + 2e^{-2\psi} - 6(\partial\psi)^2 - 4\partial^2\psi \tag{5.10a}$$

since ψ is a scalar field.

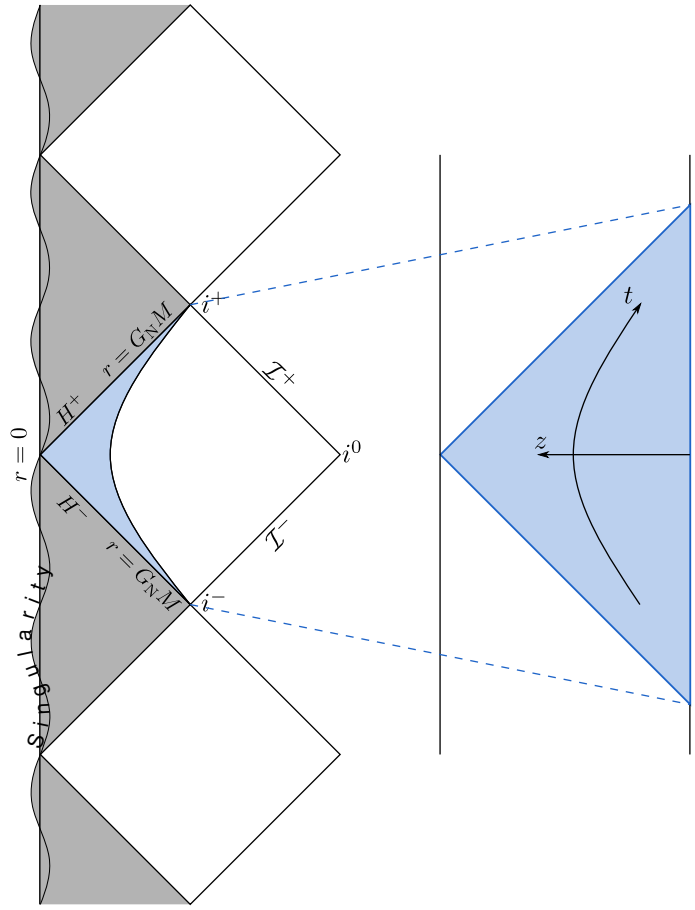

Figure 5.1: The extremal Reissner–Nordström BH. Because the horizon consists of two coinciding ones, time and space do not interchange after crossing it, unlike for a Schwarzschild BH. Therefore, we can move freely within its interior (shaded in grey) and go back to the exterior again; the diagram can be infinitely extended. Zooming in close to the horizons results in the Poincaré patch on the right.

Plugging the expression above into (5.2) with $\sqrt{-g} = \sqrt{-h}e^{2\psi}\sin\theta$, ignoring the electromagnetic contribution, and integrating out the spherical part to get 4π gives us

$$I_{\text{EH}} = \frac{4\pi}{16\pi G_{\text{N}}}\int d^2x\sqrt{-h}\left[e^{2\psi}(R_h - 6(\partial\psi)^2) + 2\right] \tag{5.11}$$

where we integrated the term containing $\partial^2\psi$ by parts to get $8e^{2\psi}(\partial\psi)^2$ and a boundary term. For the electromagnetic contribution, it is easy to obtain $F^2 = 2p^2e^{-4\psi}$. Furthermore, we define $\Phi = e^{\psi}$ such that finally

$$I = \frac{4\pi}{16\pi G_{\text{N}}}\int d^2x\sqrt{-h}\left[\Phi^2 R_h + 2(\partial\Phi)^2 + 2 - \frac{16\pi G_{\text{N}}}{2}p^2\Phi^{-2}\right] \tag{5.12}$$

The resulting action is a specific case of more general dilatonic gravity models studied in [138]

$$I = \frac{1}{16\pi G_{\text{N}}}\int d^2x\,\sqrt{-h}\left[\Phi^2 R_h + \lambda(\partial\Phi)^2 - U\left(\frac{\Phi^2}{L^2}\right)\right] \tag{5.13}$$

with dimensionless constant λ and **Dilaton** Φ^2. Since G_{N} is from a 4d parent theory, it has dimension $[G_{\text{N}}] = [\text{length}]^2$. Consequently, the dimension of the dilaton is $[\Phi^2] = [\text{length}]^2$; its value sets the area of the transverse 2-sphere. Hence, we can introduce a length parameter L in the scalar potential term U to obtain a dimensionless argument.

Our action of interest has $\lambda = 0$ – the kinetic term resides in R_h – and a linear potential $U = -2\Phi^2/l^2_{\text{AdS}}$.

5.II The JT Action

We begin by writing down the action for 2d JT gravity with metric g and dilaton ϕ coupled to conformal matter ψ ($l_{\text{AdS}} = 1$) [14, 16, 17, 138–141]

$$I_{\text{JT}}[g,\phi,\psi] = I_0[g] + I_G[g,\phi] + I_M[g,\psi] \tag{5.14a}$$

$$I_0[g] = \frac{\phi_0}{16\pi G_{\text{N}}}\left[\int_{\mathcal{M}}\sqrt{-g}R + 2\int_{\partial\mathcal{M}}\sqrt{-\gamma}K\right] \tag{5.14b}$$

$$I_G[g,\phi] = \frac{1}{16\pi G_{\text{N}}}\left[\int_{\mathcal{M}}\sqrt{-g}\phi(R+2) + 2\int_{\partial\mathcal{M}}\sqrt{-\gamma}\phi_b(K-1)\right] \tag{5.14c}$$

$$I_M[g,\psi] = I_{\text{CFT}}[g,\psi] \tag{5.14d}$$

The first action $I_0[g]$ is purely topological and adds a constant contribution $\phi_0\chi$ through the Gauss–Bonnet theorem where χ is the Euler characteristic of the corresponding manifold $\mathcal{M}$. The second action $I_G[g,\phi]$ is what we would get from dimensional reduction; hence, $\phi_0+\phi$ measures the area of the transverse space in the parent theory. Moreover, ϕ is dynamical and governed by this action where we added the usual Gibbons–Hawking–York boundary term with boundary metric γ, curvature K, and boundary value ϕ_b for the dilaton. There is an additional counterterm required to compute the on-shell action and related quantities. This explains the $(K-1)$. The last action $I_M[g,\psi]$ is simply a 2d CFT action for a matter field which does not couple to the dilaton but does backreact with it through the Einstein equation without deforming the spacetime geometry.

Varying the total action to ϕ imposes the constant curvature constraint

$$\delta(R+2) = 0 \tag{5.15}$$

In other words, the geometry is everywhere locally AdS_2 with a constant curvature. In Poincaré coordinates (F,Z) this is

$$ds^2 = \frac{-dF^2+dZ^2}{Z^2} = -\frac{4}{(X^+-X^-)^2}dX^+dX^- \tag{5.16}$$

with $X^\pm = F \pm Z$ lightcone coordinates, future and past horizon at $X^\pm = \pm\infty$, and the boundary located at $X^+ = X^-$ as per usual in the Poincaré patch $X^- \leq X^+$.

Note that this is already a fully QM feature: the dilaton acts as a Lagrange multiplier enforcing this geometry when evaluating the GPI. So, the GPI only sums over topologies which are locally AdS_2 but can differ in their Euler characteristic χ [142].

The other dynamics can be found from varying with respect to the metric and yields the Einstein equation [138–141, 143]

$$g_{\mu\nu}\Box\phi - \nabla_\mu\nabla_\nu\phi + g_{\mu\nu}\phi = 8\pi G_{\text{N}}T^m_{\mu\nu} \tag{5.17a}$$

$$T^m_{\mu\nu} = -\frac{2}{\sqrt{-g}}\frac{\delta I_M}{\delta g^{\mu\nu}} \tag{5.17b}$$

Next, we can split this equation up into a traceless and trace part

$$\frac{1}{2}g_{\mu\nu}\Box\phi - \nabla_\mu\nabla_\nu\phi = 8\pi G_{\text{N}}\left(T^m_{\mu\nu} - \frac{1}{2}g_{\mu\nu}T^m\right) \tag{5.18a}$$

$$(\Box - 2)\phi = 8\pi G_{\text{N}}T^m \tag{5.18b}$$

To look for solutions, it is easier to work in the conformal gauge

$$ds^2 = -e^{\omega(X^+,X^-)}dX^+dX^- \tag{5.19}$$

$$\Box = -4e^{-\omega}\partial_+\partial_- \tag{5.20}$$

$$R = -\Box\omega \tag{5.21}$$

and when considering semiclassical matter, the eom become (including the constraint (5.15))

$$2\partial_+\partial_-\omega + e^\omega = 0 \tag{5.22a}$$

$$-\nabla_\pm^2\phi = -e^\omega\partial_\pm(e^{-\omega}\partial_\pm\langle\phi\rangle) = \partial_\pm\phi\partial_\pm\omega - \partial_\pm^2\langle\phi\rangle = 8\pi G_\mathsf{N}\langle T^m_{\pm\pm}\rangle \tag{5.22b}$$

$$\left(\partial_+\partial_- + \frac{1}{2}e^\omega\right)\langle\phi\rangle = 8\pi G_\mathsf{N}\langle T^m_{+-}\rangle \tag{5.22c}$$

To work in the semiclassical limit, we assume that the central charge c of the conformal matter theory is large such that the graviton contribution is negligible.

Besides, the eom can be related to the Liouville equations linking JT gravity to a Liouville theory [143–146].

5.II.a The Conformal Anomaly

The conformal/trace anomaly

$$\langle T^m\rangle = \frac{c}{24\pi}R \tag{5.23}$$

can be taken care of by implementing the Polyakov action [138, 141, 143]

$$I_\mathsf{Pol} = -\frac{c}{96\pi}\int d^2x\,\sqrt{-g}R\frac{1}{\Box}R \tag{5.24}$$

With in particular $\langle T^m_{+-}\rangle = -\frac{c}{24\pi}\partial_+\partial_-\omega$, the last eom (5.18b) can be rewritten to

$$\partial_+\partial_-\langle\phi\rangle + \frac{1}{2}e^\omega\left(\langle\phi\rangle - \frac{cG_\mathsf{N}}{3}\right) = 0 \tag{5.25}$$

So the only effect the conformal anomaly has is the addition of a constant contribution: $\phi \to \phi + cG_\mathsf{N}/3$. From henceforth, we may safely set the conformal anomaly to zero in the eom as it can be absorbed in the vacuum contribution. The vacuum-subtracted semiclassical dilaton $\langle\phi_T\rangle$ then obeys the equations

$$-\nabla_\pm^2\langle\phi_T\rangle = 8\pi G_\mathsf{N}\langle T^m_{\pm\pm}\rangle \tag{5.26a}$$

$$(\Box - 2)\langle\phi_T\rangle = 0 \tag{5.26b}$$

just like in the classical case (5.18a, 5.18b) with the vacuum-subtracted, covariant stress tensor $\langle T^m_{\pm\pm}\rangle$.

Alternatively, one can achieve the same effect by rescaling the gravitational constant and thus changing the coupling constant of the Schwarzian theory (explained in the following section) [147]

$$G_\mathsf{N} \to \frac{G_\mathsf{N}}{1 - \frac{2NG_\mathsf{N}}{3\phi_b}} \tag{5.27}$$

with N the amount of matter fields. This is particularly nice in the boundary particle theory.

5.III The Boundary Particle

There is a nice perspective we will use for a boundary observer in a spacetime with an EBH – the perspective of the **boundary particle** [138, 140, 141]. From this viewpoint, the **boundary time** t becomes a preferred coordinate from which we can define a dynamical variable at the AdS_2 boundary: the dynamical time $f(t)$ which we set equal to a fixed reference time F, the Poincaré time. This preferred boundary time, associated to a boundary particle/observer, naturally describes the time evolution along the AdS_2 boundary $u = v \equiv t$. By requiring that

these boundary coordinates (u, v) coincide with the AdS_2 boundary in the Poincaré patch itself $X^+(u) = X^-(v)$, we acquire the **dynamical/holographic boundary curve**

$$X^+(t) = X^-(t) \equiv f(t) \tag{5.28}$$

We also call $f(t)$ the **time reparametrisation**. It becomes a dynamical curve in the sense that bringing in the boundary into the bulk lets it feel the effect of gravity (see Fig. 5.2).

After introducing a regulator for the AdS_2 boundary ε which moves the boundary slightly inwards, the boundary observer's coordinate frame (t, z) can be related to that of a bulk observer through

$$\frac{X^+(t+\varepsilon) + X^-(t-\varepsilon)}{2} = f(t) \tag{5.29a}$$

$$\frac{X^+(t+\varepsilon) + X^-(t-\varepsilon)}{2} = \varepsilon f'(t) \tag{5.29b}$$

where $\varepsilon f'(t)$ is equal to the distance between the holographic boundary curve and the true boundary [141].

Consequently, a boundary observer can in their frame construct a bulk frame by shooting in and collecting light rays $u = t+z, v = t-z$. They shoot in a light ray at $v = t_1$ as measured on their clock and collect it back at $u = t_2$. Now, taking this procedure to the Poincaré patch where the boundary observer sends at $F_1 = f(t_1)$ and receives at $F_2 = f(t_2)$, they can associate the coordinates $X^- = F_1, X^+ = F_2$ to every bulk point. From this they can construct a unique bulk frame and metric – the **radar definition** of the bulk [142, 148]

$$X^+(u) = f(u) \tag{5.30a}$$

$$X^-(v) = f(v) \tag{5.30b}$$

$$ds^2(f) = \frac{f'(u)f'(v)}{[f(u) - f(v)]^2}(dz^2 - dt^2) \tag{5.30c}$$

This procedure is boundary-intrinsic and is constructed via local operations from the boundary observer perspective. The transformation fits within the larger context of quantum reference systems [149].

Allowing QM fluctuations: the boundary observer experiences a fixed bulk location but fluctuating metric whilst a Poincaré observer would see a fuzzy bulk location and a fixed metric [142].

For these dynamics to be consistent with the dilaton, we should specify a boundary condition [138, 140, 141]

$$g_{tt}\Big|_{\partial\mathcal{M}} = \frac{1}{\varepsilon^2} \tag{5.31a}$$

$$\phi\Big|_{\partial\mathcal{M}} = \phi_b = \frac{\phi_r}{\varepsilon} \tag{5.31b}$$

where ϕ_b is large and ϕ_r is a fixed constant. In this approach, the JT action reduces to a boundary term and the theory becomes a Schwarzian theory in one less spatial dimension

$$\begin{aligned} I_G &\to -\frac{\phi_r}{8\pi G_N}\int \frac{dt}{\varepsilon}\frac{K-1}{\varepsilon} \\ &= -\frac{\phi_r}{8\pi G_N}\int dt\{f(t), t\} \end{aligned} \tag{5.32}$$

with induced metric dt/ε and extrinsic curvature

$$K = 1 + \varepsilon^2\{f(t), t\} \tag{5.33}$$

It enjoys a $\mathrm{SL}(2,\mathbb{R})$ symmetry of the reparametrisation $f(t)$ precisely because the **Schwarzian** is invariant under such transformations.

$$S(f(t),t) \equiv \{f(t),t\} = \frac{f'''}{f'} - \frac{3}{2}\left(\frac{f''}{f'}\right)^2 \tag{5.34}$$

with Möbius transformation

$$f \to \frac{af+b}{cf+d}, \qquad ad-bc=1 \tag{5.35}$$

With the aforementioned result, the Arnowitt–Deser–Misner (ADM) energy can be computed directly by relating the action (5.32) to the boundary Hamiltonian

$$E(t) = -\frac{\phi_r}{8\pi G_{\mathrm{N}}}\{f(t),t\} \tag{5.36}$$

Originally, this computation was done via the boundary stress tensor by means of holographic renormalisation [138–140, 150].

As a side note, while the Einstein–Hilbert part of the JT action is invariant under the reparametrisation $t \to f(t)$, it maps cutouts of the hyperbolic disk $(F(t), Z(t))$ in Euclidean AdS_2 to another cutout. But this does not leave the boundary trajectory invariant. Again, the $\mathrm{SL}(2,\mathbb{R})$ of the full reparametrisation group do leave this boundary trajectory invariant. One can think of the cutouts spontaneously breaking it down to $\mathrm{SL}(2,\mathbb{R})$ with $f(t)$ the associated Goldstone modes and a zero action since it has no spatial dimension, only a zero wavelength mode remains. The dilaton lifts the large degeneracy of the Einstein–Hilbert action [134, 140].

5.III.a Energy from the Boundary

The authors of [141] used this Schwarzian theory to construct a Hamiltonian formalism from which they found how the energy changes with respect to the boundary time, crucial for our discussion on EBHs and which nicely shows the Unruh effect (see Fig. 5.2 again for the following discussion). Just as before, the boundary stress tensor can be identified with the boundary Hamiltonian $H = T_{tt}$ and the ADM energy can be similarly found in a doubled phase space; the boundary action contains third order derivatives such that more conjugate variables are needed. This formalism is reminiscent of a dynamical moving mirror to simulate Hawking radiation, backreacting when hit by matter [151–153].

When allowing for backreaction in a semiclassical setup, the rate at which the ADM energy changes is merely equal to a net flux of the energy flow

$$\frac{\mathrm{d}E}{\mathrm{d}t} = T_{vv}(t) - T_{uu}(t) \tag{5.37}$$

where the stress tensors showing up are the covariant ones [135, 154]

$$T_{uu} = -\frac{c}{12\pi}\left[(\partial_u\omega)^2 + \partial_u^2\omega\right] + :T_{uu}: \tag{5.38a}$$

$$T_{vv} = -\frac{c}{12\pi}\left[(\partial_v\omega)^2 + \partial_v^2\omega\right] + :T_{vv}: \tag{5.38b}$$

$$T_{uv} = -\frac{c}{12\pi}\partial_u\partial_v\omega \tag{5.38c}$$

for a spacetime $ds^2 = -e^{2\omega(u,v)}dudv$.

The second term is the normal ordered stress tensor which is chirally conserved and frame-dependent since normal ordering is always with respect to a certain vacuum. This normal ordered term is exactly what one would measure via a detector calibrated to their

vacuum, by subtraction of the first term. However, this term transforms noncovariantly under a general conformal transformation $(X^+(u), X^-(v))$ due to the conformal anomaly and gives rise to the Unruh effect

$$:T_{uu}: = \left(\frac{\partial X^+}{\partial u}\right)^2 :T_{++}: -\frac{c}{24\pi}\{X^+, u\} \tag{5.39a}$$

$$:T_{vv}: = \left(\frac{\partial X^-}{\partial v}\right)^2 :T_{--}: -\frac{c}{24\pi}\{X^-, v\} \tag{5.39b}$$

also called the Virasoro anomaly.

Observe how for a Möbius transformation the anomalous transformation disappears. This is directly related to the fact that these transformations leave the vacuum state invariant; hence the stress tensors related to this vacuum as well.

Only the total sum is covariant in the sense that $\nabla_\mu T^{\mu\nu} = 0$ and transforms as a tensor. These properties are important to be consistent with the Einstein equation: the stress tensor has to transform in an equivalent way to the Ricci tensor.

By giving an operational meaning to this equation, it solves the Unruh backreaction paradox. The Minkowski vacuum by an accelerated observer looks like a thermal Rindler vacuum, if this backreacts on the spacetime it leads to an inconsistency. However, what the accelerated observer measures, as stated, is the normal ordered piece and not the total covariant stress tensor. So by adding the vacuum/Casimir piece – the first term – to their measurement, the effect cancels out and no backreaction is happening [154].

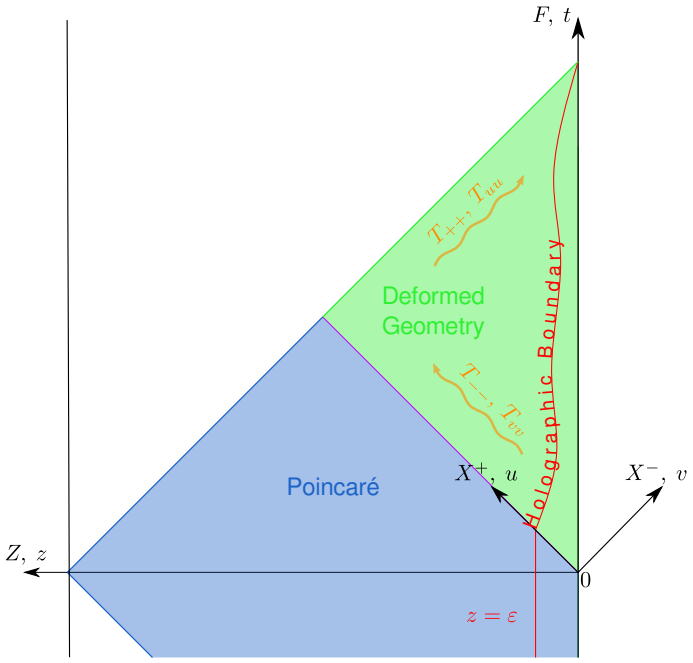

Figure 5.2: The holographic boundary curve. In the green patch, the stress tensors are nonzero leading to a deformed geometry with respect to the Poincaré patch. The difference between the two fluxes determines how the holographic boundary curve evolves and how both frames are related.

The case for JT gravity is special because at the boundary $u = v = t$

$$-\frac{c}{12\pi}\left[(\partial_t\omega)^2 + \partial_t^2\omega\right] = \frac{c}{24\pi}\{f(t), t\} \tag{5.40}$$

which means the Casimir piece of both stress tensors (5.38a, 5.38b) are equal to the expression above

$$T_{uu} = \frac{c}{24\pi}\{f(t), t\} + :T_{uu}: \tag{5.41a}$$

$$T_{vv} = \frac{c}{24\pi}\{f(t), t\} + :T_{vv}: \tag{5.41b}$$

such that for the difference they cancel each other out

$$\frac{\mathrm{d}E}{\mathrm{d}t} = T_{vv}(t) - T_{uu}(t) = :T_{vv}(t): - :T_{uu}(t): \tag{5.42}$$

This can also be acquired from plugging (5.30a, 5.30b) into (5.39a, 5.39b).

5.IV Solving the eom

5.IV.a The Static Black Hole Solution

For cases in which the stress tensor vanishes and with metric (5.16), we obtain the static BH background with mass $M = E$ and dilaton profile

$$\phi = 2\phi_r \frac{1 - (\pi T)^2 X^+ X^-}{X^+ - X^-} \tag{5.43}$$

at Hawking temperature T in AdS_2 [141].

The time reparametrisation in this case $f(t)$ becomes

$$f(t) = \frac{1}{\pi T}\tanh(\pi T t) \tag{5.44}$$

which is a solution for a constant Schwarzian

$$\{f(t), t\} = -\frac{2\pi^2}{\beta^2} \tag{5.45}$$

From this follows the metric and dilaton in boundary coordinates (u, v) through $(X^+(u), X^-(v))$

$$ds^2 = -\frac{4(\pi T)^2}{\sinh^2[\pi T(u-v)]} du dv \tag{5.46a}$$

$$\phi = 2\phi_r \pi T \coth[\pi T(u-v)] \tag{5.46b}$$

Both expressions are periodic in Euclidean time with period β.

This spacetime has a future and past horizon where $u = +\infty, v = -\infty$ which translates in Poincaré coordinates to

$$X^{\pm} = \pm\frac{1}{\pi T} \tag{5.47}$$

These two points are exactly where the boundary particle meets the AdS_2 boundary for $X^{\pm} = f(t \to \pm\infty)$ at the two points respectively.

The Penrose diagram, depicted in Fig. 5.3, is a smaller triangular region inside the full Poincaré patch due to the finite horizons and becomes smaller as the energy increases. This effect can be seen from the expression for the energy which is $\propto T^2$ and can be found by plugging in the time reparametrisation (5.44) into (5.36)

$$E(t) = \frac{\pi\phi_r}{4G_N} T^2 \tag{5.48}$$

One obtains the the full Poincaré patch in the limit $E, T \to 0$.

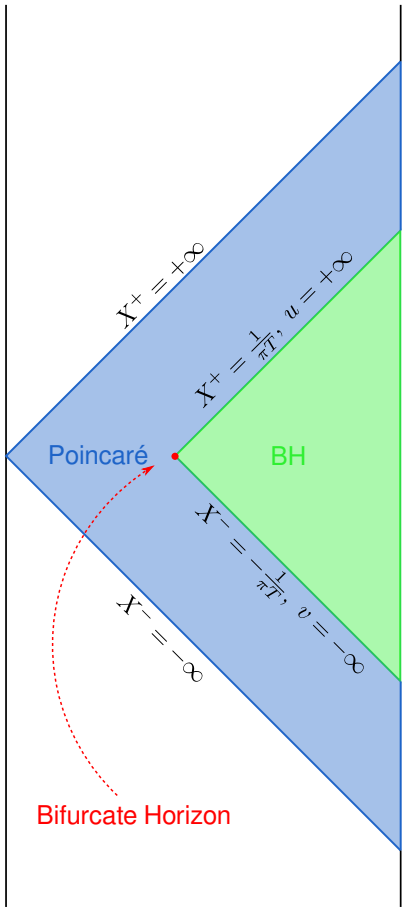

Figure 5.3: Penrose diagram for the static BH. The smaller green patch corresponds to the BH patch and is a part of the larger Poincaré patch (blue). The horizons are also shown; the bifurcate horizon is located where the horizons intersect.

Next, let us calculate the entropies of this spacetime, starting with the thermodynamical entropy by making use of (5.48)

$$\frac{\delta S}{\delta E} = \frac{1}{T} \tag{5.49a}$$

$$\Rightarrow S_{\text{Th}} = \frac{\phi_0}{4G_{\text{N}}} + 2\sqrt{\frac{\pi\phi_r}{gG_{\text{N}}}E} \tag{5.49b}$$

$$= \frac{\phi_0}{4G_{\text{N}}} + \frac{2\pi\phi_r}{4G_{\text{N}}}T \tag{5.49c}$$

where the first term is an integration constant which we fixed by demanding that at $E = T = 0$ the thermodynamical entropy is equal to its extremal value.

Successively, we can look at the BH entropy determined by the value of the dilaton at the horizon (3.21). Remember, the horizon is a codimension-2 surface which in our 2d spacetime translates to a point. Due to the value of the dilaton being related to the area of the transverse space of the parent theory, the BH entropy is determined by the dilaton at the horizon

$$S_{\text{BH}} = \frac{\phi_0}{4G_{\text{N}}} + \frac{\phi\big|_h}{4G_{\text{N}}} \tag{5.50}$$

The horizon is as usual found by the condition $g_{tt}\big|_h = 0$ and coincides with the bifurcate

horizon (5.47) which we can plug into (5.43) to obtain

$$S_{\text{BH}} = \frac{\phi_0}{4G_{\text{N}}} + \frac{2\pi\phi_r}{4G_{\text{N}}}T \tag{5.51}$$

The HEE computed via the RT formula is all what remains. Again, we need to find a codimension-2 minimal surface which is homologous to the boundary. The dilaton perfectly fits the bill as the homology is guaranteed through a spacelike interval connecting it to the boundary; it is even homotopic to it. To find the minimal surface we need to extremise $\phi(X^+, X^-)$ (5.43) with respect to its location

$$\partial_+\phi = 0 = \frac{-(\pi T)^2 X^-}{X^+ - X^-} - \frac{1-(\pi T)^2 X^+X^-}{(X^+ - X^-)^2} \tag{5.52a}$$

$$\partial_-\phi = 0 = \frac{-(\pi T)^2 X^+}{X^+ - X^-} + \frac{1-(\pi T)^2 X^+X^-}{(X^+ - X^-)^2} \tag{5.52b}$$

The solution is easy to find by adding both equations to each other, solving to one variable, and subsequently plugging it back into one of the above. In the end, one acquires the bifurcate horizon (5.47). Accordingly, we need to evaluate the dilaton at this minimal surface and we get an entropy equal to that of the BH entropy.

In conclusion, we computed the entropy in three different ways and find them all to be equal to each other

$$S_{\text{Th}} = S_{\text{BH}} = S_{\text{RT}} \tag{5.53}$$

This shows the strength of the RT formula!

To end our discussion, we can maximally extend this spacetime to a two-sided AdS_2 BH by defining Kruskal–Szekeres coordinates $W^\pm$ which are just Möbius transformations of the Poincaré coordinates $X^\pm$ [121, 147]

$$W^+ = +\frac{1+\pi T X^+}{1-\pi T X^+} = +e^{2\pi T u} \tag{5.54a}$$

$$W^- = -\frac{1-\pi T X^-}{1+\pi T X^-} = -e^{2\pi T v} \tag{5.54b}$$

with inverse

$$X^\pm = \pm\frac{1}{\pi T}\frac{W^\pm \mp 1}{W^\pm \pm 1} \tag{5.55}$$

The boundary is now at $W^+W^- = -1$, as observed in the metric and dilaton profile

$$ds^2 = -\frac{4}{(1+W^+W^-)^2}dW^+dW^- \tag{5.56a}$$

$$\phi = 2\phi_r\pi T\frac{1-W^+W^-}{1+W^+W^-} \tag{5.56b}$$

These transformations can be used in the evaporating case as well. The Penrose diagram is depicted in Fig. 5.4.

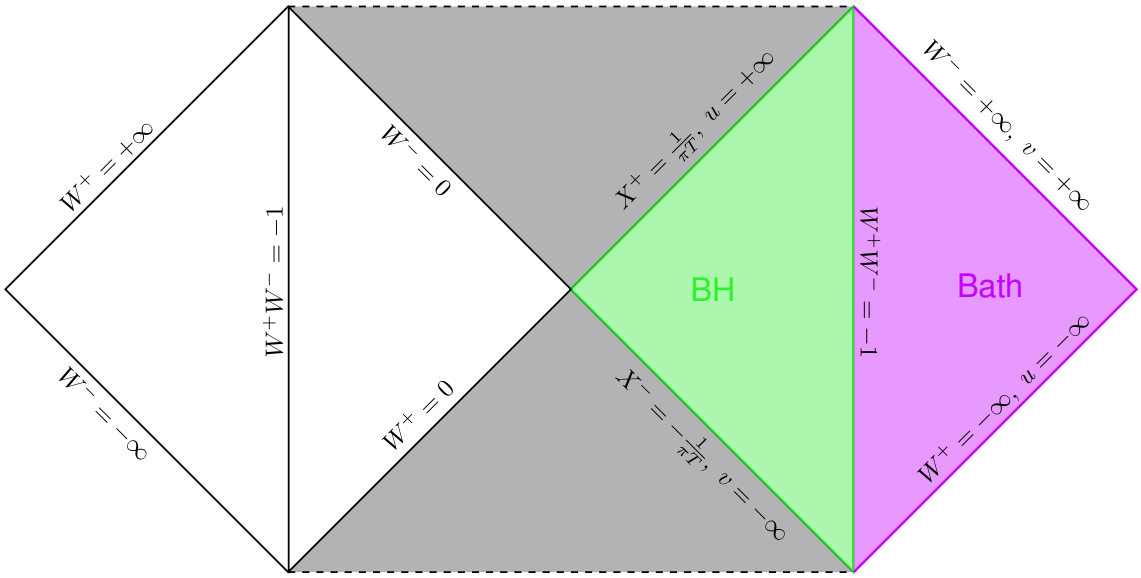

Figure 5.4: The maximally extended static BH. In the middle we have a two-sided AdS_2 BH. The Kruskal–Szekeres $W^\pm$ and boundary coordinates (u, v) also define a bath region (in purple) behind the boundary. Gluing such an external heat bath to define the radiation region is usually done in literature to find islands.

5.IV.b A General Solution

For a nonvanishing stress tensor, the eom (5.26a, 5.26b) can be directly integrated through the method of Green's functions [138, 141, 143]

$$\phi = 2\phi_r \frac{1 - (\pi T)^2 (I_+ + I_-)}{X^+ - X^-} \tag{5.57a}$$

$$I_\pm(u, v) = \pm \int_{\pm\infty}^{X^\pm} ds (s - X^\pm)(s - X^\mp) T^m_{\pm\pm}(s) \tag{5.57b}$$

Luckily, there is a particular, nicer solution in the case of purely infalling matter $T^m_{++} = 0$ [147]. To this end, we start by solving the $(++)$-equation (5.26a) and combine this with the $(+-)$-equation (5.26b) to obtain

$$\phi = 2\phi_r \left[\frac{1}{2} \partial_- h(X^-) + \frac{h(X^-)}{X^+ - X^-} \right] \tag{5.58}$$

Now solving the $(--)$-equation (5.26a) determines $h(X^-)$

$$T^m_{--}(X^-) = -\frac{\phi_r}{8\pi G_N} \partial_-^3 h(X^-) \tag{5.59}$$

and can also be found from varying the boundary action to t. The static BH solution (5.43) corresponds to $h(X^-) = 1 - (\pi T)^2 (X^-)^2$.

When describing EBHs it turns out that we can link this function to the time reparametrisation.

5.V The Evaporating Black Hole

Using (5.42) and imposing certain BC we can obtain a model for a static and EBH spacetime [141, 148, 154]. We start with the extremal BH/Poincaré patch and form a BH by sending in a

classical matter pulse at $t = 0$ with fixed energy E_0

$$\frac{\mathrm{d}E}{\mathrm{d}t} = E_0\delta(t) + :T_{vv}(t): - :T_{uu}(t): \tag{5.60}$$

The Poincaré coordinates always describe the Poincaré patch such that $:T_{++}(t): = 0 = :T_{--}(t):$ for all times t.

Before the pulse $t < 0$ there is nothing ingoing or outgoing such that $T_{uu} = 0 = T_{vv}, E = 0$. So the equations to solve (5.36, 5.60) become

$$\{f(t), t\} = 0 \tag{5.61a}$$

$$\frac{\mathrm{d}}{\mathrm{d}t}\{f(t), t\} = 0 \tag{5.61b}$$

which has as solution $f(t) = t$, not surprising since we started from the Poincaré patch. A boundary observer would also measure the Poincaré vacuum $:T_{vv}: = 0 = :T_{uu}(t):$.

After we have sent in the pulse $t > 0$ we do not throw anything in anymore: $T_{vv} = 0 = T_{uu}$. By imposing reflecting BC, the Hawking radiation sent out by the BH eventually falls back into it again and feeds the BH such that it remains at a constant energy. $X^{\pm}$ still describe the Poincaré vacuum; but since the energy after the pulse is nonzero, this vacuum described from the BH frame (u, v) has a nonzero Schwarzian contribution (5.39a, 5.39b)

$$:T_{uu}: = :T_{vv}: = -\frac{c}{24\pi}\{f(t), t\} \tag{5.62}$$

Equations (5.36, 5.60) now dictate that the energy stays constant at E_0

$$\{f(t), t\} = E_0 \tag{5.63a}$$

$$\frac{\mathrm{d}}{\mathrm{d}t}\{f(t), t\} = 0 \tag{5.63b}$$

These two conditions lead to the static BH solution with reparametrisation (5.44) and Hawking temperature (5.48). Hence, as viewed from the BH frame we obtain an eternal Unruh heat bath

$$:T_{vv}: = :T_{vv}: = \frac{\pi c}{12\beta^2} \tag{5.64}$$

whilst it is just the Poincaré vacuum from the bulk perspective: the Unruh effect at work!

To let our BH evaporate, we take away the Hawking radiation sent by the BH. We can imagine a boundary observer moving along the holographic boundary curve and who holds an Unruh detector perfectly absorbing all Hawking radiation the BH emitted; hence $:T_{vv}: = 0$. There is no ingoing flux feeding the BH. The Hawking radiation emitted from the BH is nonzero and measured from the boundary becomes

$$:T_{uu}: = -\frac{c}{24\pi}\{f(t), t\} \tag{5.65}$$

We now have a nonzero energy rate (5.60) $\dot{E} = - :T_{uu}:$ and together with the ADM energy (5.36) we have to solve the following system

$$\frac{\mathrm{d}E}{\mathrm{d}t} = -kE \tag{5.66a}$$

$$\Rightarrow E(t) = E_0 e^{-kt} \tag{5.66b}$$

after implementation of the initial value $E(0) = E_0$ and where we defined the **evaporation rate** k as

$$k = \frac{cG_{\mathsf{N}}}{3\phi_r} \tag{5.67}$$

with units $[k] = [\text{energy}]^{-1}$. We obtain an exponentially decaying energy and with this we can find the reparametrisation through

$$\{f(t), t\} = -2(\pi T)^2 e^{-kt} \tag{5.68a}$$
$$f(0) = 0, \quad f'(0) = 1, \quad f''(0) = 0 \tag{5.68b}$$

with the BC stemming from gluing along the pulse at $t = 0$ which also determines E_0 in terms of the temperature via (5.48). The solution is pretty complicated and contains the modified Bessel functions of the first and second kind [14, 141, 148]

$$f(t) = \frac{1}{\pi T} \frac{I_0[\alpha]K_0[\alpha e^{-\frac{kt}{2}}] - K_0[\alpha]I_0[\alpha e^{-\frac{kt}{2}}]}{I_1[\alpha]K_0[\alpha e^{-\frac{kt}{2}}] + K_1[\alpha]I_0[\alpha e^{-\frac{kt}{2}}]} \tag{5.69}$$
$$\alpha = \frac{2\pi T}{k}$$

Note that this function is essentially a Möbius transformation of the ratio K_0/I_0. Although we could alternatively use this reparametrisation which is undoubtedly easier to use, the BC (5.68b) become a lot more difficult [121].

Moreover, $f(t)$ increases monotonically and asymptotes to a fixed value for $t \to +\infty$ beyond the horizon of the static BH case. However, it does not reach the original Poincaré horizon as shown in Fig. 5.5

$$f_\infty = f(t \to +\infty) = \frac{1}{\pi T} \frac{I_0[\alpha]}{I_1[\alpha]} \tag{5.70}$$

Poincaré time even stops flowing as $f'(t \to +\infty) \to 0$ [141]. This result will turn out to be of crucial importance when trying to find islands in this setup.

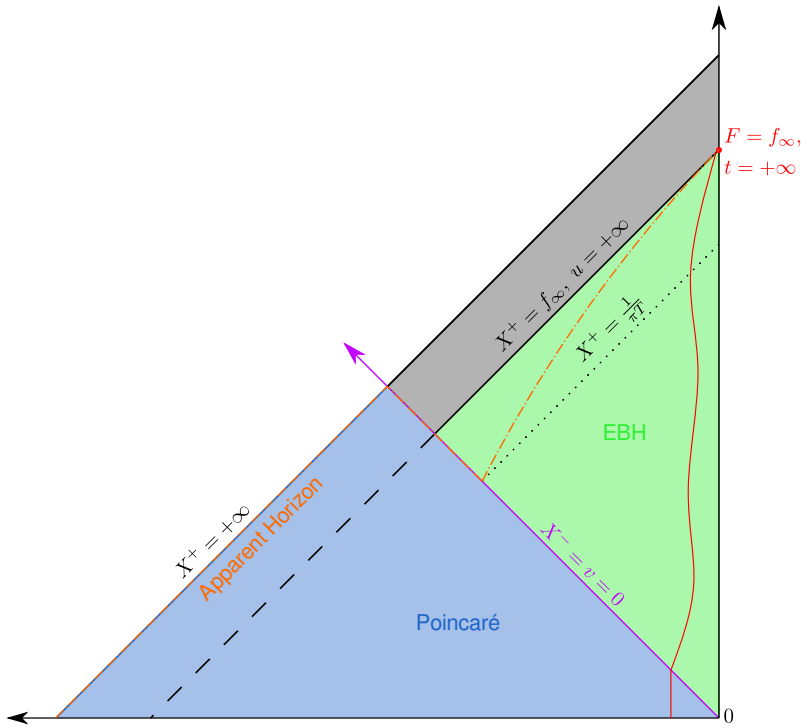

Figure 5.5: The EBH. From the Poincaré patch we sent in a pulse at $t = 0$ to form a BH. If the BH were static, the (u, v) coordinates could only describe up to the would-be horizon $X^+ = \frac{1}{\pi T}$; the starting point of the apparent horizon. In the EBH case, these coordinates describe the patch up to f_∞.

In the limit of large k, the evaporation happens instantaneously resulting in the original Poincaré patch again; whilst for very small k. the parametrisation becomes that of the eternal BH where evaporation is turned off. Different profiles are plotted in Fig. 5.6.

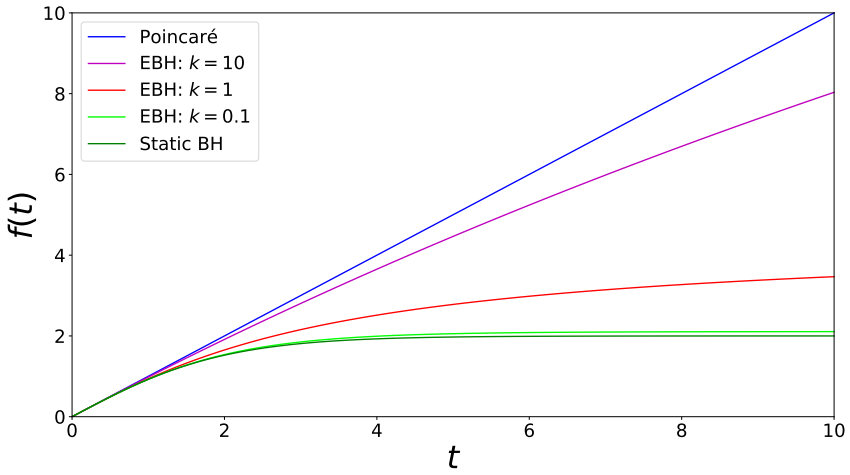

Figure 5.6: Reparametrisation profiles for the different scenarios. The time reparametrisation of the EBH interpolates between the static BH and the Poincaré patch for increasing evaporation rate k.

As seen in the figure above, a small k gives rise to a reparametrisation resembling the static case. In this limit, the reparametrisation and horizon value can be approximated by the following expressions (B.2, B.18)

$$f(t) \approx f_\infty \tanh\left(\frac{2\pi T}{k}\left[1 - e^{-\frac{k}{2}t}\right]\right) \tag{5.71a}$$

$$f_\infty = \frac{1}{\pi T} + \mathcal{O}(k) \tag{5.71b}$$

and indeed looks similar to the case of a static BH (5.44). When considering early times $kt \ll 1$, the exponential within the argument can be further expanded. The result is a parametrisation equivalent to the one for a static BH at temperature T (5.44). The Unruh heat bath immediately appears after the pulse is sent in!

From the decaying energy, it is possible to define an effective/quasistatic Hawking temperature [141]

$$T_{\text{eff}}(t) = Te^{-\frac{k}{2}t} \tag{5.72}$$

Moreover, this exponentially decaying energy is what would be expected from a quasistatic computation through the Stefan–Boltzmann law in 2d

$$\frac{\mathrm{d}E}{\mathrm{d}t} \propto -\sigma_{\text{SB}}T^2 \propto -\sigma_{\text{SB}}E \tag{5.73}$$

The setup we described here varies from the usual setup in most papers [14, 18, 20, 121, 122, 155–158] in which they glued a flat spacetime to the holographic boundary (as in Fig. 5.4). This extra spacetime acts as a heat bath collecting the Hawking radiation but where gravity is effectively turned off. Before the pulse is sent in, these two spacetimes do no interact with each other and the boundary is assumed to be perfectly reflecting, whereas after the coupling it becomes transparent. As a result, a BH forms due to an energy pulse resulting from this coupling; this is reminiscent of a quench procedure (see appendix of [127]). This is not what happened in our setup, we simply shot in a classical pulse and artificially absorbed all Hawking radiation reaching the boundary through an Unruh detector without making assumptions about

an extra heat bath. The result is the same reparametrisation, but the physical implications are different as we will see when determining the bulk entropy. We come back to this discussion in the next Section 5.VI, Chapter 7 and in the Outlook 8.

5.V.a Forgetting the Memory Integrals

To find the expression for the dilaton, we make use of the procedure in Subsect. 5.IV.b; it turns out the function $h(X^-)$ (5.58, 5.59) can be related to the time reparametrisation [121]. The same result was also found by the authors of [122] by directly integrating the general expression for the dilaton.

From the condition of perfect absorption $:T_{vv}: = 0$ and the covariant stress tensor (5.41b) follows

$$T_{vv} = \frac{c}{24\pi}\{f(v), v\} \tag{5.74}$$

at the boundary where $v = t$. Since this really transforms as a tensor we get

$$T_{--} = \frac{1}{f'(v)^2} T_{vv} \tag{5.75}$$

Together with the following expression as a result from (5.36, 5.66a)

$$\frac{\mathrm{d}}{\mathrm{d}v}\{f(v), v\} = -k\{f(v), v\} \tag{5.76}$$

we find (5.67)

$$T_{--} = -\frac{\phi_r}{8\pi G_\mathsf{N}} \frac{1}{f'(v)^2} \partial_v \{f(v), v\} \tag{5.77}$$

Using the chain rule to write $\partial_v = f'(v)\partial_-$, and using the Leibniz rule to acquire

$$\begin{aligned} f''(v) &= \partial_v f'(v) \\ &= f'(v)\partial_- f'(v) \end{aligned} \tag{5.78a}$$

$$\begin{aligned} f'''(v) &= f'(v)\partial_- f''(v) \\ &= f'(v)\left[\partial_- f'(v)\right]^2 + f'(v)^2 \partial_-^2 f'(v) \end{aligned} \tag{5.78b}$$

To promote clarity, we did not write $v(X^+)$ explicitly. Next, we can work out the derivative acting on the Schwarzian (5.34)

$$\begin{aligned} \{f(v), v\} &= -\frac{1}{2}[\partial_- f'(v)]^2 + f'(v)\partial_-^2 f'(v) \\ \Rightarrow \frac{1}{f'(v)^2}\partial_v\{f(v), v\} &= \partial_-^3 f'(v) \end{aligned} \tag{5.79}$$

such that (5.77)

$$T_{--} = -\frac{\phi_r}{8\pi G_\mathsf{N}} \partial_-^3 f'(v) \tag{5.80}$$

Identification with (5.59) leads to the conclusion

$$h(X^-) = f'[v(X^-)] \tag{5.81}$$

and plugging this into the general expression (5.58) brings about an expression for the dilaton in terms of the reparametrisation $f(t)$

$$\phi = 2\phi_r \left[\frac{1}{2}\frac{f''(v)}{f'(v)} + \frac{f'(v)}{f(u) - f(v)}\right] \tag{5.82}$$

Using the reparametrisation $f(t) = t$ results in the dilaton profile for the Poincaré vacuum. Likewise, using the one from the static BH solution (5.44) leads to (5.43).

5.VI The Semiclassical Entanglement Entropy

To find islands through the QES formula, we require an expression for the semiclassical entropy of the bulk fields across the spacelike interval between the island and the boundary. The fact that this interval is anchored on the holographic boundary provides us with an entropy evolving in boundary time t. Since the matter sector does not couple to the dilaton directly, we can treat it as a QFT on a fixed background. Moreover, since information is preserved along null lines, we will be able to interpret our setup as a boundary observer with an Unruh detector calibrated according to their vacuum in boundary coordinates (u, v) who measures the entanglement between the radiation already captured (early time) and the radiation yet to come out of the EBH (late time). Our setup differs from most papers given that we are removing one set of movers by absorbing it through the Unruh detector, effectively turning it into a chiral CFT (more on this in the following chapter).

Let us start in flat space $ds^2 = -dX^+dX^-$ and measure the entropy across a single interval for a massless free scalar with respect to the vacuum $|0_+\rangle$ [43, 148, 154, 159]. For a free massless scalar, the CFT decouples in a rightmoving and leftmoving part, thus we can calculate the contribution to the entropy from these modes separately across intervals $[X_1^+, X_2^+]$ and $[X_1^-, X_2^-]$

$$S = \frac{c}{12} \ln \frac{(X_1^+ - X_2^+)^2}{\delta_1 \delta_2} + (X_i^+ \to X_i^-) \tag{5.83}$$

where δ_i are the cutoffs in the points (X_i^+, X_i^-) as measured by an observer in their frame.

Alternatively, we can look at the entropy with respect to another vacuum $|0_u\rangle$ related to the original vacuum by a conformal transformation $u(X^+)$, similarly for $v(X^-)$

$$S = \frac{c}{12} \ln \frac{(u_1 - u_2)^2}{\hat{\delta}_1 \hat{\delta}_2} + (u_i \to v_i) \tag{5.84}$$

with cutoffs $\hat{\delta}_i$ as measured by an observer in the (u, v) frame.

These cutoffs are related to how the clocks tick for the observers in the different frames $\hat{\delta}_i = u_i' \delta_i$ which is not surprising as they have their detectors calibrated to a different vacuum; hence also to a different time coordinate with respect to which they define positive frequency modes. Plugging this relation into (5.84) leads to

$$S = \frac{c}{12} \ln \frac{(u_1 - u_2)^2}{u_1' u_2' \delta_1 \delta_2} + (u_i \to v_i) \tag{5.85}$$

which is invariant under Lorentz boosts because the product of the cutoffs on the leftmoving and rightmoving modes is boost-invariant and can be interpreted as the square of a proper length measured on a spatial slice [159]. In these new coordinates, the metric is $ds^2 = -\partial_u X^+ \partial_v X^- du dv = -e^{2\omega} du dv$ and the entropy can alternatively be written as

$$S = \frac{c}{6}(\omega_1 + \omega_2) + \frac{c}{12} \ln \frac{(u_1 - u_2)^2}{\delta_1 \delta_2} + (u_i \to v_i) \tag{5.86}$$

In [159] it was conjectured that this is the correct analogue for a curved spacetime as there is no global inertial frame; we are free to choose coordinates and measure the entropy with respect to the vacuum accordingly. Local Lorentz transformations leaving the metric in $X^\pm$ invariant also leave the entropy invariant and moreover, this expression is invariant under Möbius transformations of (u, v) which preserve the metric and stress tensors.

We can now apply this procedure to our setup in AdS_2

$$ds^2 = -\frac{4}{(X^+ - X^-)^2} dX^+ dX^- = -\frac{4 \partial_u X^+ \partial_v X^-}{(X^+ - X^-)^2} du dv \tag{5.87}$$

A bulk interval is depicted in Fig. 5.7. By following [148] we obtain

$$S_{\text{bare}} = \frac{c}{6}\left(\ln\frac{2}{X_1^+ - X_1^-} + \ln\frac{2}{X_2^+ - X_2^-}\right) + \frac{c}{12}\ln\frac{(X_1^+ - X_2^+)^2}{\delta_1\delta_2} + (X_i^+ \to X_i^-) \tag{5.88}$$

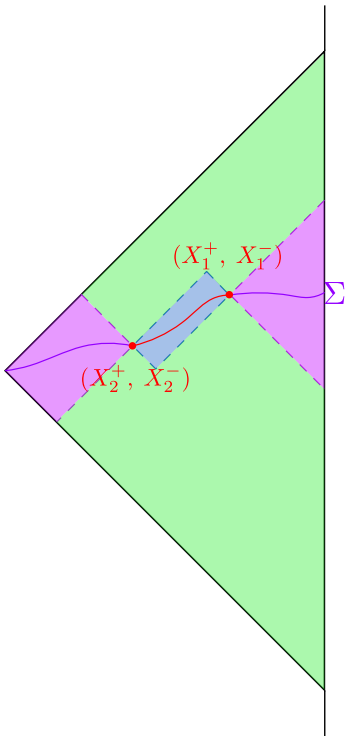

Figure 5.7: Entropy measured across a bulk interval. The entanglement wedges for the bipartitioning of the Cauchy slice Σ are also depicted.

However, a boundary observer in the coordinate frame (u, v) would calibrate their Unruh detector with respect to their vacuum, so we should subtract a reference entropy

$$\begin{aligned} S_{\text{ref}} =& \frac{c}{6}\left(\ln\frac{2\partial_u X_1^+ \partial_v X_1^-}{X_1^+ - X_1^-} + \ln\frac{2\partial_u X_2^+ \partial_v X_2^-}{X_2^+ - X_2^-}\right) \\ &+ \frac{c}{12}\ln\frac{(u_1 - u_2)^2}{\delta_1\delta_2} + (X_i^+ \to X_i^-, u_i \to v_i) \end{aligned} \tag{5.89}$$

from the bare entropy to obtain a renormalised quantity

$$\begin{aligned} S_{\text{ren}} &= S_{\text{bare}} - S_{\text{ref}} \\ &= \frac{c}{12}\ln\frac{(X_1^+ - X_2^+)^2}{\partial_u X_1^+ \partial_u X_2^+ (u_1 - u_2)^2} + (X_i^+ \to X_i^-, u_i \to v_i) \end{aligned} \tag{5.90}$$

Note that is indeed what a boundary observer would measure, for the expression does not rely on any boundary-intrinsic UV cutoff anymore. Both S_{ref} and S_{ren} have a similar UV cutoff behaviour near the boundary.

The same formula can be found by starting with the expression for the entropy in $X^\pm$ (5.83) and subsequently subtract a reference entropy with $X^+(u) = u, X^-(v) = v$ by making the analogy with a moving mirror [43]. In this context, the authors established a relation between the renormalised entropy and the two-point correlation function of the stress tensor $C(z_1, z_2)$. They obtained a negative renormalised entropy, suggesting that the vacuum has less correlations and is therefore more disordered

$$S_{\text{ren}} = -\frac{c}{24}\ln\frac{C}{C_0} \tag{5.91}$$

It is reminiscent of the Casimir effect and vacuum polarisation near BH horizons.

For a two-sided interval, the procedure can be repeated by adding a term $\frac{c}{6}\ln\eta$ dependent on the cross ratio

$$\eta = \frac{X_1^+ - X_1^-}{X_1^+ - X_2^-}\frac{X_2^+ - X_2^-}{X_2^+ - X_1^-} \tag{5.92}$$

One could argue that we are working in a boundary CFT. For that reason, we should add to the one-sided interval the Affleck–Ludwig boundary entropy $\ln g$, and to the two-sided case a term $\ln G(\eta)$ related to the operator product expansion (OPE) coefficient of the two-point function [160]. However, by setting absorbing BC the boundary can be seen as 'transparent' and this term is therefore not vital.

5.VI.a Twist Fields Derivation

The formula (5.86) has been proven in [14] by making use of the twist fields we introduced in Subsect. 2.II.a, we reconstruct the argument here.

The replica manifold has singularities at the endpoints of the interval, so we introduce an IR length scale and set it equal to the AdS scale to define renormalised entropies. This local regulator gets absorbed into the normalisation of the twist fields.

Under our Weyl transformation of interest $g \to e^{2\omega}g$, Eqs. (2.52, 2.55) become

$$\left\langle \mathcal{T}_1\tilde{\mathcal{T}}_2\right\rangle_{e^{2\omega}g} = (e^{-\omega_1})^{h_n}(e^{-\omega_2})^{h_n}\left\langle \mathcal{T}_1\tilde{\mathcal{T}}_2\right\rangle_g \tag{5.93a}$$

$$S_{e^{2\omega}g} = S_g + \frac{c}{6}\sum_{\text{endpoints}}\omega \tag{5.93b}$$

When the interval only contains one point in the bulk and the other one is anchored to the boundary, we only need one insertion; for twist fields inserted at the boundary are topological and contribute nothing

$$\left\langle \mathcal{T}(Z^+,Z^-)\right\rangle = \frac{g_n}{(Z^+-Z^-)^{h_n}} \tag{5.94}$$

The coordinates $Z^\pm$ are the Weyl-rescaled coordinates associated with the Weyl-rescaled metric g. In the $n\to 1$ limit we find the vN entropy through (2.54)

$$S = \frac{c}{6}\ln\left(Z^+ - Z^-\right) + \ln g \tag{5.95}$$

where the last term is the Affleck-Ludwig boundary entropy: $\ln g = -\lim_{n\to 1}\partial_n \ln g_n$ by using l'Hôpital's rule [160].

For a two-sided interval, we have to take the cross ratio into account (5.92), but in the Weyl-rescaled coordinates $Z^\pm$. Furthermore, the OPE coefficient of the two-point function for twist fields has no fixed form, it depends on the theory of interest

$$\left\langle \mathcal{T}_1\tilde{\mathcal{T}}_2\right\rangle = \frac{G_n(\eta)}{[(Z_1^+ - Z_2^+)(Z_1^- - Z_2^-)\eta]^{h_n}} \tag{5.96}$$

Again, we take the limit $n\to 1$ (2.54) to acquire

$$S = \frac{c}{6}\ln[(Z_1^+ - Z_2^+)(Z_1^- - Z_2^-)] + \frac{c}{6}\ln\eta + \ln G(\eta) \tag{5.97}$$

Now, by setting $Z^\pm = X^\pm$ and rescaling the metric with the appropriate Weyl factor (5.87)

$$ds^2 = -dZ^+dZ^- \to -\frac{4}{(X^+-X^-)^2}dX^+dX^- \tag{5.98}$$

followed by applying the transformation formula (5.93b) to (5.97), we obtain the same formula (5.88) from our previous heuristic derivation. There are no cutoffs δ_i present as they were assumed to be absorbed in the twist field normalisation.

Chapter 6

An Archipelago from the Boundary

In this chapter we search for islands in the setup we described in Sect. 5.V. Additionally, we give an operational meaning to the different regions in our spacetime from the perspective of the boundary observer. For the entropy we employ the usual method, i.e. the 'drop the boundary cutoff' method. We will take the cutoff into account and use the renormalised entropy to find islands in the following chapter.

The first section forms one of the cornerstones of this thesis as it gives a natural perspective for the entropy as measured by a boundary observer. Of course, this point of view makes more sense when using the renormalised entropy due to the calibration of the observer's Unruh detector. Afterwards, a warning is appropriate as we enter the more technical parts and at last set sail towards an archipelago.

6.I The Boundary Observer Perspective

In the previous chapter we introduced our model for an EBH in JT gravity without specifying a heat bath. We took the perspective of a boundary observer who follows the holographic boundary curve with an Unruh detector in hand, absorbing all the outgoing radiation from the BH. This effectively turned our CFT into a chiral CFT since only one set of movers remains.

As a direct consequence, to calculate the entropy of a bulk interval we need not make use of the image charge trick [143]. Since information is preserved along null lines, the entropy of an interval is determined by the radiation which goes through this interval. If we had two sets of movers and reflecting BC, an outgoing mode could get reflected off the boundary, become an ingoing mode and get captured by the interval. Equivalently in computing this entropy, one could mirror the interval with respect to the boundary and use transparent BC. An outgoing mode would then get captured by this image interval instead of reflecting off the boundary first. This entropy becomes a two-sided interval entropy; hence one should use the prefactor $c/6$ and add an extra contribution stemming from the cross ratio η. This situation is depicted in Fig. 6.1.

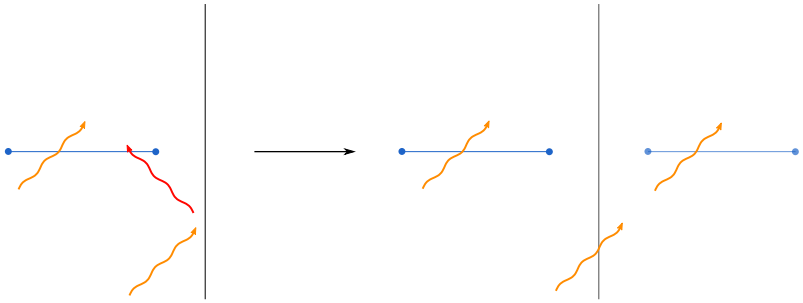

Figure 6.1: The image charge trick. Left we have a CFT with reflecting BC; an initial rightmover reflects off the boundary and gets captured by the interval. Right we show the same computation by using transparent BC; the same rightmover will now get caught by this illusionary interval behind the boundary.

For the radiation region, we take it to be the interval stretching from (σ, σ) up until $(u = t,\ \sigma/2)$ along the pulse [148]. We can imagine that as soon as the Unruh detector starts absorbing radiation, a heat bath develops behind the boundary which grows as more radiation is getting absorbed – some kind of internal spacetime for the detector. In this heat bath, a horizontal slice is equivalent to the radiation region as the latter can be mapped to the interval by moving along an outgoing null ray. This links our setup with the usual setup in which a flat space heat bath is glued to the boundary. However, we need not specify a particular metric for this region. The only property it needs is for it to act as a heat bath for the radiation. A full Cauchy slice of this extended spacetime is nothing more than the union of these three intervals: $\mathcal{I} \cup \mathcal{BH} \cup \mathcal{R}$. This view is illustrated in Fig. 6.2.

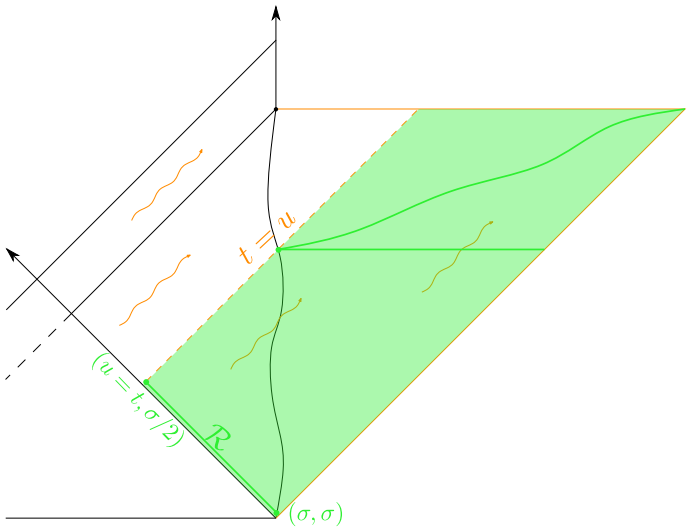

Figure 6.2: The external heat bath. The mentioned radiation region along the pulse is shown, σ is small to keep the interval spacelike. We can add an external system where the radiation caught by the observer is stored. No metric is required to be defined in this region. Actually, every interval beginning at the left null ray and ending on the right one constitutes a correct radiation region. In particular, a part of the boundary suffices.

This information preservation along null lines also give rises to a nice interpretation of the island. Given that all radiation can be seen as originating from the pulse $v = 0$, to each interval along the pulse we can associate an interval which lies along the holographic boundary curve by shifting it over an outgoing null line (as shown in Fig. 6.3). An observer starting at $t = 0$ moving along the boundary will start collecting radiation and its associated interval along the pulse will grow. The entropy the observer measures is then a measure for the entanglement between the early radiation – the collected radiation $\mathcal{R}$ and the island region $\mathcal{I}$ – and the late

radiation – the radiation yet to escape $\mathcal{BH}$. Hence, for each t we can divide our boundary and pulse into three intervals each encoding a specific part of the total radiation. Since an island region extending to the exterior captures the part between the island and the horizon, we call this the very late radiation. The two points dividing the pulse in these three parts are the location of the boundary observer $u = t$ (early vs late) and the island itself (late vs very late) giving the dilatonic contribution.

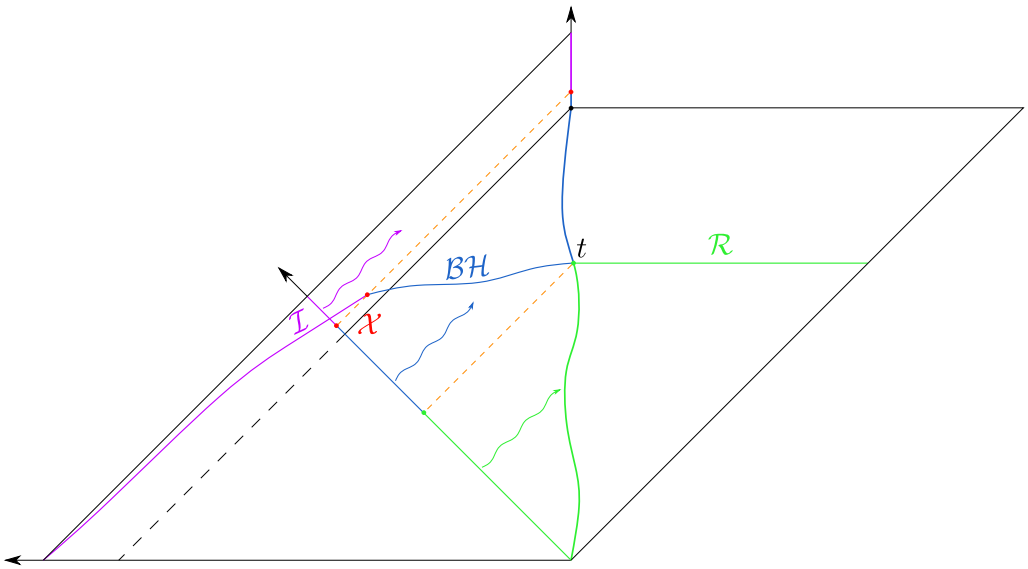

Figure 6.3: The division of the outgoing radiation. Each part of the radiation originating from the pulse gets captured by the associated boundary interval. Specifically, the green interval is what the observer already detected. Again, the island lacks a scrambling time behind the boundary time.

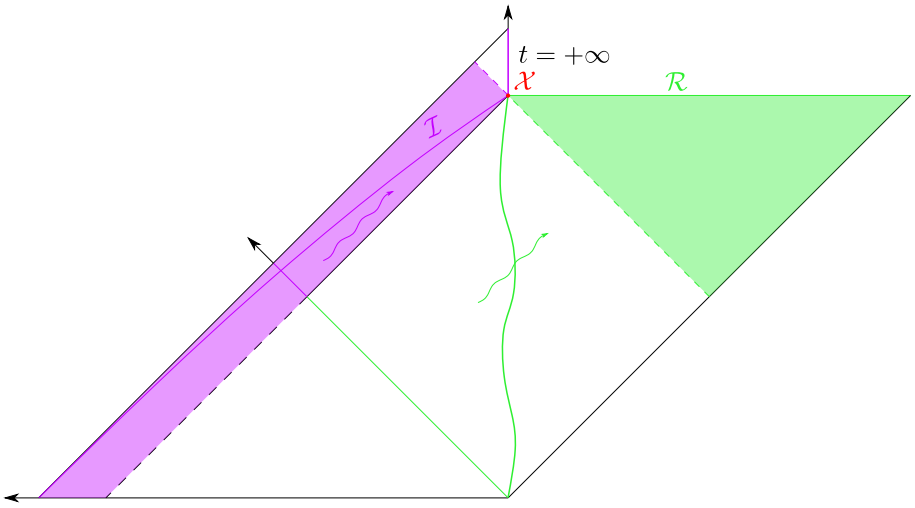

Figure 6.4: The final island. The island eventually ends up at the same location as the observer on the boundary. There is no $\mathcal{BH}$ anymore, a full Cauchy slice is given by $\mathcal{I} \cup \mathcal{R}$. At this point, the observer has caught all the outgoing radiation and can construct the interior (in purple).

As the boundary observers moves to $t \to +\infty$ and ends at f_∞, the Unruh detector will have collected all the outgoing radiation from the EBH resulting in full knowledge and a zero entropy: $\mathcal{I}$ and $\mathcal{BH}$ continuously claim less and less of the radiation. Eventually, $\mathcal{BH}$ disappears and a full Cauchy slice is now established by $\Sigma = \mathcal{I} \cup \mathcal{R}$ (see Fig. 6.4). If the quantum state was pure on this Cauchy slice, then surely $S(\mathcal{BH}) = S(\mathcal{I} \cup \mathcal{R}) = S(\Sigma) = 0$. Therefore,

we expect that the island eventually recedes to this boundary point for $t \to +\infty$. The captured radiation can be used to almost fully reconstruct the BH interior – the part lying within the EW of the island and the only region relevant for the observer. Notice how the island region is associated to the remaining interval above the boundary point at f_∞. Had we not taken this into account, information had been lost and the observer would not be able to reconstruct the interior. This is a clear difference between information loss and preservation when incorporating the existence of such an island. At this point, the scrambling time is zero since the island and the boundary observer coincide; all the information is immediately available!

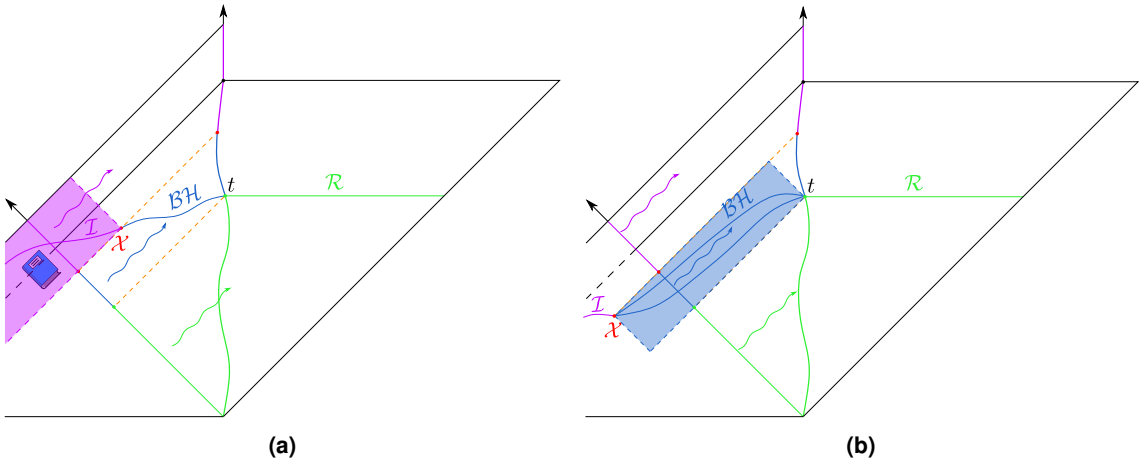

Figure 6.5: (a) An island in front of the horizon after the pulse. The observer could by acting on his radiation $\mathcal{R}$ decode everything which lies inside the purple EW of the island region, including a diary. This EW partially consists of the outgoing radiation which has yet to be released – the very late radiation. **(b)** The island before the pulse. We are free to deform $\mathcal{BH}$ within its EW, doing so leads to a different intersection with the pulse. To be consistent, it must capture the radiation stemming from the part lying within the EW.

It is interesting to discuss the difference between the island lying in the interior or in the exterior – Fig. 6.3 vs Fig. 6.5a. An island which lies in front of the horizon captures a part of the radiation the observer has yet to capture, we called this the very late radiation. Additionally, the EW of the island extends to the exterior meaning that the observer can reconstruct that part of spacetime with the radiation he already has access to. This includes a diary which enters the EW of the island but has not reached the horizon yet. One could ask themselves whether it violates causality or not. The first appearance of such an island was in [155] for an eternal AdS_2 BH; causality was restored by means of the quantum focussing conjecture [161]. Other cases also report a possible island extending to the outside [157, 162–166]. Considering quantum corrections to the event horizon, it was suggested that the island may be inside the stretched horizon [167] but outside the classical horizon [164]. In higher-dimensional systems this effect can be explained in terms of EW nesting [104, 106, 162, 168].

Finally, for the island lying before the pulse there is another interesting phenomenon (Fig. 6.5b). Since radiation only departs from the pulse onwards, it should not capture any outgoing radiation: there is no EBH sending out radiation yet. If the island is nontrivial, the island region actually captures nothing but has a contribution only stemming from its boundary. Nevertheless, the BH region now also partially lies in this region of spacetime without radiation. Naturally, one would think that the radiation which gets captured would be that between $u = t$ and where $\mathcal{BH}$ intersects the pulse. Despite that, from Ch. 2 we know we can freely deform the interval within its causal diamond – the EW. Hence, we can deform the interval such that the intersection with the pulse changes, resulting in an increase or decrease in the amount of radiation it captures. This seems paradoxical at first because such deformations leave the entropy invariant, yet we can 'freely' choose how much radiation it captures. Analo-

gously, this would also change the interval on the boundary curve it describes. The island after the pulse has no such problems. It would be therefore more natural if the BH region captures only the radiation within its EW. This would be the radiation between $u = t$ and the island mapped to the pulse along a null line. Only in this way the description remains consistent.

6.I.a Poincaré vs Boundary Coordinates

In Ch. 5 we found the time reparametrisation associated to an EBH (5.69). Furthermore, we observed that by using this coordinate transformation $X^+(u) = f(u),\ X^-(v) = f(v)$, the boundary coordinates (u, v) can only look up to the horizon at $X^+ = f_\infty$ (Fig. 5.5). Hence, we immediately encounter a difficulty; when looking for islands using the boundary coordinates we can never find an island lying behind the horizon. So, one would be tempted to always use the Poincaré coordinates. This is not immediately feasible when searching for islands behind the pulse because the dilaton expression can only be written using the parametrisation if one uses the boundary coordinate v (5.82). Since generally $v \leq t$, and thus $f(v) \leq f(t)$, it poses no problem to use v as we will not be reaching the limit value in this direction. It only excludes a small region of possible islands – the region above $F = f_\infty$. However, such islands would always lie inside the lightcone of the boundary observer, resulting in a timelike interval $t > v$. Alternatively, one could use the integral expression instead which is reconcilable with Poincaré coordinates at the cost of analytical simplicity(5.57a, 5.57b).

Due to these considerations, we could look for islands using mixed coordinates (X^+, v) in this regime. The use of mixed coordinates is indeed what is done in some papers. However, this is generally not a good idea because the value of the entropy can differ in mixed coordinates. Whilst the dilaton as a scalar is invariant under coordinate transformations, the entropy is only invariant under Möbius transformations because it are precisely only these ones which leave the vacuum and stress tensor invariant. In mixed coordinates, we would replace X^- by a conformal transformation $X^-(v) = f(v)$. This does not leave the vacuum and entropy invariant because of the anomalous transformation in the stress tensor (5.39a, 5.39b). Accordingly, one would find different islands in these setups and a different Page curve as well.

Some authors prefer to use mixed coordinates with the Kruskal–Szekeres coordinate W^+ instead, they have a similar form as those in the static case (5.54a, 5.54b). Although this is just a Möbius transformation of the Poincaré coordinates, it is a conformal transformation of the boundary coordinates. Hence, we can apply the previous discussion on this mixing as well. Another reason would be that if one uses the cross ratio (5.92) one needs to apply an equal Möbius transformation on each point in order for it remain a projective invariant. This is certainly not the case for the Kruskal–Szekeres coordinates.

The bottom line is to be careful when using mixed coordinates; it is advised to stick to a singular coordinate system instead and evaluate the full Page curve with respect to that system. In certain cases, which we will encounter in the following sections, it can happen that both coordinate systems or mixed coordinates provide us with the same entropy and island. But this is not true in general. Especially since this requires the island to lie outside the horizon, otherwise the mapping $X^+(u) = f(u)$ does not work.

This discussion will be of importance in the next chapter where we make use of the renormalised entropy (5.90), forcing us to only use boundary coordinates.

6.II The Radiation and Bekenstein–Hawking Entropy

In Subsect. 6.I we took our radiation region $\mathcal{R}$ to lie along the pulse; this is the interval between (σ, σ) and $(u = t,\ \sigma/2)$ where σ is very small and only there to keep it spacelike (Fig. 6.2) [148].

Without loss of generality we set $\phi_0 = 0$ and work in units of $2\phi_r/4G_\mathsf{N}$ for all coming computations; the evaporation rate k was given in (5.67).

We could now do a quick computation of the entropy solely attributed to this region, equal to plugging the trivial island $\mathcal{I} = \emptyset$ into the island formula (4.21).

With $\sigma \approx 0$ we have $f(\sigma) \approx 0, f'(\sigma) \approx 1, f''(\sigma) \approx 0$ such that (5.88)

$$S(\mathcal{R}) = k \ln 4 \tag{6.1}$$

which has no dilaton contribution and is completely time-independent. The time-dependence actually resides in the cutoff $\delta_{X_2^+} = f'(t)\delta$

$$S[\mathcal{R}(t)] = -2k \ln \frac{f'(t)\delta}{2} \tag{6.2}$$

This entropy diverges for $t \to +\infty$ since $f'(t) \to 0$.

Because we chose to not take the cutoffs into account in this chapter, we do not discuss this further and do not use it for our results in the following sections.

The same calculation by making use of the renormalised entropy (5.90) was first done in [148], through the same steps as before

$$S_\mathsf{ren}[\mathcal{R}(t)] = \frac{k}{2} \ln \frac{f(t)^2}{f'(t)t^2} \tag{6.3}$$

This entropy starts at 0 and quickly reaches a fixed value, as is seen in Fig. 6.6a, determined by the limit of $f'(t)t^2$ found from (B.7a, B.8a, B.9).

$$\begin{aligned} \lim_{t\to+\infty} f'(t)t^2 &= \frac{1}{\alpha^2} \lim_{t\to+\infty} \left(\frac{t}{N(t)}\right)^2 \\ &= \left(\pi T I_1\left[\frac{2\pi T}{k}\right]\right)^{-2} \end{aligned} \tag{6.4}$$

Since by making use of l'Hôpital's rule

$$\begin{aligned} \lim_{t+\to\infty} \frac{t}{N(t)} &= \frac{1}{I_1[\alpha]} \lim_{t\to+\infty} \frac{t}{K_0[\alpha e^{-\frac{k}{2}t}]} \\ &\overset{H}{=} \frac{2}{\alpha k I_1[\alpha]} \lim_{t\to+\infty} \frac{e^{\frac{k}{2}t}}{K_1[\alpha e^{-\frac{k}{2}t}]} \\ &= -\frac{2}{\alpha k I_1[\alpha]} \alpha \end{aligned} \tag{6.5}$$

Subsequently, by making use of the limit value (5.70) we end up with

$$\lim_{t\to+\infty} S_\mathsf{ren}[\mathcal{R}(t)] = k \ln I_0\left[\frac{2\pi T}{k}\right] \tag{6.6}$$

The plot 6.6a shows $\tilde{S} = S/k$ as a function of kt since both are dimensionless quantities. We refer to the latter as the **island time**; it sets a natural timescale for the evolution of the island. Actually, we could have worked with $kf(kt)$ in the entropy $\tilde{S}(kt)$ instead; or work in $e^{-kt/2}$. Similarly for the coordinates $kX^\pm$, ku, kv. In this case, our model would truly have been dimensionless and the only relevant parameter in our theory would be the ratio $\frac{k}{T}$ – the **island parameter (IP)**. It determines how rapidly $f(t)$ reaches the horizon value f_∞. Alternatively, we could have multiplied $f(t)$ and the locations with the temperature T instead, also producing a dimensionless model. However, in light of the island time it seems more natural to use k.

Regarding the IP, the two limit scenarios can be explained as well.

- **Static BH limit:** this coincides with the IP going to zero via $k \to 0$ or $T \to +\infty$. The first one is directly equivalent to no evaporation, as seen from the Schwarzian (5.68a) or the exponential dependence in (5.69). Since $k \propto c$, this can be seen as decreasing the amount of evaporation channels the BH has access to, slowing down the evaporation. We should be careful in this regard, we implicitly assumed a large central charge c in order for the graviton contribution to be negligible. The latter corresponds to shooting in a pulse with infinite energy (5.36). It is 'non-evaporating' in the sense that the energy is infinite and hence decays sluggishly.

- **Poincaré limit:** this corresponds to a diverging IP. Either by instant evaporation $k \to +\infty$ or by having no pulse at all $T \to 0$.

Unfortunately, in what follows we did not follow this approach. Instead, we varied k and kept the temperature fixed at $T = \frac{1}{2\pi}$.

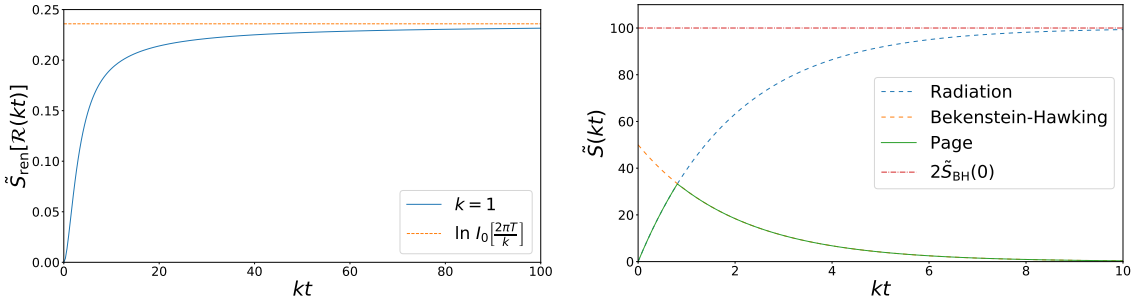

(a) **(b)**

Figure 6.6: **(a)** The renormalised radiation entropy (6.3) for $k = 1$ and $T = \frac{1}{2\pi}$. It starts at 0 and asymptotes to the value given by (6.6). **(b)** The quasistatic approximations. Following the minimum results in the Page curve. Also note how the radiation asymptotes to twice the initial BH value.

Interestingly, we can repeat the story for a macroscopic BH. We already know such BHs have a sluggish evaporation rate $k \ll 1$ since the evaporation time is huge (3.26). Therefore, we can make use of the approximations of the modified Bessel functions (B.1a, B.1a). In [148] they found that for such a BH

$$S_{\text{ren}}[\mathcal{R}(t)] \approx 2\pi T \left(1 - e^{-\frac{k}{2}t}\right) \tag{6.7}$$

In this case, the BH entropy can be quasistatically approximated by the entropy of the static solution (5.49c) with the time-dependent effective temperature (5.72)

$$S_{\text{BH}}(t) = \pi T e^{-\frac{k}{2}t} \tag{6.8}$$

in our chosen units.

By following the minimum of these two curves shown in Fig. 6.6b we obtain the Page curve with accompanying Page time

$$kt_{\text{Page}} = 2\ln\frac{3}{2} \tag{6.9}$$

However, only the radiation entropy is a fine-grained entropy and stems from using the island rule; the Bekenstein–Hawking entropy is rather coarse-grained. The QES prescription/island rule dictates that we should take the minimum between two fine-grained entropies, the Bekenstein–Hawking entropy is generally not associated to an island to begin with. Without the island formula, there is no instruction telling us to take the minimum. Either way, this

curve would be consistent with unitarity.

Besides, observe how the radiation entropy goes to twice that of the initial BH value $S_{\text{ren}}[\mathcal{R}(t \to +\infty)] = 2S_{\text{BH}}(t=0)$. This is not a coincidence, because when we look at their variation we unearth

$$\delta S_{\text{ren}}[\mathcal{R}(t)] = -2\delta S_{\text{BH}}(t) \tag{6.10}$$

It satisfies Zurek's irreversibility argument [148, 159, 169]. Zurek argued that an EBH in empty space of D spatial dimensions ends with a Bekenstein–Hawking entropy which is a factor $(D+1)/D$ larger than the initial value; it is an irreversible process. This factor originates from comparing the increasing entropy of a free Boson gas at T_H with the decreasing entropy of a BH

$$\delta S = \frac{D+1}{D}\frac{E}{T_H}dt, \qquad \delta S_{\text{BH}} = -\frac{E}{T_H}dt \tag{6.11}$$

Note that in this case, the factor appears between the Bekenstein–Hawking entropy and a fine-grained entropy instead; a result from the domination of correlations across the horizon.

6.III The Generalised Entropy

We want to navigate towards the islands, so we begin by denoting the most general expression for the entropy consisting of the dilaton contribution (5.82) and that of the bulk quantum fields (5.88) for an interval $(u_1, v_1) \to (u_2, v_2)$

$$\begin{aligned} S = &\left[\frac{1}{2}\frac{f''(v_2)}{f'(v_2)} + \frac{f'(v_2)}{f(u_2)-f(v_2)}\right] + k\ln\left(4\frac{X_1^+ - X_2^+}{X_1^+ - X_1^-}\frac{X_1^- - X_2^-}{X_2^+ - X_2^-}\right) \\ &- \frac{k}{2}\ln \delta_{X_1^+}\delta_{X_2^+}\delta_{X_1^-}\delta_{X_2^-} \end{aligned} \tag{6.12}$$

and as a reminder: $X^+(u) = f(u), X^-(v) = f(v)$. One of our points is anchored to the boundary, hence we push (u_1, v_1) to this boundary by setting (5.29a, 5.29b)

$$u_1 = v_1 = t \tag{6.13a}$$
$$f(u_1) = f(v_1) = f(t) \tag{6.13b}$$
$$f(u_1) - f(v_1) = 2\varepsilon f'(t) \tag{6.13c}$$

and rename $(u_2, v_2) \equiv (u, v)$ which eventually becomes the location of the island

$$S(t,u,v) = \left[\frac{1}{2}\frac{f''(v)}{f'(v)} + \frac{f'(v)}{X^+ - X^-}\right] + k\ln\left(2\frac{f(t)-X^+}{\varepsilon f'(t)}\frac{f(t)-X^-}{X^+ - X^-}\right) \tag{6.14}$$

We ignored the cutoffs. One could argue that we are simply adding a local term to counter the contribution from the cutoffs, a similar remark can be made for ε, but it is not immediately clear how we can give this an operational meaning.

We could have chosen to ignore ε as well since its value has no influence on the location of the island; it only leads to an additive contribution in all cases. But, we keep it in the expression such that the argument of the logarithm remains dimensionless: it is a spacetime cutoff and has the same dimension as $X^\pm$. When discussing results, this contribution will not be added to our entropy. Because the value is quite arbitrary, it would not be representative to include this contribution when comparing the entropy with the BH result (6.8) which does not contain this cutoff.

6.IV The Pre-Pulse Island

For islands before the pulse, they must satisfy $v \leq 0 \leq t \leq u$ or $X^- \leq 0 \leq f(t) \leq X^+$. In this regime we have $f(v) = v = X^-$ and the entropy reduces to (6.14)

$$S_{\text{pre}}(t, X^+, X^-) = \frac{1}{X^+ - X^-} + k \ln\left(2\frac{f(t) - X^+}{\varepsilon f'(t)}\frac{f(t) - X^-}{X^+ - X^-}\right) \tag{6.15}$$

6.IV.a Finding the Island

To find the island $\mathcal{X}$, we extremise over the location (X^+, X^-) leading to the system

$$\partial_+ S_{\text{pre}} = 0 = \frac{-1}{(X^+ - X^-)^2} - k\left(\frac{1}{f(t) - X^+} + \frac{1}{X^+ - X^-}\right) \tag{6.16a}$$

$$\partial_- S_{\text{pre}} = 0 = \frac{1}{(X^+ - X^-)^2} + k\left(\frac{-1}{f(t) - X^-} + \frac{1}{X^+ - X^-}\right) \tag{6.16b}$$

There is one solution corresponding to the bifurcate horizon at $(+\infty, -\infty)$ with $\mathcal{BH}$ being a full Cauchy slice of the Poincaré patch. At this location, the entropy is equal to the extremal entropy and a diverging contribution from the bulk, so we will not look further into this solution. Such an island is equivalent to the trivial island: $\mathcal{BH} \cup \mathcal{R}$ constitutes a full Cauchy slice in our extended geometry.

To find nontrivial islands, we start by summing both equations to get

$$\begin{aligned} \frac{1}{X^+ - f(t)} + \frac{1}{X^- - f(t)} &= 0 \\ \Rightarrow X^+ + X^- &= 2f(t) \end{aligned} \tag{6.17}$$

Naturally, we assumed both $X^\pm \neq f(t)$ which would otherwise imply $u = v = t$: a point on the holographic boundary. By solving for one coordinate and plugging it in either equation effortlessly leads to the solution

$$X^+_{\mathcal{X}} = f(t) + \frac{1}{2k}, \qquad X^-_{\mathcal{X}} = f(t) - \frac{1}{2k} \tag{6.18}$$

with generalised entropy (6.15)

$$S_{\text{pre}}[\mathcal{X}(t)] = k[1 - \ln\big(2\varepsilon k f'(t)\big)] \tag{6.19}$$

Clearly, this entropy starts at a nonzero value and increases limitlessly but with a decreasing rate (see Fig. 6.7). This sort of island is equivalent to the picture in Fig. 6.5b.

In Ch. 4 we discussed the Hayden–Preskill protocol and determined the scrambling time (3.28): the minimum time for information to come out if we throw in a diary. For islands, we established that this is equivalent to the diary entering the EW of the island. Since it takes t_{scr} for the information to return, the island lies along an incoming null ray a scrambling time in the past of the boundary observer

$$t_{\text{scr}} = t - v_{\mathcal{X}} \tag{6.20}$$

In this case when recast in island time, we acquire (6.18)

$$k t_{\text{scr}}(t) = k[t - f(t)] + \frac{1}{2} \tag{6.21}$$

As time increases, the scrambling time becomes infinitely large and thrown in information is lost forever.

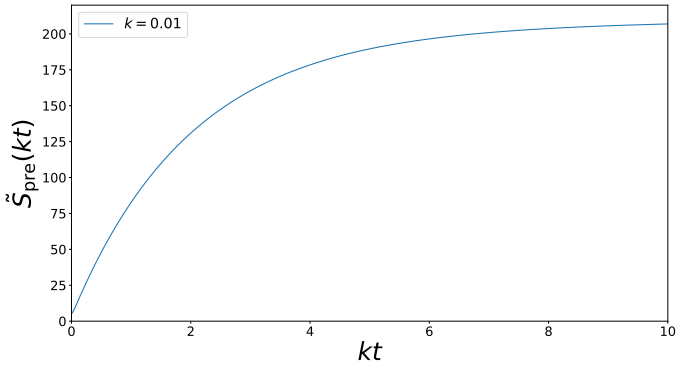

Figure 6.7: Evolution of the entropy associated to the pre-pulse island (6.19) for $k = 0.01$ and $T = \frac{1}{2\pi}$.

One might wonder, in light of the discussion in Subsect. 6.I.a, if either using the Poincaré or boundary coordinates would result in the same island and the same entropy. Although this is obvious for the v coordinate, there is a slight ambiguity whether we should use $X^+(u) = u$ or $X^+(u) = f(u)$ in this part of our spacetime with $u > 0$.[1] From the structure of the expression (6.15) follows $\partial_u S_{\text{pre}}(t, u, X^-) = f'(u)\partial_+ S_{\text{pre}}(t, X^+, X^-) = 0$ as the first island condition. For general finite u, the derivative $f'(u)$ is nonzero and can be discarded. Hence, we would end up with the same island and the same entropy if we had used $X^+(u) = f(u)$ instead. The only difference that might appear is in the existence of the island: u cannot look behind the horizon, so if the island crosses it – and it will – the solution for u ceases to exist. However, if the island remains outside for all t there will always be an appropriate u leading to the same value for the entropy.

6.IV.b Existency Conditions

On account of searching before the pulse, the island is only physical if $X^- \leq 0$, or if (6.18)

$$kf(t) \leq \frac{1}{2} \tag{6.22}$$

Since our reparametrisation starts at $f(0) = 0$, this island remains physical for at least a certain time range depending on the IP. The reparametrisation increases monotonically and reaches it maximum value f_∞ at $t \to +\infty$, so we can have an island which is supported for all boundary times t only if

$$kf_\infty \leq \frac{1}{2} \tag{6.23}$$

The horizon value kf_∞ was found earlier (5.70), but we retake it here

$$kf_\infty = \frac{1}{\pi T}\frac{I_0[\frac{2\pi T}{k}]}{I_1[\frac{2\pi T}{k}]} \tag{6.24a}$$

$$= \frac{k}{\pi T} + \left(\frac{k}{2\pi T}\right)^2 + \mathcal{O}\left[\left(\frac{k}{T}\right)^3\right] \tag{6.24b}$$

In the last line we expanded for small values of the IP, or equivalently for large arguments of the modified Bessel functions, making use of (B.2) [14].

Whilst not very elucidating, using this expansion we can make a crude estimation for the

[1] In the next chapter we will elaborate further on this ambiguity.

IP at which this condition is saturated

$$\begin{aligned} kf_\infty &= \frac{1}{2} \\ \Rightarrow \frac{k}{\pi T} + \frac{1}{4}\left(\frac{k}{\pi T}\right)^2 &= \frac{1}{2} \end{aligned} \tag{6.25}$$

which is a quadratic equation in $\frac{k}{\pi T}$ and can be easily solved to the sole positive solution

$$\frac{k}{T} = 2\pi\left(-1+\sqrt{\frac{3}{2}}\right) \approx 1.412 \tag{6.26}$$

Clearly, this approximation is crude because we were expanding for large arguments but for this value $\frac{2\pi T}{k} \approx 4.45$, neither big nor small. A numerical computation gives $\frac{k}{T} \approx 1.3846$; maybe our approximation was not that bad after all.

In summary, depending on the IP we obtain two scenarios

- $\frac{k}{T} \leq 1.3846$: the island is supported for all t;
- $\frac{k}{T} > 1.3846$: the island is only supported for a finite range in t.

Therefore, by decreasing the IP we can make sure the island is always physical. In particular, this holds for macroscopic BHs.

As for the case of the island only having finite support, the boundary time t_e when it ceases to exist satisfies

$$kf(t_e) = \frac{1}{2} \tag{6.27}$$

This should be found numerically in terms of the modified Bessel functions $kf(t_e)(\frac{k}{T})$ and decreases for an increasing IP. This condition can also be found from plugging $X^- = 0$ into the equations and solving for $(X^+, f(t))$. In the Poincaré limit, the reparametrisation becomes $kf(t) = kt$ and the island is only supported at $kt \leq \frac{1}{2}$. The location of the island on the pulse would be the origin.

Regarding the Hayden–Preskill protocol, islands without full support for the boundary time range do not have a diverging scrambling time; it rather saturates to $t_{\text{scr}} = t_e$ (6.21), not very surprising.

As f_∞ is the horizon of the EBH, we can determine if the island lies in front of or behind it: $X^+ > f_\infty$. Due to monotonicity, the island remains inside if it was initially behind or on the horizon at $t = 0$

$$kf_\infty \leq \frac{1}{2} \tag{6.28}$$

which is exactly the same condition as for the island to exist for all t (6.23). If not, the island starts in front of the horizon and crosses it at t_h when

$$kf(t_h) + \frac{1}{2} = kf_\infty \tag{6.29}$$

For this horizon crossing to be physical the island still needs to exist, or equivalently $t_h \leq t_e$, or using the monotonicity of $f(t)$

$$\begin{aligned} kf(t_h) &\leq kf(t_e) \\ \Rightarrow kf_\infty &\leq 1 \end{aligned} \tag{6.30}$$

We can again determine when this value is saturated and coincides with the scenario in which the island exactly ends at the intersection of the horizon and the pulse. The crude approximation can be reused to give

$$\frac{k}{T} = 2\pi(-1+\sqrt{2}) \approx 2.603 \tag{6.31}$$

Again this is even cruder than the one before, yet it lies close to the numerical computation: $\frac{k}{T} = 2.4312$.

We can conclude

- $\frac{k}{T} \leq 2.4312 \Rightarrow t_h \leq t_e$: the island crosses the horizon in finite time and stays behind it until t_e;
- $\frac{k}{T} > 2.4312 \Rightarrow t_h > t_e$: the island forever stays in front of the horizon until t_e.

Adjoining this to our previous discussion leads to three scenarios depending on the IP (Fig. 6.8 shows this dependence):

1. $\frac{k}{T} \leq 1.3846$: the island exists for all t, lies behind the horizon, and has a diverging scrambling time;
2. $1.3846 < \frac{k}{T} < 2.4312$: the island starts in front of the horizon, crosses it in finite time t_h and stays behind it until $t_e > t_h$. It has a finite scrambling time;
3. $\frac{k}{T} \geq 2.4312$: the island starts in front of the horizon and stays there until it reaches its end at the pulse in finite t_e with a finite scrambling time as well.

It is interesting to observe that by increasing the IP, we not only limit its existence but also extract it from behind the horizon. A similar scenario will not happen in the renormalised case. As argued in Section 6.I.a, the boundary coordinates (u, v) are not fit for islands behind the horizon.

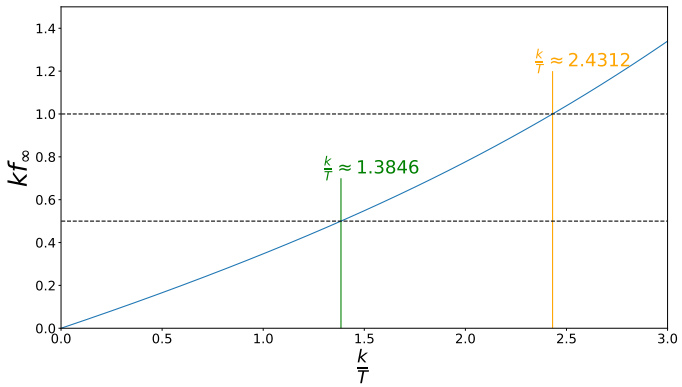

Figure 6.8: Dependence of the horizon value kf_∞ on the IP. The two saturation values (6.23) and (6.30) are shown as well.

From the solution (6.18) we can extract its trajectory in the Poincaré patch as

$$F_{\text{pre}}[\mathcal{X}(t)] = \frac{X^+_{\text{pre}} + X^-_{\text{pre}}}{2} = f(t) \tag{6.32}$$

$$Z_{\text{pre}}[\mathcal{X}(t)] = \frac{X^+_{\text{pre}} - X^-_{\text{pre}}}{2} = \frac{1}{2k} \tag{6.33}$$

The island only evolves in boundary time t at the same rate as $f(t)$, whereas it remains stationary in the spatial dimension. Considering the three scenarios above, if k remains fixed

and we change the IP only by changing the temperature T, all three scenarios are part of the same Z-slice at $kZ = \frac{1}{2}$.

From this viewpoint it is not hard to recast our conditions (6.23, 6.30) into a geometrical picture, illustrated in Fig. 6.9. Due to the island moving vertically through our Penrose diagram, t_e is exactly the time when the island reaches the matter pulse. Hence, there can be no horizon crossing if the island lies to the right of the intersection between the matter pulse and the horizon at $Z = \frac{f_\infty}{2}$, and this gives rise to the second condition for the horizon crossing (6.30).

The island is perennial and never reaches the pulse if it stays to the left of the intersection between the horizon and the Z-axis. This point coincides with the intersection of the horizon in the X^+ and X^- directions: $X^+ = -X^- = f_\infty$ and leads to the position $Z = f_\infty$. Again, the island staying to the left of this point is exactly equivalent to the first condition (6.23).

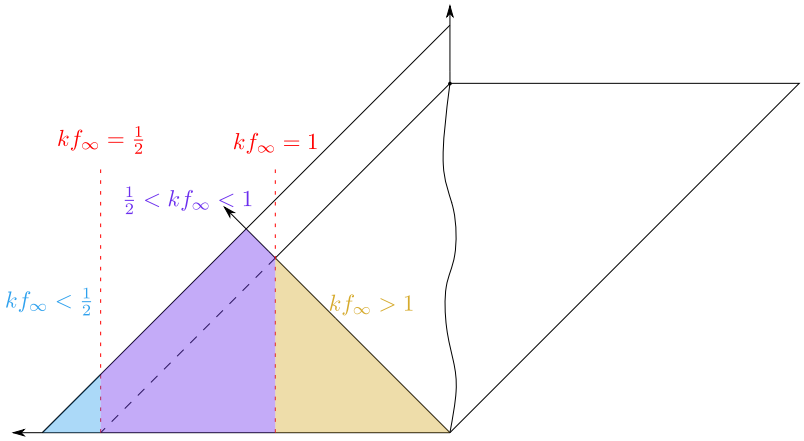

Figure 6.9: Geometrical representation of the three scenarios.

6.V The Post-Pulse Island

For islands after the pulse, we are searching in the regime $0 \leq v \leq t \leq u$ or $0 \leq X^- \leq f(t) \leq X^+$, and we need to use the most general expression for the entropy (6.14)

$$S_{\text{post}}[t, X^+, v] = \left[\frac{1}{2}\frac{f''(v)}{f'(v)} + \frac{f'(v)}{X^+ - f(v)}\right] + k \ln\left(2\frac{f(t) - X^+}{\varepsilon f'(t)}\frac{f(t) - f(v)}{X^+ - f(v)}\right) \tag{6.34}$$

Whilst the expression for the bulk entropy stays the same, we should insert $X^- = f(v)$ precisely because the dilaton needs to be rewritten into a function of v if we do not want to make use of the memory integrals (5.57b). A consequence of this fact is that we cannot look behind the horizon in the X^--direction, but this poses no problem as argued in Subsect. 6.I.a.

6.V.a Finding the Island

We start by extremisation with respect to X^+

$$\partial_+ S_{\text{post}} = 0 = \frac{-f'(v)}{[X^+ - f(v)]^2} - k\left(\frac{1}{f(t) - X^+} + \frac{1}{X^+ - f(v)}\right) \tag{6.35}$$

to find a solution in terms of (t, v)

$$X^+_{\mathcal{X}}(t, v) = \frac{f'(v)f(t) - kf(v)[f(t) - f(v)]}{f'(v) - k[f(t) - f(v)]} \tag{6.36a}$$

$$= f(t) + k\frac{f(t) - f(v)}{f'(v)}\left[\frac{1}{f'(v)} - f(v)\right] + \mathcal{O}(k^2) \tag{6.36b}$$

In the last line we expanded the denominator to linear order in k, one should actually think of this as expanding $kX^+_{\mathcal{X}}$ for small values of the IP.

Note that if $t \to +\infty$, automatically $u \to +\infty$ due to the condition $t \leq u$. Plugging this into the above equation results in $X^- = X^+ = f_\infty$. This is exactly what we would expect from our discussion in Sect. 6.I: the island ends on the boundary point where the observer ends. It remains to be seen whether $v \to +\infty$ satisfies the second condition or not of course.

Should we be careful in using mixed coordinates (X^+, v)? Because the entropy (6.34) only explicitly depends on X^+, one would have $\partial_u S_{\text{post}}(t,u,v) = f'(u)\partial_+ S_{\text{post}}(t, X^+, v) = 0$, so the same remarks can be made as in the pre-pulse case.

The other condition is much harder to solve, precisely due to the complicated expression for the dilaton

$$\begin{aligned}\partial_v S_{\text{post}} = 0 =& \frac{1}{2}\partial_v \frac{f''(v)}{f'(v)} + \frac{f''(v)}{X^+ - f(v)} + \left(\frac{f'(v)}{X^+ - f(v)}\right)^2 \\ &+ kf'(v)\left[\frac{1}{X^+ - f(v)} - \frac{1}{f(t) - f(v)}\right]\end{aligned} \tag{6.37}$$

in which we should set $X^+ \to X^+_{\mathcal{X}}(t,v)$. Using the solution (6.36a) we can simplify this expression somewhat

$$\begin{aligned}X^+_{\mathcal{X}}(t,v) - f(v) &= \frac{f(t) - k\frac{f(v)}{f'(v)}[f(t) - f(v)]}{1 - \frac{k}{f'(v)}[f(t) - f(v)]} - f(v) \\ &= \frac{f(t) - f(v)}{1 - \frac{k}{f'(v)}[f(t) - f(v)]} \\ \Rightarrow \frac{f'(v)}{X^+_{\mathcal{X}}(t,v) - f(v)} &= \frac{f'(v)}{f(t) - f(v)} - k\end{aligned} \tag{6.38}$$

such that the first term of this expression cancels out with the last term in the v-condition (6.37)

$$\partial_v S_{\text{post}} = 0 = \frac{1}{2}\partial_v \frac{f''(v)}{f'(v)} + \frac{f''(v)}{X^+_{\mathcal{X}}(t,v) - f(v)} + \left(\frac{f'(v)}{X^+_{\mathcal{X}}(t,v) - f(v)}\right)^2 - k^2 \tag{6.39}$$

It is interesting to see that to linear order this condition reduces to $\partial_v S_{\text{dilaton,post}} = 0$ which would be the one stemming from the RT formula. On the other hand, this condition gives the trajectory of the apparent horizon in terms of $X^+_{ah}(v)$ in function of the independent parameter v if we did not specify X^+. Perspicuously, since we have the extra condition on X^+ this differs from the apparent horizon as solving this equation results in $v_{\mathcal{X}}(t)$. The quantum contribution is purely the last term $-k^2$ due to the particular form of $X^+_{\mathcal{X}}(t,v)$.

The dilaton contribution still remains as complex as ever. By using some results from Appendix B.II we try to reduce the complexity as fit for a numerical approach. To this end, we start with grouping the results as a good reference point for later

$$f(t) = \frac{1}{\pi T}\frac{A(t)}{N(t)} \tag{6.40a}$$

$$f'(t) = \frac{1}{[\alpha N(t)]^2} \tag{6.40b}$$

$$f''(t) = 2\pi T e^{-\frac{k}{2}t} f'(t)\frac{B(t)}{N(t)} \tag{6.40c}$$

$$\partial_t \frac{f''(t)}{f'(t)} = 2(\pi T)^2 e^{-kt}\left[-1 + \left(\frac{B(t)}{N(t)}\right)^2\right] \tag{6.40d}$$

with functions

$$A(t) = I_0\left[\frac{2\pi T}{k}\right] K_0\left[\frac{2\pi T}{k}e^{-\frac{k}{2}t}\right] - K_0\left[\frac{2\pi T}{k}\right] I_0\left[\frac{2\pi T}{k}e^{-\frac{k}{2}t}\right] \tag{6.41a}$$

$$N(t) = K_1\left[\frac{2\pi T}{k}\right] I_0\left[\frac{2\pi T}{k}e^{-\frac{k}{2}t}\right] + I_1\left[\frac{2\pi T}{k}\right] K_0\left[\frac{2\pi T}{k}e^{-\frac{k}{2}t}\right] \tag{6.41b}$$

$$B(t) = K_1\left[\frac{2\pi T}{k}\right] I_1\left[\frac{2\pi T}{k}e^{-\frac{k}{2}t}\right] - I_1\left[\frac{2\pi T}{k}\right] K_1\left[\frac{2\pi T}{k}e^{-\frac{k}{2}t}\right] \tag{6.41c}$$

Note that all functions can be rewritten in terms of the variable $\exp\left(-\frac{k}{2}t\right)$, this can be exploited in a numerical setup.

First, notice that since $f''(v) \propto f'(v)$, the second term in the v-condition (6.39) can be written as

$$\frac{f''(v)}{X^+_{\mathcal{X}}(t,v) - f(v)} = 2\pi T e^{-\frac{k}{2}v}\frac{B(v)}{N(v)}\frac{f'(v)}{X^+_{\mathcal{X}}(t,v) - f(v)} \tag{6.42}$$

From this we can write the second and third term as

$$\begin{aligned}\partial_v \frac{f'(v)}{X^+ - f(v)}\bigg|_{X^+_{\mathcal{X}}(v,t)} &= \left[\frac{f''(v)}{f'(v)} + \frac{f'(v)}{X^+_{\mathcal{X}}(v,t) - f(v)}\right]\frac{f'(v)}{X^+_{\mathcal{X}}(t,v) - f(v)} \\ &= \left[2\pi T e^{-\frac{k}{2}v}\frac{B(v)}{N(v)} + \frac{f'(v)}{X^+_{\mathcal{X}}(t,v) - f(v)}\right]\frac{f'(v)}{X^+_{\mathcal{X}}(t,v) - f(v)}\end{aligned} \tag{6.43}$$

Combining this with (6.38) we ultimately obtain

$$\begin{aligned}0 = (\pi T)^2 e^{-kv}&\left[-1 + \left(\frac{B(v)}{N(v)}\right)^2\right] \\ &+ \left[2\pi T e^{-\frac{k}{2}v}\frac{B(v)}{N(v)} + \frac{f'(v)}{f(t) - f(v)} - k\right]\left[\frac{f'(v)}{f(t) - f(v)} - k\right] - k^2\end{aligned} \tag{6.44}$$

We can now already verify our prediction to which we alluded before by taking the limit $v \to +\infty$. Hence, $f(v) \to f_\infty,\ f'(v) \to 0$ and by combining (6.40a, 6.40c) with (B.7a, B.7b)

$$\lim_{v\to+\infty} e^{-\frac{k}{2}v}\frac{B(v)}{N(v)} \propto \lim_{x\to 0} x\frac{K_1[\alpha x]}{K_0[\alpha x]} = 0 \tag{6.45}$$

So, the limit $v \to +\infty$ indeed satisfies the condition and we have therefore proven our prediction. One may now ask whether we should have taken the limit $t \to +\infty$ first; and yes, this is indeed the correct order. By employment of l'Hôpital's rule one can easily check that the condition is again satisfied

$$\lim_{v\to+\infty}\frac{f'(v)}{f_\infty - f(v)} \overset{H}{=} -\lim_{v\to+\infty}\frac{f''(v)}{f'(v)} \propto \lim_{v\to+\infty} e^{-\frac{k}{2}v}\frac{B(v)}{N(v)} = 0 \tag{6.46}$$

Since we have to find $v_{\mathcal{X}}$ numerically, there is not an immediate expression available for the scrambling time. But it is expected to be decreasing as the island recedes to the boundary where the scrambling time is zero.

6.V.b The Initial Island

We expect that as t increases, so does $v_{\mathcal{X}}$ until it reaches its final value at the boundary $X^+ = X^- = f_\infty$. It follows that the earliest moment t_0 for the island to come into existence is when $v_{\mathcal{X}} = 0$. This leads to the quadratic equation (6.44)

$$(\pi T)^2 - \frac{1}{f(t)^2} + \frac{2k}{f(t)} = 0 \tag{6.47}$$

and can easily be solved to get the result

$$\frac{1}{kf(t_0)} = 1 + \sqrt{1 + \left(\frac{\pi T}{k}\right)^2} \tag{6.48}$$

where we chose the plus sign to acquire a positive answer. This can be inverted to

$$\begin{aligned} kf(t_0) &= \frac{1}{1 + \sqrt{1 + \left(\frac{\pi T}{k}\right)^2}} \\ &= \left(\frac{k}{\pi T}\right)^2 \left[\sqrt{1 + \left(\frac{\pi T}{k}\right)^2} - 1\right] \end{aligned} \tag{6.49}$$

The expression is what one would expect from solving the quadratic equation to $g(t) = \frac{1}{f(t)}$, observe how this initial time is only dependent on the IP.

By considering the limit values of the IP, we find that $kf(t_0)$ is bounded by 0 and $\frac{1}{2}$

$$\lim_{\frac{k}{T}\to 0} \frac{1}{1 + \sqrt{1 + \left(\frac{\pi T}{k}\right)^2}} = 0 \tag{6.50a}$$

$$\lim_{\frac{k}{T}\to +\infty} \frac{1}{1 + \sqrt{1 + \left(\frac{\pi T}{k}\right)^2}} = \frac{1}{2} \tag{6.50b}$$

From (6.49) we can find the starting value kt_0 for every IP and it turns out to be bounded as well

$$0 \leq kt_0 \leq \frac{1}{2} \tag{6.51}$$

For large values of the IP, the initial time quickly asymptotes to $kt_0 = \frac{1}{2}$ precisely because $f(t) \to t$ in this limit.

We can plug this into (6.38) to find the initial location on the pulse, we could call the combination (kt_0, kX_0^+) the **IP address** of the island

$$kX_0^+(t_0, 0) = \frac{kf(t_0)}{1 - kf(t_0)} \tag{6.52a}$$

$$= \frac{1}{\sqrt{1 + \left(\frac{\pi T}{k}\right)^2}} \tag{6.52b}$$

This expression is the same as the one found in [14] when looking close to the pulse. Moreover, because $kf(t_0)$ is bounded, we also find a bound on this quantity

$$0 \leq kX_0^+ \leq 1 \tag{6.53}$$

From this perspective, the two special values for the IP from the discussion in the pre-pulse island do not translate to special scenarios for the post-pulse island (Subsect. 6.IV.b).

Of particular interest, we can look for which IP the island already starts behind the horizon kf_∞. For this purpose, however, it is easier to check whether the initial location can even reach the would-be horizon $\frac{k}{\pi T}$ associated to the static solution

$$\begin{aligned} kX_0^+(0, t_0) &= \frac{k}{\pi T} \\ \Rightarrow \frac{\pi T}{k} &= \sqrt{1 + \left(\frac{\pi T}{k}\right)^2} \end{aligned} \tag{6.54}$$

Obviously, this leads to a false equation except in the limit for the IP to 0, and the would-be horizon just becomes the origin at $kX^+ = 0$. Therefore, the island inevitably starts on the pulse in front of the would-be horizon; this value increases more rapidly than $kX_0^+(0, t_0)$. Consequently, the island never starts at or behind the true horizon. The behaviour of all mentioned functions are shown in Fig. 6.10.

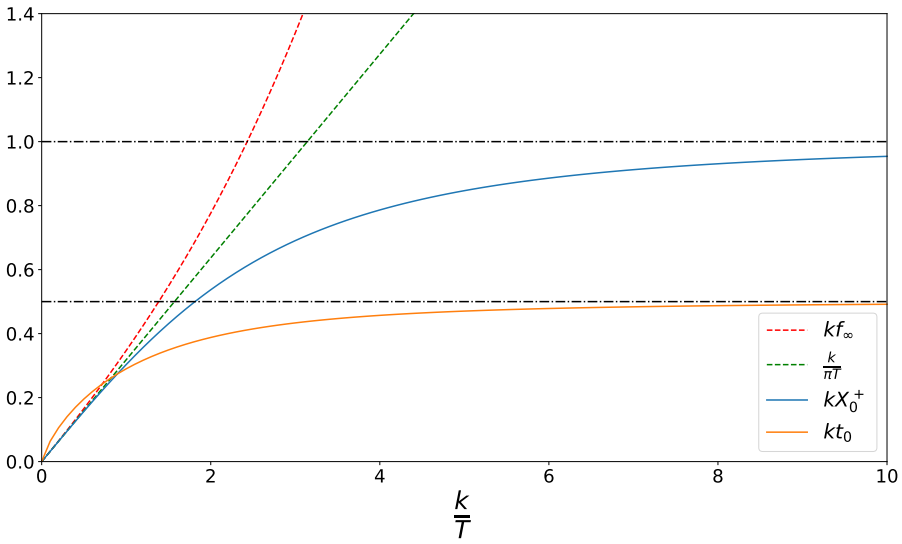

Figure 6.10: The IP address. The initial values $(kt_0,\ kX_0^+)$ plotted as a function of the IP. The would-be and true horizon are also plotted as a reference, along with the bounds $kt_0 = \frac{1}{2}$ and $kX_0^+ = 1$.

We can also infer the initial entropy (6.34, 6.52b)

$$\begin{aligned} S_{\text{post}}(t_0,\ X_0^+,\ 0) &= \frac{1}{X_0^+} + k \ln\left(2\frac{f(t_0) - X_0^+}{\epsilon f'(t_0)}\frac{f(t_0)}{X_0^+}\right) \\ &= k\left[\sqrt{1 + \left(\frac{\pi T}{k}\right)^2} + \ln\left(2\frac{k}{\epsilon}\frac{f(t_0)^2}{f'(t_0)}\right)\right] \end{aligned} \tag{6.55}$$

This expression depends on the IP through t_0, but there is also an explicit k-dependence within the logarithm. Its value diverges for IP $\to 0$.

6.V.c Using the Approximation

If the IP is very small, we can make use of the approximations (B.18–B.21)

$$f(t) = f_\infty \tanh\left(\frac{2\pi T}{k}[1 - e^{-\frac{k}{2}t}]\right) \tag{6.56a}$$

$$f'(t) = \pi T f_\infty e^{-\frac{k}{2}t}\left[1 - \left(\frac{f(t)}{f_\infty}\right)^2\right] \tag{6.56b}$$

$$f''(t) = -\frac{k}{2}f'(t)\left[1 + \frac{4\pi T}{kf_\infty}e^{-\frac{k}{2}t}f(t)\right] \tag{6.56c}$$

$$\partial_t \frac{f''(t)}{f'(t)} = -\frac{2\pi T}{f_\infty}e^{-\frac{k}{2}t}\left[f'(t) - \frac{k}{2}f(t)\right] \tag{6.56d}$$

We start with

$$\frac{f''(v)}{X_{\mathcal{X}}^+(t,v) - f(v)} = -\frac{k}{2}\left[1 + \frac{4\pi T}{kf_\infty}e^{-\frac{k}{2}v}f(v)\right]\frac{f'(v)}{X_{\mathcal{X}}^+(t,v) - f(v)} \tag{6.57}$$

from which follows that the second derivative in the v-condition combined with (6.38) results in

$$\partial_v \frac{f'(v)}{X^+ - f(v)}\bigg|_{X^+_{\mathcal{X}}(t,v)} = \left[\frac{f'(v)}{f(t)-f(v)} - k\right]\left[\frac{f'(v)}{f(t)-f(v)} - \frac{3}{2}k - \frac{2\pi T}{f_\infty}e^{-\frac{k}{2}v}f(v)\right] \tag{6.58}$$

The equation to solve becomes (6.39)

$$\begin{aligned} 0 = &-\frac{\pi T}{f_\infty}e^{-\frac{k}{2}v}\left[f'(v) - \frac{k}{2}f(v)\right] \\ &+ \left[\frac{f'(v)}{f(t)-f(v)} - k\right]\left[\frac{f'(v)}{f(t)-f(v)} - \frac{3}{2}k - \frac{2\pi T}{f_\infty}e^{-\frac{k}{2}v}f(v)\right] - k^2 \end{aligned} \tag{6.59}$$

6.VI Results & the Page Curve

The result of the post-island entropy for $k = 0.01$ is plotted in Fig. 6.11, this was numerically computed by making use of the approximated equations mentioned in the previous subsection.

Immediately apparent from the figure is the similar behaviour between the total entropy and the BH entropy. This is due to the tiny bulk contribution such that the dilaton dominates the total entropy leading to similar behaviour for both. It seems to confirm the claim that the entropy beyond the Page time can be well approximated by the BH entropy to which we alluded in Subsect. 4.III. However, the bulk contribution slightly increases with island time. This is not what we would expect: since the island moves towards the horizon, the bulk interval decreases in size until it vanishes at infinity (see Fig. 6.13). This contribution might start decreasing at a later time not on the figure, this requires a large precision numerically.

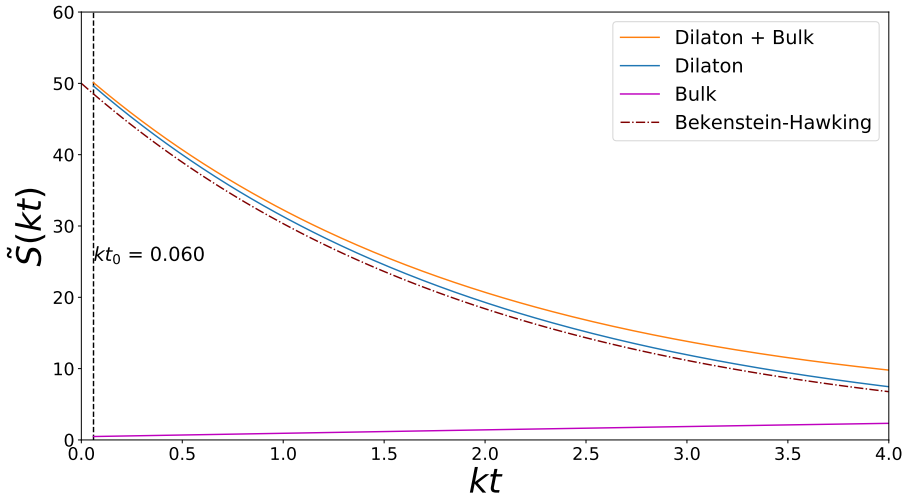

Figure 6.11: The post-island entropy for $k = 0.01,\ T = \frac{1}{2\pi}$ computed via Eq. (6.59). We show how both contributions, dilaton and bulk, contribute to the total entropy. The BH entropy is also plotted and lies very close to the dilaton part. The initial time according to (6.49) is depicted as the vertical line.

Combining the result from the post-island with those of the pre-island (6.19) finally leads to the Page curve as depicted in Fig. 6.12. As is evident, the Page curve first follows the entropy associated to the pre-pulse island and switches dominance at the Page time. At this moment, the post-pulse island becomes the new minimum and leads to a decrease reminiscent of the

BH formula. Eventually, the entropy returns to zero after an infinite boundary time.[2]

How the island exactly moves through the Poincaré patch is illustrated in Fig. 6.13. The pre-pulse island in this case corresponds to an IP value of 2 which constitutes the second scenario in 6.IV.b. The vertical trajectories of the pre-pulse island for different IP values only differ in the Z-direction whilst the trajectories for the post-pulse island remain qualitatively the same.

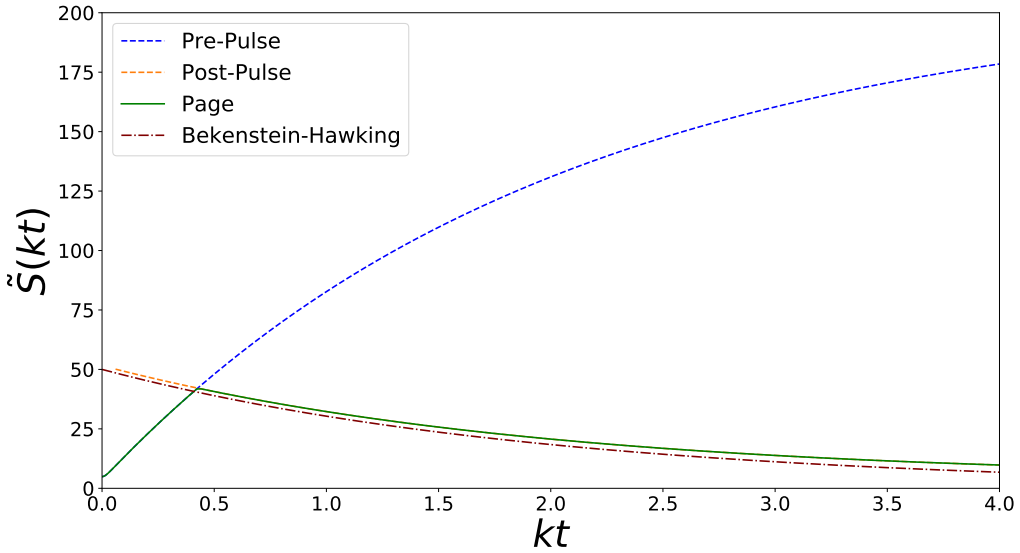

Figure 6.12: The Page curve for $k = 0.01$, $T = \frac{1}{2\pi}$ computed via the approximation for small k. The Page curve itself is shown in green: it starts at a nonzero values, rises due to the pre-pulse island and eventually jumps to the post-pulse island at the Page time to decrease.

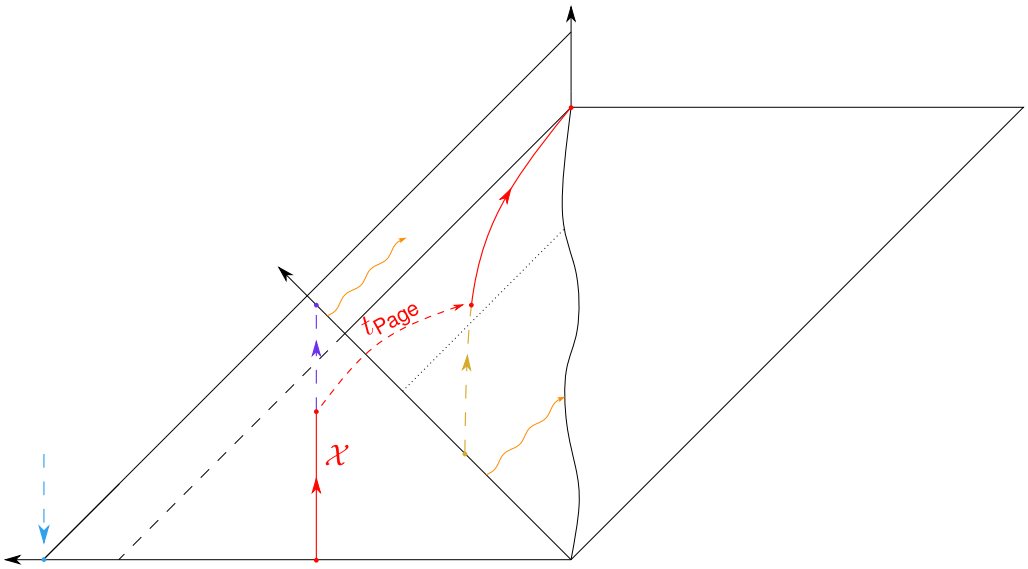

Figure 6.13: The island trajectory for $k = \frac{1}{\pi}$, $T = \frac{1}{2\pi}$ corresponding to an IP of 2. The island giving the Page curve is depicted in red. At the Page time, the island switches dominance to the post-pulse case. Eventually, it ends on the same boundary point as the observer. The pre-pulse island ceases to exist when it hits the matter pulse. The bifurcate island with a diverging entropy is denoted as well.

[2] One could find an approximate formula for the Page time by equalling the two entropies and expanding them for small values of t. However, the Page time is not that small, it would probably not yield a very accurate result. This approach is explained briefly in Appendix B.IV.

For $k = \frac{1}{\pi}$ we cannot make use of the approximate expressions anymore and have to solve (6.44) with the reparametrisation including the modified Bessel functions. The results for the post-island entropy and the Page curve in this case are shown respectively in Fig. 6.14a and 6.14b.

The birth of the post-pulse island now happens at a later time, in accordance with (6.49). Although the total entropy, dilaton and BH entropy behave in a similar way, they do quite differ in their values. Even the bulk entropy remains relatively large with respect to the total entropy and the dilaton contribution, and increases more rapidly than for smaller values of k. We expect the BH approximation to break down for increasing values of the evaporation rate k or even the IP, this formula was only valid for small values anyway.

A similar observation can be made from the Page curve. The BH entropy decreases more rapidly, its initial value lies closer to that of the pre-island, and the Page time is larger. It seems that a larger IP value also yields a smaller distance between the initial time for the post-island and the Page time. We suspect that in the limit of large IPs they coincide or perhaps the Page transition rather becomes discontinuous if $t_{\text{Page}} > t_0$. Since the pre-pulse island is not perennial for this IP, it may be that at larger values there is a gap in the entropy if the initial time of the post-pulse island is larger than the end time of the pre-pulse island.

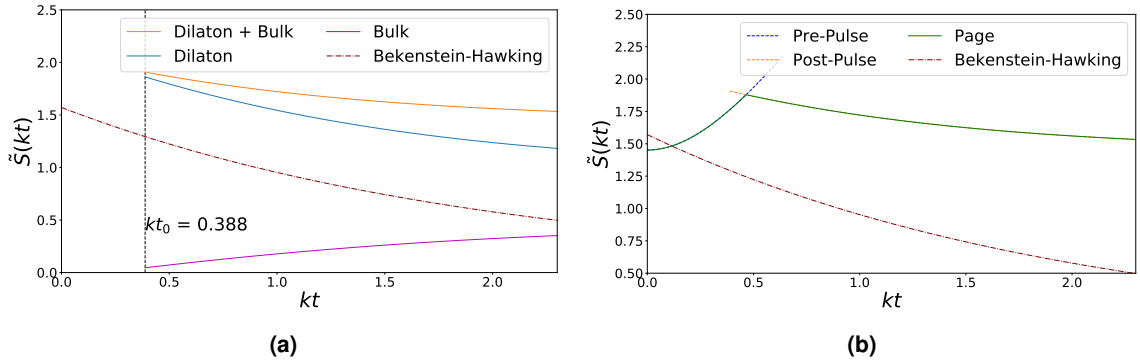

(a) **(b)**

Figure 6.14: **(a)** The post-island entropy for $k = \frac{1}{\pi}$, $T = \frac{1}{2\pi}$. Its birth is at a later time, the contribution of the bulk entropy is relatively larger and the Bekenstein–Hawking entropy does not form a good approximation. **(b)** The Page curve for $k = \frac{1}{\pi}$, $T = \frac{1}{2\pi}$. It has a larger Page time than the previous case, it also lies closer to the initial time of the post-pulse island. Because of the limited existence of the pre-pulse island, it perishes at kt_e determined by (6.27).

As a side note, we plotted the scrambling time for the post-pulse island in Fig. 6.15. Obviously, the initial scrambling time is equal to the initial time of the post-pulse island when $v_{\mathcal{X}} = 0$. Afterwards, it increases with a rate which slows down. When the post-pulse island eventually recedes to the boundary point, its scrambling time should vanish accordingly: $t = v_{\mathcal{X}}$ at that point. From this observation, there will be a point from henceforth it starts to dwindle. This explains the behaviour seen in the graph.

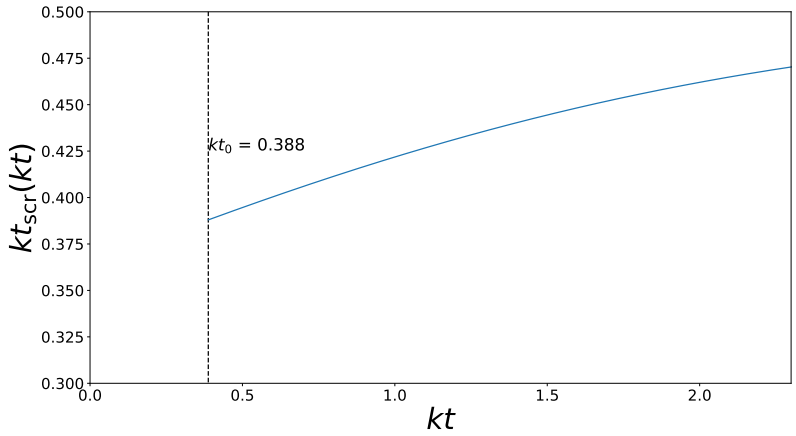

Figure 6.15: The post-pulse scrambling time for $k = \frac{1}{\pi}$, $T = \frac{1}{2\pi}$. Initially, it starts at the same value as the initial island time and increases up to a certain point. Afterwards, it should abate towards zero for an infinite boundary time.

At last, we can take a look at the Zurek argument presented in Sect. 6.II. Numerical calculations show that for $k = 0.01$ and $k = \frac{1}{\pi}$ respectively

$$\frac{\delta S_{\text{pre}}}{\delta S_{\text{post}}} = -4 \to -5, \qquad \frac{\delta S_{\text{pre}}}{\delta S_{\text{post}}} = -4 \to -20 \tag{6.60}$$

Despite being a varying value and its absolute value increasing with time, its larger than the expected value of 2. This happens more quickly for a higher value of the IP. Zurek's irreversibility argument is not satisfied.

Chapter 7

Renormalised Islands

Previously in this thesis, we explored the calculations involving islands like how they are usually done in literature, i.e. by ignoring the cutoff contributions $\delta_{f(t)} = f'(t)\delta$. In this chapter, we finally take these contributions into account by employing the renormalised entropy derived in Sect. 5.VI. This quantity is independent of the cutoffs and naturally gives a measure for the entanglement a boundary observer would measure. The perspective from this boundary observer, discussed in Sect. 6.I, is still valid. We need not be careful about the coordinates we adopt since we will always be working in boundary coordinates (u, v), except for one particular choice.

Qualitatively, the outline of this chapter mimics that of the previous one.

7.I The Generalised Entropy

Again, we first write down the most general expression for the entropy in this case. The dilaton part stays the same as (5.82) but the bulk entropy is now replaced by the renormalised expression (5.90) resulting in

$$\begin{aligned} S = &\left[\frac{1}{2}\frac{f''(v_2)}{f'(v_2)} + \frac{f'(v_2)}{f(u_2)-f(v_2)}\right] \\ &+ \frac{k}{2}\ln\frac{[f(u_1)-f(u_2)]^2}{f'(u_1)f'(u_2)(u_1-u_2)^2} + \frac{k}{2}\ln\frac{[f(v_1)-f(v_2)]^2}{f'(v_1)f'(v_2)(v_1-v_2)^2} \end{aligned} \tag{7.1}$$

Once more, we push one point to the boundary by making use of (6.13a, 6.13b)

$$\begin{aligned} S(t,u,v) = &\left[\frac{1}{2}\frac{f''(v)}{f'(v)} + \frac{f'(v)}{f(u)-f(v)}\right] \\ &+ \frac{k}{2}\ln\frac{[f(t)-f(u)]^2}{f'(u)(t-u)^2} + \frac{k}{2}\ln\frac{[f(t)-f(v)]^2}{f'(v)(t-v)^2} - k\ln f'(t) \end{aligned} \tag{7.2}$$

7.I.a Ambiguity for the Pre-Pulse Island

Similarly, we start with the region before the pulse corresponding to $v \leq 0 \leq t \leq u$ such that $f(v) = v$ and we explicitly write $X^+(u) = f(u)$. The entropy (7.2) becomes

$$S_{\text{pre}}(t,u,v) = \frac{1}{X^+(u)-v} + \frac{k}{2}\ln\frac{[f(t)-X^+(u)]^2}{\partial_u X^+(u)(t-u)^2} + \frac{k}{2}\ln\frac{[f(t)-v]^2}{(t-v)^2} - k\ln f'(t) \tag{7.3}$$

We retake our discussion on what coordinates to use from Sect. 6.I.a. Whilst it is necessary to work with the coordinate u, it leaves an ambiguity whether we should re-express the Poincaré coordinate X^+ as u or $f(u)$. Earlier on, we had the freedom to choose one or

the other since $\partial_u S_{\text{pre}}(u) = f'(u)\partial_+ S_{\text{pre}}(X^+)$. But now the expression above has an explicit u-dependence which nullifies this statement. The choice is related to a conformal transformation leading to a different evolution of the island, ergo the entropy. One could argue that it is more natural to set $X^+(u) = u$; because for an observer who also existed before the pulse was shot in, the geometry was unperturbed. Despite that, the island clearly depends on the geometry before the BH was formed, so it is like the BH remembers some of this information in order for its entropy to be determined by the island formula. From this viewpoint, it may be more logical for the boundary observer to use $X^+ = f(u)$ instead, with $u > 0$, as if the horizon has always been present. Nonetheless, we explore both choices and try to draw a conclusion from its consequences for the island. We call the situation with $X^+(u) = f(u)$ the **Horizon geometry** and $X^+(u) = u$ the **Poincaré geometry**.

7.II The Pre-Pulse Island: Horizon geometry

In this section, we begin by setting $X^+(u) = f(u)$ in (7.3) and extremise with respect to both u and v independently

$$\partial_u S_{\text{pre}} = 0 = \frac{-f'(u)}{[f(u)-v]^2} + k\left[\frac{-f'(u)}{f(t)-f(u)} + \frac{1}{t-u} - \frac{1}{2}\frac{f''(u)}{f'(u)}\right] \tag{7.4a}$$

$$\partial_v S_{\text{pre}} = 0 = \frac{1}{[f(u)-v]^2} + k\left[\frac{-1}{f(t)-v} + \frac{1}{t-v}\right] \tag{7.4b}$$

One is always free to plug the second condition into the first one to acquire

$$f'(u)\left[\frac{1}{t-v} - \frac{1}{f(t)-v} - \frac{1}{f(t)-f(u)}\right] + \frac{1}{t-u} - \frac{1}{2}\frac{f''(u)}{f'(u)} = 0 \tag{7.5}$$

The v-condition (7.4b) can be solved exactly, leading to two solutions

$$\begin{aligned} v_{\mathcal{X}}^{\pm}(t,u) = {} & \frac{1}{2}\frac{t+f(t)-2kf(u)[t-f(t)]}{1-k[t-f(t)]} \\ & \pm \frac{1}{2}\frac{t-f(t)}{1-k[t-f(t)]}\sqrt{1+4k\frac{[t-f(u)][f(t)-f(u)]}{t-f(t)}} \end{aligned} \tag{7.6}$$

with k-expansions

$$\begin{aligned} v_{\mathcal{X}}^{\pm}(t,u) = {} & \frac{1}{2}[t+f(t)] + \frac{k}{2}[t-f(t)][t+f(t)-2f(u)] \\ & \pm \frac{1}{2}[t-f(t)] \pm \frac{k}{2}\Big([t-f(t)]^2 + 2[t-f(u)][f(t)-f(u)]\Big) + \mathcal{O}(k^2) \end{aligned} \tag{7.7}$$

from which we can separately calculate

$$v_{\mathcal{X}}^{+}(t,u) = t + k[t-f(u)]^2 + \mathcal{O}(k^2) \tag{7.8a}$$

$$v_{\mathcal{X}}^{-}(t,u) = f(t) - k[f(t)-f(u)]^2 + \mathcal{O}(k^2) \tag{7.8b}$$

We can plug the solutions (7.6) back into the u-condition (7.4a) and resort to numerical measures to find $u_{\mathcal{X}}$. Because of the structure of this condition, it is not very illuminating to fill in all the functions in terms of $A(u), B(u), N(u)$, etc.

Although from numerical computations it turns out that for every t there is indeed a solution giving a finite $u_{\mathcal{X}}$, plugging this back into the expression for $v_{\mathcal{X}}^{\pm}$ returns a positive value in both cases. So these islands would lie behind the pulse, contradicting our assumption. Therefore, we will not look at the expression for its scrambling time.

Nevertheless, we find three possible islands by sending either $u_{\mathcal{X}} \to +\infty$, $v_{\mathcal{X}} \to -\infty$, or both simultaneously.

7.II.a Back to the Past

One island lies on the past horizon $\mathcal{I}^-$: $v_{\mathcal{X}} \to -\infty$, immediately giving an infinite scrambling time. It is easy to verify that this satisfies the v-condition (7.4b) for finite t and u. The u-condition (7.4a) consequently reduces to

$$0 = \frac{-f'(u)}{f(t) - f(u)} + \frac{1}{t-u} - \frac{1}{2}\frac{f''(u)}{f'(u)} \tag{7.9}$$

and is effectively the condition $\partial_u S_{\text{pre, bulk}} = 0$ since the dilaton term vanishes.

Solutions can be found numerically and result in $u_{\mathcal{X}} \approx t$ for finite t. Since $u_{\mathcal{X}}$ is not exactly equal to t, it is important to take the high precision of the terms $f(t) - f(u)$ and $t - u$ into account. Especially since $f(t)$ rapidly asymptotes to f_∞.

The entropy (7.3) now reduces to a pure bulk contribution

$$S_{\mathcal{I}^-}[t, u_{\mathcal{X}}(t)] = \frac{k}{2} \ln \frac{[f(t) - f(u_{\mathcal{X}})]^2}{f'(u)(t - u_{\mathcal{X}})^2} - k \ln f'(t) \tag{7.10}$$

Notice that this island lies on the null line $u \approx t$ and intersects the pulse very closely to the endpoint of the radiation region $\mathcal{R}$. Thereby, the BH region $\mathcal{BH}$ only captures a very small amount of radiation resulting in a small entropy, whereas the rest of the radiation gets captured by a large island which reduces as t increases. This island exists for all t, starts with an entropy almost equal to 0, and increases indefinitely. Eventually, it ends at $(f_\infty, -\infty)$.

The entropy can be well approximated by taking the limit $t \to u$ leading to a factor of $f'(t)^2$ within the argument of the logarithm

$$S_{\mathcal{I}^-}(t) \approx -\frac{k}{2} \ln f'(t) \tag{7.11}$$

7.II.b On the Horizon

The second solution can be found from sending $u_{\mathcal{X}} \to +\infty$. Since in this limit $f(u) \to f_\infty$, it is rather easy to see it indeed satisfies the u-condition (7.4a) when combined with (6.40b, 6.45, 6.46) for finite v, t.

The v-coordinate just becomes $v^{\pm}_{\mathcal{X}}[t, f(u) = f_\infty]$ (7.6) with $v^-_{\mathcal{X}}$ staying positive for all t. The other solution $v^+_{\mathcal{X}}$ only becomes negative after a time t_0 and moves towards the pulse to ultimately remain stationary at a fixed value. The condition for this starting time t_0 is when $v^+_{\mathcal{X}} \to -\infty$, i.e. it starts at the 'bifurcate' horizon $(f_\infty, -\infty)$, happening when

$$k[t_0 - f(t_0)] = 1 \tag{7.12}$$

which is clearly a quantity only depending on the IP if solved for kt_0.

The asymptotic value for the island on the horizon can be found by first setting $f(u) \to f_\infty$ and subsequently taking the limit $t \to \infty$ in (7.6)

$$v^{\pm}_{f_\infty} \to \frac{1}{2}\frac{1}{1 - k(t - f_\infty)} \left[t + f_\infty - 2kf_\infty(t - f_\infty) \pm (t - f_\infty)\right] \tag{7.13}$$

such that

$$kv^+_{f_\infty} \to kf_\infty - 1 \tag{7.14a}$$

$$kv^-_{f_\infty} \to kf_\infty \tag{7.14b}$$

Clearly, $kv^-_{f_\infty}$ asymptotes to a positive value and moreover, $kv^+_{f_\infty}$ forever stays negative only when

$$kf_\infty \leq 1 \tag{7.15}$$

It tells us that for certain IPs this island is physical for all $t \geq t_0$. If not, it hits the pulse when $v^+_{f_\infty}(t_e) = 0$. It is similar to one of the conditions of the previous chapter (6.30).

The scrambling time is divergent at t_0 but rapidly approaches the value

$$kt_{\text{scr},f_\infty}(t) = k(t - f_\infty) + 1 \tag{7.16}$$

and diverges again when $t_e \to +\infty$.

When taking the limit in the entropy expression (7.3), the difficulty only resides in the second term. Since $f(u) - f_\infty$ is very small but nonzero, we need to look at the limit of $f'(u)(t-u)^2$. This limit was already found in the previous chapter (6.4) and the entropy becomes

$$\begin{aligned} S_{f_\infty}[t, v^+_{\mathcal{X}}(t)] =& \frac{1}{f_\infty - v^+_{\mathcal{X}}(t)} + k \ln\left(\pi T I_1\left[\frac{2\pi T}{k}\right]\right) + k \ln \frac{f(t) - f_\infty}{f'(t)} \\ &+ k \ln \frac{f(t) - v^+_{\mathcal{X}}(t)}{t - v^+_{\mathcal{X}}(t)} \end{aligned} \tag{7.17}$$

Its asymptotic value can be determined from (7.14a). It boils down to evaluating the following expression

$$\lim_{t\to+\infty} \ln \frac{f(t) - f_\infty}{ktf'(t)} \tag{7.18}$$

It is rather easier to evaluate the inverse argument

$$\lim_{t\to+\infty} \frac{ktf'(t)}{f(t) - f_\infty} \overset{H}{=} \lim_{t\to+\infty} k\left[1 + \frac{tf''(t)}{f'(t)}\right] \tag{7.19}$$

in which we used l'Hôpital's rule because

$$\lim_{t\to+\infty} tf'(t) \propto \lim_{t\to+\infty} \frac{t}{N(t)^2} = 0 \tag{7.20}$$

after a computation along similar lines as (6.4). Next, by making use of (6.40b, 6.40c, 6.41b, 6.41b, B.7a, B.7b) we evaluate

$$\begin{aligned} \lim_{t\to+\infty} \frac{tf''(t)}{f'(t)} &= 2\pi T \lim_{t\to+\infty} te^{-\frac{k}{2}t} \frac{B(t)}{N(t)} \\ &= -2\pi T \lim_{t\to+\infty} t \frac{K_1[\alpha e^{-\frac{k}{2}t}]}{K_0[\alpha e^{-\frac{k}{2}t}]} \\ &= -2\pi T \frac{2}{\alpha k} = -2 \end{aligned} \tag{7.21}$$

Clearly, the limit does not exist because the result is the logarithm of a negative number.

7.II.c Chasing the new Bifurcate Horizon

We can also take both limits $u_{\mathcal{X}} = -v_{\mathcal{X}} \to +\infty$ leading to an island which for all t stays stationary on the 'bifurcate' horizon $(X^+, X^-) = (f_\infty, -\infty)$ and has an infinite scrambling time. It is easy to check this satisfies both conditions by setting $-v = u$ in (7.4a, 7.4b), the only limit left to check explicitly is

$$\lim_{u\to+\infty} \frac{-f'(u)}{[f(u) + u]^2} \propto \lim_{u\to+\infty} \frac{1}{[uN(u)]^2} = 0 \tag{7.22}$$

by making use of (B.7a)

$$\lim_{u\to+\infty} uK_1\left[\alpha e^{-\frac{k}{2}u}\right] = +\infty \tag{7.23}$$

The entropy becomes fairly easy for this solution as we just apply the appropriate limit to either of the expressions for the preceding islands (7.10, 7.17)

$$S_{\text{bifur, hor}}(t) = k\ln\left(\pi T I_1\left[\frac{2\pi T}{k}\right]\right) + k\ln\frac{f(t)-f_\infty}{f'(t)} \tag{7.24}$$

and is purely a bulk contribution. For $t\to+\infty$ it should become equal to the entropy associated to the island on the past horizon which diverges due to (6.46). It also gives the starting value for the island on the true horizon at t_0 from (7.12).

7.II.d An Archipelago

Combining the island solutions previously mentioned, we arrive at the graph in Fig. 7.1 for $k = 0.01$. As a comparison, the renormalised radiation entropy (6.3) computed in the foregoing chapter is plotted as well.

As is apparent from the graph, the islands lying on the horizon and bifurcate horizon have an entropy greater than the one on the past horizon. In agreement with (7.12), the island on the horizon only comes into existence after a certain amount of island time has passed with an entropy equal to the one on the bifurcate horizon. Their values continue to lie close to each other. Additionally, we plotted the approximate formula for the island on the past horizon (7.11). It fits perfectly with the more general solution from solving (7.9). Ultimately, this island will also end up at the same divergent entropy for the bifurcate horizon due to (6.46) after an infinite boundary time. It might be that after a huge amount of time has elapsed, the island jumps to the one on the horizon.

Whilst the entropy associated to the island on the past horizon is not exactly equal to the radiation entropy, it does have a similar behaviour.

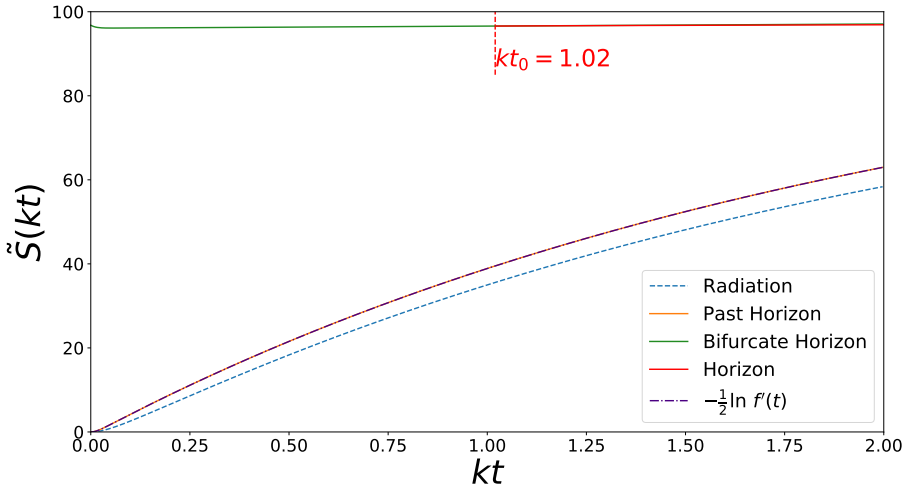

Figure 7.1: Evolution of the entropy associated to the pre-pulse archipelago for $k = 0.01$ and $T = \frac{1}{2\pi}$ in the Horizon geometry. The entropy of the island on the past horizon looks similar to the radiation entropy and is equivalent to (7.11). We also depicted the starting time for the island on the horizon, when (7.12) is satisfied.

7.III The Pre-Pulse Island: Poincaré geometry

As originally intended, we additionally look at the case in which we set $X^+(u) = u$ instead. Plugging this into (7.4a, 7.4b) gives us the following island equations

$$\partial_u S_{\text{pre}} = 0 = \frac{-1}{(u-v)^2} + k\left[\frac{-1}{f(t)-u} + \frac{1}{t-u}\right] \tag{7.25a}$$

$$\partial_v S_{\text{pre}} = 0 = \frac{1}{(u-v)^2} + k\left[\frac{-1}{f(t)-v} + \frac{1}{t-v}\right] \tag{7.25b}$$

Right off the bat, the original Poincaré bifurcate horizon is an appropriate island solution. Even when taking either $u \to +\infty$ or $v \to -\infty$ first, it forces the other coordinate to diverge as well. The scrambling time is infinite and the entropy is just the last term in (7.3)

$$S_{\text{bifur, Poincaré}}(t) = -k \ln f'(t) \tag{7.26}$$

which equals twice the value of (7.11).

There are two sets of nontrivial islands when solving the system analytically

$$\begin{aligned} u^{\pm}_{\mathcal{X}}(t) = {} & \frac{[t+f(t)][1-4k^2 t f(t)] + 4k^2[t^3+f(t)^3]}{2[1+4k^2(t-f(t))^2]} \\ & \pm \frac{t-f(t)}{2\sqrt{1+4k^2[t-f(t)]^2}}[1-2k(t-f(t))] \end{aligned} \tag{7.27a}$$

$$\begin{aligned} v^{\pm}_{\mathcal{X}}(t) = {} & \frac{t+f(t)}{2} \\ & \pm \frac{t-f(t)}{2\sqrt{1+4k^2[t-f(t)]^2}}[1+2k(t-f(t))] \end{aligned} \tag{7.27b}$$

The sets of islands are $(u^+_{\mathcal{X}}, v^-_{\mathcal{X}})$ and $(u^-_{\mathcal{X}}, v^+_{\mathcal{X}})$. However, the latter is not a physical solution: $v^+_{\mathcal{X}}(t) > 0$ since notably $t - f(t) > 0$. Both solutions do coincide at their starting value for $t = f(t) = 0$, equivalent to the origin of the Penrose diagram.

The physical island solution has as expansion in k

$$\begin{aligned} u^+_{\mathcal{X}}(t) &= t - k[t-f(t)]^2 + \mathcal{O}(k^2) \\ &= 2t - [f(t) + t_{\text{scr}}(t)] + \mathcal{O}(k^2) \end{aligned} \tag{7.28a}$$

$$v^-_{\mathcal{X}}(t) = f(t) - k[t-f(t)]^2 + \mathcal{O}(k^2) \tag{7.28b}$$

with associated scrambling time

$$\begin{aligned} t_{\text{scr}}(t) &= \frac{t-f(t)}{2}\left[1 + \frac{1+2k[t-f(t)]}{\sqrt{1+4k^2[t-f(t)]^2}}\right] \\ &= [t-f(t)][1+k(t-f(t))] + \mathcal{O}(k^2) \end{aligned} \tag{7.29}$$

Again, it diverges for $t \to +\infty$.

Finally, the entropy (7.3) can be expressed as follows

$$\begin{aligned} S_{\text{pre}}[\mathcal{X}(t)] = {} & \frac{\sqrt{1+4k^2[t-f(t)]^2}}{t-f(t)} \\ & + k \ln \frac{4k[t-f(t)][\sqrt{1+4k^2[t-f(t)]^2} - 2k(t-f(t))] - 1}{f'(t)} \end{aligned} \tag{7.30}$$

To find how the island moves through our geometry, we compute its trajectory analogously to (6.32, 6.33)

$$F_{\text{pre}}[\mathcal{X}(t)] = \frac{t+f(t)}{2} - \frac{k[t-f(t)]^2}{\sqrt{1+4k^2[t-f(t)]^2}} \tag{7.31a}$$

$$Z_{\text{pre}}[\mathcal{X}(t)] = \frac{t-f(t)}{2\sqrt{1+4k^2[t-f(t)]^2}} \tag{7.31b}$$

As mentioned earlier, this island starts in the origin and eventually goes to the bifurcate horizon of the Poincaré geometry for $t \to +\infty$. However, even if it starts in the origin it first moves through the region after the pulse and then crosses it at another time t_0 when $v^-_{\mathcal{X}}(t_0) = 0$. Thus, the island is only a physical solution from t_0 onwards. Starting from the island Eqs. (7.25a, 7.25b), this is equivalent to solving

$$\frac{1}{t_0} - \frac{1}{f(t_0)} - \frac{1}{f(t_0)-u_0} + \frac{1}{t_0-u_0} = 0 \tag{7.32}$$

with u_0 the coordinate where its trajectory intersects the pulse

$$ku_0 = \sqrt{\frac{t_0 f(t_0)}{k[t_0-f(t_0)]}} \tag{7.33}$$

Surprisingly, this island goes back in time. A comparable island was already found in the case of dS space [170]. It was argued by using the EW construction hypothesis that the island has to move back in time to not violate the no-cloning theorem.

The numerical results for both islands are shown in Fig. 7.2. Again, the radiation entropy is plotted for comparison (6.3).

We already established that the entropy associated to the bifurcate horizon is twice that of (7.11), so naturally it is not equivalent to the radiation entropy, yet it behaves similarly. The other island is only physical from the moment t_0 determined by (7.32). At an early time there is already an exchange of dominance between the two islands. However, they meet again in the limit $t \to +\infty$ because the second island recedes to the bifurcate horizon with a diverging entropy. It will turn out this exchange happens after the Page time.

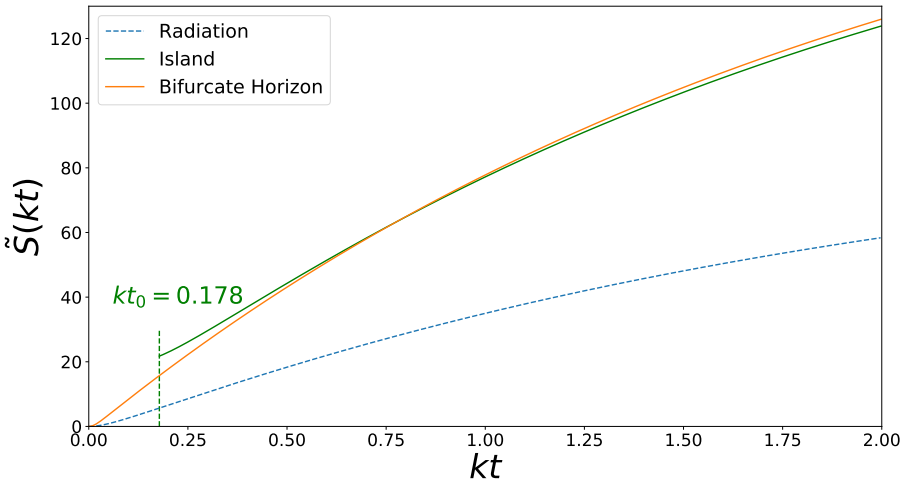

Figure 7.2: Evolution of the entropy associated to the pre-pulse archipelago for $k = 0.01$ and $T = \frac{1}{2\pi}$ in the Poincaré geometry. Both entropies are not well approximated by the radiation entropy. We also depicted the time when the second island becomes physical (7.32).

7.IV The Post-Pulse Island

We finally arrive at the islands which are the hardest discover, namely those behind the pulse $0 \leq v \leq t \leq u$ with the most general entropy expression (7.2) which we retake here

$$S_{\text{post}}(t,u,v) = \left[\frac{1}{2}\frac{f''(v)}{f'(v)} + \frac{f'(v)}{f(u)-f(v)}\right] + \frac{k}{2}\ln\frac{[f(t)-f(u)]^2}{f'(u)(t-u)^2} + \frac{k}{2}\ln\frac{[f(t)-f(v)]^2}{f'(v)(t-v)^2} - k\ln f'(t) \tag{7.34}$$

leading to the island conditions

$$\partial_u S_{\text{post}} = 0 = -\frac{f'(u)f'(v)}{[f(u)-f(v)]^2} + k\left[\frac{-f'(u)}{f(t)-f(u)} + \frac{1}{t-u} - \frac{1}{2}\frac{f''(u)}{f'(u)}\right] \tag{7.35a}$$

$$\partial_v S_{\text{post}} = 0 = \frac{1}{2}\partial_v\frac{f''(v)}{f'(v)} + \frac{f''(v)}{f(u)-f(v)} + \left(\frac{f'(v)}{f(u)-f(v)}\right)^2 + k\left[\frac{-f'(v)}{f(t)-f(v)} + \frac{1}{t-v} - \frac{1}{2}\frac{f''(v)}{f'(v)}\right] \tag{7.35b}$$

The first condition almost resembles that of the pre-pulse case (7.4a) except for the extra factor of $f'(v)$ in the first term. Therefore, for finite v this condition is fulfilled for an island on the horizon $u_{\mathcal{X}} \to +\infty$ due to its similarity with Sect. 7.II.b. Plugging this into the second condition results in $f(u) \to f_\infty$ and after some numerical techniques it seems there is no finite v for which the second condition holds. There is no possible island which lies on the horizon forever. A nontrivial island needs to be checked numerically.

Can we already verify our prediction from the previous chapter that the island ends on the boundary at $X^+ = f_\infty = X^-$, requiring $u_{\mathcal{X}} = v_{\mathcal{X}} \to +\infty$? A lot of the limits are similar to those in the previous cases. By combining (6.40c, 6.40d, 6.45, 6.46), every term can be explicitly checked to be vanishing. This indeed confirms our prediction and the island will eventually end on the boundary point where the observer ends as well. Furthermore, the entropy correctly vanishes in this limit. For instance, when we equally divide the last term in expression (7.34) among the two prior, what remains is the following limit

$$\lim_{u\to t}\frac{[f(t)-f(u)]^2}{f'(t)f'(u)(t-u)^2} = \frac{f'(t)^2}{f'(t)^2} = 1 \tag{7.36}$$

7.IV.a The Initial Island & a Phase Transition

Just as before, the earliest possible island is one at the pulse itself $v_{\mathcal{X}} = 0$. By using Eqs. (6.40d, 7.35a, 7.35b), this is when

$$-\frac{f'(u_0)}{f(u_0)^2} + k\left[\frac{-f'(u_0)}{f(t_0)-f(u_0)} + \frac{1}{t_0-u_0} - \frac{1}{2}\frac{f''(u_0)}{f'(u_0)}\right] = 0 \tag{7.37a}$$

$$-(\pi T)^2 + \frac{1}{f(u_0)^2} + k\left[\frac{1}{t_0} - \frac{1}{f(t_0)}\right] = 0 \tag{7.37b}$$

The second condition can be directly solved to

$$kf(u_0) = \frac{k}{\pi T}\frac{1}{\sqrt{1+\left(\frac{k}{\pi T}\right)^2\left[\frac{1}{kf(t_0)} - \frac{1}{kt_0}\right]}} \tag{7.38}$$

The difficulty lies in the first condition. One could for small values of the IP use the approximation (6.56a) to obtain an analytical expression for the inverse $u = f^{-1}$. But this becomes

convoluted rather quickly and we resort to a numerical approach.

We do have an analytical expression for its IP address already giving us some insight. Since $t - f(t) \leq 0$, it immediately follows that $\frac{1}{f(t)} - \frac{1}{t} \geq 0$ as well. No matter what value for the IP we take and regardless of the exact t_0, the denominator in the expression above will be larger than unity. Due to this reasoning, we can conclude the island always starts before the would-be horizon, and hence also before the true horizon. Only for the IP being zero it starts on the would-be horizon, being zero as well. This is not surprising since we had been working in the boundary coordinates (u, v) all this time and already concluded that an island on the horizon for finite t is not a good solution in general.

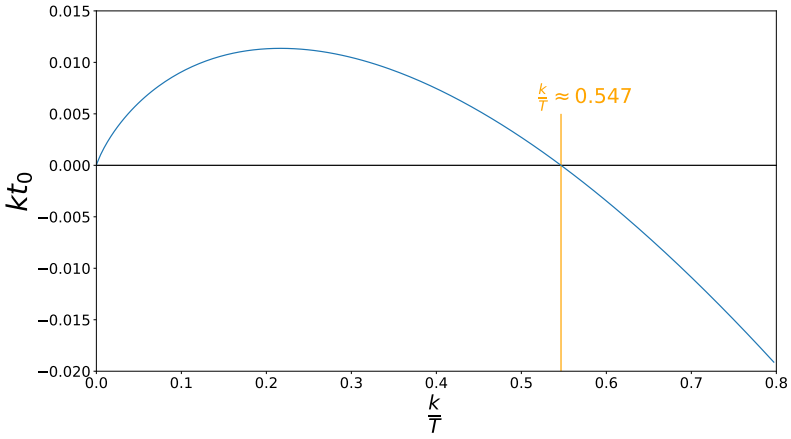

Figure 7.3: The initial time as function of the IP. Beyond the threshold value, depicted in orange, we enter the no-island phase.

The initial time for different values of the IP is plotted in Fig. 7.3. Immediately surprising is the appearance of a threshold value beyond which the initial time becomes negative. This threshold is $\frac{k}{T} = 0.547$ and the island then starts at the would-be horizon $kf(u_0) = \frac{k}{\pi T}$. One would first conclude that for values beyond the threshold the island does not start on the pulse but rather somewhere else; the initial island conditions break down. However, numerics show that those islands lie within the lightcone of the boundary observer: $v < t$ is violated. As such, these islands are not suitable.

Although this value was determined at a fixed T, rewriting the equations into a manifestly dimensionless form by expressing them in island time reveals that the same value for the threshold is obtained.[1] It seems there is an apparent phase transition between an island phase and a no-island phase with the transition happening at $\frac{k}{T} = 0.547$. Additionally, a Page transition will not happen in the no-island phase. There will be nor a Page curve nor unitarity – information is lost.

7.V Results & the Page Curve

First, the result for the post-island entropy with $k = 0.01$ is depicted in Fig. 7.4.

What one should notice immediately is how the contribution of the dilaton and the BH entropy almost exactly coincide. Even more so than in the previous chapter. Besides, the bulk entropy is tiny and decreases at a sluggish pace. This decrease is in accordance with a decreasing $\mathcal{BH}$ region, something which did not happen previously. Therefore, the total entropy is almost that of the dilaton, and hence almost equal to the BH result. Again, the claim that the post-island entropy can be traced by the BH value to a great extent is verified.

[1] We alluded to such a dimensionless description in Sect. 6.II.

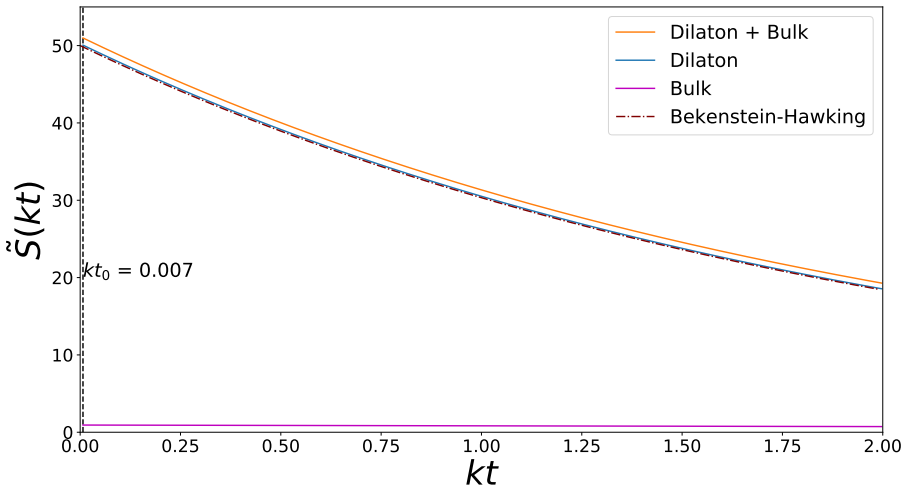

Figure 7.4: The post-island entropy for $k = 0.01$, $T = \frac{1}{2\pi}$. We show how both contributions, dilaton and bulk, contribute to the total entropy. The BH entropy is also plotted and almost exactly coincides with the dilaton. The initial time is depicted as the vertical line.

We combine this result with those of the pre-pulse islands, only keeping the relevant terms; these are the minimal entropies before the Page time for both geometries. The result is shown in Fig. 7.5 – it forms the crux of this thesis!

As was established earlier, the BH entropy is a good fit for the entropy associated to the post-island which gives the decreasing contribution to the Page curve. While the behaviour in both geometries for the increasing part is similar – the only difference being a factor of two – it is only in the Horizon geometry that it can be relatively well approximated by the radiation entropy. Therefore, to a considerable degree, the Page curve for an EBH in JT gravity closely resembles the one obtained from first following the radiation entropy à la Hawking and subsequently following the BH entropy. This is a remarkable result! The previous chapter could only produce halve of this claim and to a lesser extent than when using the renormalised entropy.[2]

Notice that this argument is in favour of using the Horizon geometry for the island in the pre-pulse case.

All the island solutions' trajectories as well as the one associated to the Page curve are illustrated in Fig. 7.6a and 7.6b according to the Horizon and Poincaré geometry respectively.

In Sect. 4.III we noticed how the rising part of the Page curve is associated to a trivial island; for Schwarzschild this was one all the way down to $r = 0$. Such an island would have an entropy associated to it purely equal to that of the radiation region. The falling part was attributed to a nontrivial island behind the horizon.

In our setup, the island inevitably lies in the exterior which is due to our choice of describing the problem in boundary coordinates (u, v). For the Poincaré geometry, the island associated to the rising part is indeed the trivial island on the bifurcate horizon. This could be used as an argument to favour the Poincaré geometry over the Horizon geometry. The island for the Horizon geometry constitutes a nontrivial island region $\mathcal{I}$ but is trivial in the sense that it has no dilaton contribution due to being on the past horizon. However, the trivial island in the Poincaré geometry has an entropy associated to it which deviates more from the radiation entropy than the one in the Horizon geometry, as previously observed.

[2] The Page time is larger than in the previous case, so the same remarks apply. See B.IV.

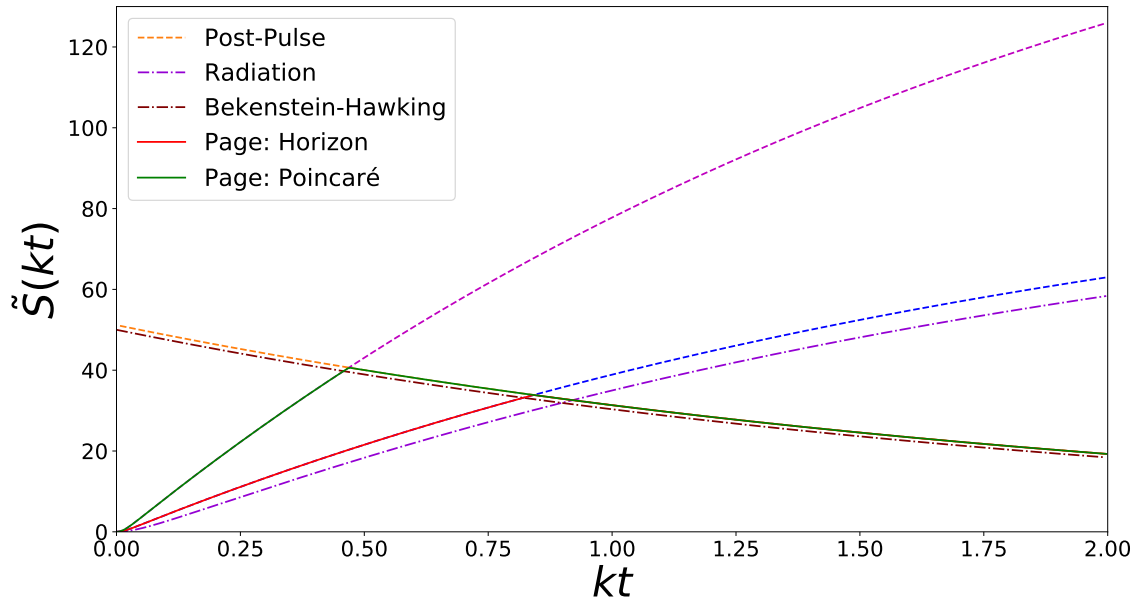

Figure 7.5: The Page curve for $k = 0.01$, $T = \frac{1}{2\pi}$ in both geometries. In both cases, the island jumps to the same post-island at the Page time. Before the Page time, we either follow the increasing green or red curve depending on the geometry.

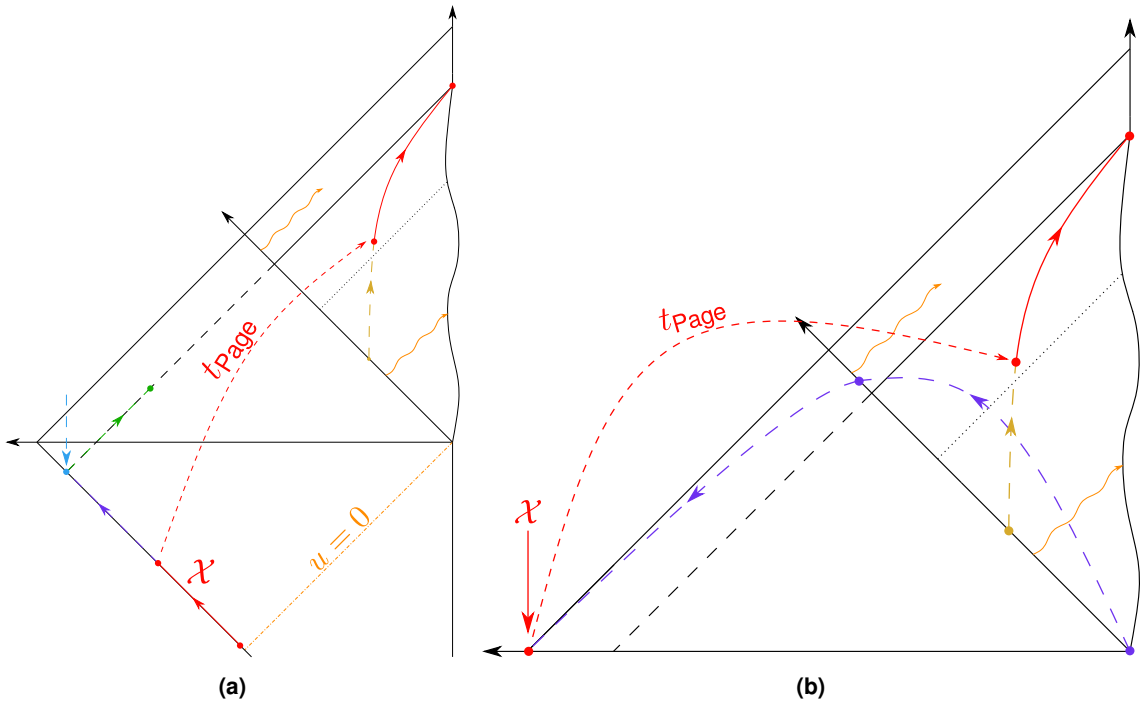

Figure 7.6: **(a)** The archipelago and island trajectories for the Horizon geometry in the pre-pulse region. **(b)** The archipelago and island trajectories for the Poincaré geometry in the pre-pulse region. Observe how the island solution in purple goes back in time and first crosses a region behind the pulse. In both cases, the island giving the Page curve is depicted in red.

As a side note again, we plot the scrambling time for the post-pulse island in Fig. 7.7. The same remarks as before can be made.

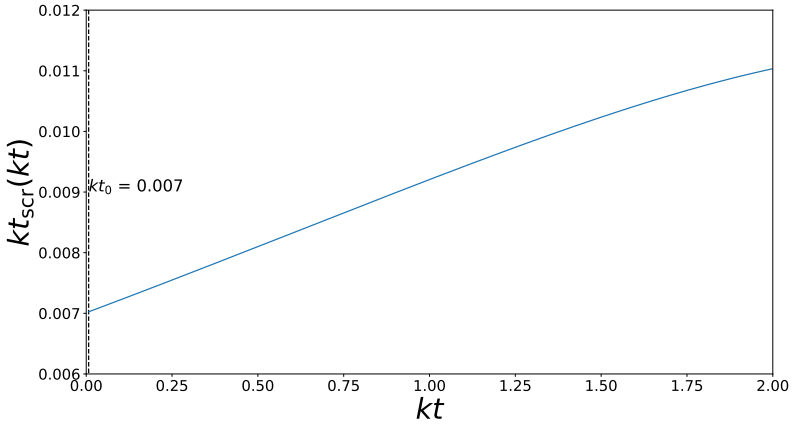

Figure 7.7: The post-pulse scrambling time for $k = 0.01,\ T = \frac{1}{2\pi}$. Initially, it starts at the same value as the initial island time and increases up to a certain point. Afterwards, it should abate towards zero for an infinite boundary time.

A last argument in favour of the Horizon geometry is obtained when investigating Zurek's irreversibility argument using some numerics. For the Horizon and Poincaré geometry respectively

$$\frac{\delta S_{\text{pre, Horizon}}}{\delta S_{\text{post}}} = -2, \qquad \frac{\delta S_{\text{pre, Poincaré}}}{\delta S_{\text{post}}} = -4 \tag{7.39}$$

In contrast with the previous chapter, both values are now constant. The Poincaré value is even twice that of the Horizon geometry value; this is not surprising since this is the same for their entropies. However, it is remarkable how only the Horizon geometry reproduces Zurek's irreversibility argument perfectly with the correct factor argued in Sect. 6.II. This is another win for the Horizon geometry.

Chapter 8

Summary & Outlook

The best way to tame a mystery is with another mystery.

Oreki Houtarou

We have come a long way. Starting with a preliminary on holography and a chapter on EE, we eventually ended at the renowned island formula and a review of semiclassical JT gravity. In that chapter, we built the foundation for our setup of an EBH which we further developed in Ch. 6 by using its properties as a chiral CFT. Finally, we ventured out and found an archipelago using the old and new ways, both leading to the Page curve.

In what follows, we give a succinct summary of the main interpretations and results first. Afterwards, we discuss some recent developments and formulate a possible outlook.

8.I Summary & Conclusion

Because our model for an EBH largely differs from the ones in the literature, we juxtapose both models depicted in Fig. 8.1a and 8.1b.

The first model glues an external, flat heat bath to the boundary of AdS_2 to define the region in which the radiation escapes. For $t < 0$ the boundary between these two spacetimes is reflecting; they do not couple with each other. At $t = 0$ the coupling between both is turned on, leading to a pulse which forms the BH; reminiscent of a quench procedure. To allow evaporation, the boundary is transparent for $t > 0$ and both left and rightmovers are present in both spacetimes.

Our model is different, we did not glue any spacetime to the boundary, but take the perspective of a boundary observer. This boundary observer moves along the holographic boundary associated to the Poincaré patch for $t < 0$. Subsequently, they shoot in a classical pulse at $t = 0$ to form the BH. Evaporation for $t > 0$ is achieved by the observer collecting the outgoing Hawking radiation with an Unruh detector (see Sect. 5.V). This turned the CFT into a chiral CFT with only outgoing modes present. In Sect. 6.I we showed how this can be related to a model with an external heat bath in which this bath can be reinterpreted as the internal spacetime of the Unruh detector. However, we need not make any assumptions about its properties or more specifically, its metric. We argued that the island eventually ends up at the same boundary point as our observer for $t \to +\infty$ such that the island region entails the part of the spacetime our observer would not have access to without it.

A second difference is our use of the renormalised entropy of Sect. 5.VI. We took the Poincaré geometry as a reference and formulated a more natural measure for the entropy with respect to this reference geometry. As a consequence, we had to use boundary coordinates (u, v); islands were forced to float in front of the horizon (see Sect. 6.I.a).

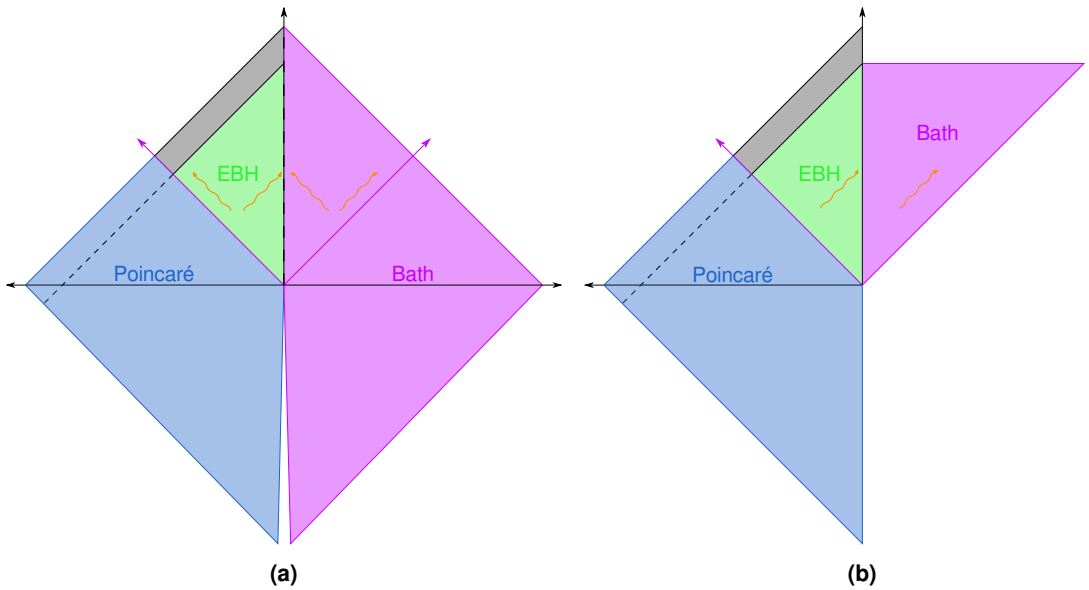

Figure 8.1: (a) The setup in literature. Due to the coupling at $t = 0$ a pulse is sent in forming the BH. By setting transparent BC, evaporation is achieved and we have radiation in both directions. **(b)** Our setup of an EBH. A classical pulse is sent in and outgoing radiation is absorbed by the boundary observer. Nothing is reflected back in again.

In Ch. 7 we set sail towards the archipelago in this model and found quite an amount of islands. The only problem was a possible ambiguity for islands in the pre-pulse region: whether we should set $X^+(u) = f(u)$ or $X^+(u) = u$; the Horizon and Poincaré geometry respectively. At the end, we found that the Horizon geometry had the most striking results.

First of all, the Page curve was computed for both cases and depicted in Fig. 7.5. Remarkably, the Page curve associated to the horizon geometry can be well approximated by first following the Hawking result and then the BH entropy. This was also apparent from Fig. 7.4: the bulk entropy almost contributes nothing and the dilaton coincides with the BH entropy nearly perfectly. It affirms the claim made in Ch. 4.

The second result is the appearance of a phase transition for the post-island. For values of the IP beyond the threshold 0.547, computed in the dimensionless model, we found that islands lie within the lightcone of the observer. Hence, they violate $v < t$. Consequently, the post-pulse island for such BHs cannot save the paradox; there is no decreasing part for the Page curve and the entropy rises indefinitely.

Finally, both geometries have a constant ratio of $\delta S_{\text{pre}}/\delta S_{\text{post}}$. But, only the Horizon geometry results in a ratio of -2, consistent with Zurek's irreversibility argument presented in Sect. 6.II.

We presented a **bathless** model for an EBH in JT gravity and subsequently used the QES/island formula to compute the **Page curve**. It substantially follows the Hawking calculation and BH entropy before and after the Page time respectively. This was done by means of a **renormalised entropy**, the cutoffs were accounted for. Moreover, this setup has a natural interpretation in terms of a **boundary observer** collecting the radiation with an Unruh detector. Besides, this model satisfies **Zurek's irreversibility argument** and exhibits a **phase transition** between an island phase and a no-island phase regarding the post-pulse region.

8.II Other Developments & Outlook

In this last section, we start with an unpedantic overview of some of the recent developments and then formulate an outlook.[1]

- **The Unitary Gauge Construction:** presented by Y. Nomura [171, 172], it is an equivalent perspective on the paradox by means of a Legendre duality. Whilst the island perspective makes the interior manifest and unitarity obscure, the unitary gauge construction makes unitarity manifest and the interior obscure instead. In this construction, three sets of modes are investigated along with the dynamics of the stretched horizon: hard modes within the zone ($\nu > 2\pi T_H$), soft modes ($\nu < 2\pi T_H$) and far modes (radiation);

- **Soft Hair:** H. Verlinde et al. their idea is to reinvestigate the role of soft hair in the paradox [21, 173, 174]. This soft hair stems from the infinite amount of conservation laws in asymptotically flat spacetimes due to Bond–Metzner–Sachs (BMS) supertranslation symmetries. Closely related is the exchange of soft gravitons, they are the Goldstone bosons associated to the supertranslation symmetry breaking [175];

- **The Principle of Holographic Information:** proposed by S. Raju et al. [23, 24, 176], it suggests that all the information about massless excitations can be obtained from a neighbourhood near the past boundary of future null infinity. Moreover, any information on future null infinity is also available from any cut to its past. Similar principles can be formulated for past null infinity as well. These principles are suggested in the context of 4d asymptotically flat spacetimes, they are oft-abbreviated as 'information is always outside'. Applied to the heat bath argument, an external nongravitating heat bath is nonphysical in the sense that gravitational effects will in reality be very weak. But, as long as gravity is present, regardless of how weak, information is stored locally instead of holographically. Criticism entails the fact that the Page curve is due to the factorisation of the Hilbert space in a bipartite way. However, in a theory of dynamical gravity this factorisation is rendered moot and the Page curve would just be flat. This led to a fierce debate during the *Island Hopping 2020: from Wormholes to Averages* conference.
  Another effect of this coupling to an external heat bath would be the rise of a massive graviton [177];

- **Cosmological Islands:** a plethora of work has also been done in the context of dS space and models more related to cosmology. These include the entropy associated to the cosmological horizons, wormholes, or even islands within bubble Universes [170, 178–188];

- **Replica Wormholes:** there also exists a perspective from the replica trick applied to the GPI [19, 20, 122, 189]. If we go to the replicated manifold and consider the GPI, then we need to sum over all possible geometries; these include geometries representing multiple wormholes between the replica manifolds. Apparently, Hawking's result is associated to the completely disconnected geometry whilst the completely connected case represents the QES solution leading to unitarity. They are depicted in Fig. 8.2a and 8.2b respectively. This GPI is often interpreted as an ensemble average. For JT gravity this is closely related to an ensemble of SYK models (see Appendix A). The island equations can also be derived from the analytic continuation.

[1] The literature is quite extensive, so we likely have not cited every existing paper on a specific topic.

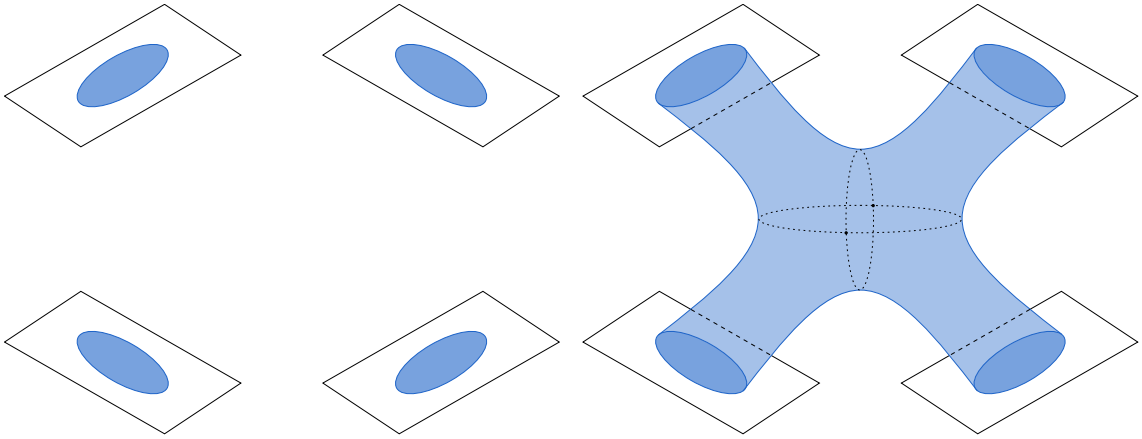

Figure 8.2: **(a)** The disconnected geometry leading to the Hawking result. **(b)** The connected geometry leading to the QES result. Replica wormholes connect the different replica manifolds.

Future work can be directed towards some of these developments described above.

Specifically within the framework of this thesis, it might be interesting to investigate this phase transition into more detail. It might be that for large values of the IP, suitable islands reemerge. For such an approach, the dimensionless model argued in Sect. 6.II is ideal.

As mentioned in Ch. 4, use of the island formula is hard due to the expression of the entropy of a union of intervals. Authors then assume the total state to be pure such that the QES formula may be used instead. It would be interesting to explicitly employ both formulas within the same model to verify whether this assumption is valid or not.

Perhaps it proves insightful to study the role of the heath bath in further detail. Clearly, there is a lot of debate on the dynamics of this extra spacetime; it plays a crucial role in a considerable amount of models. In our case, we did not have to specify any properties of the heat bath. It might be that starting from a bathless model in some other spacetime leads to specific constraints when mapping it to the same model with this extra region. Whether such a mapping exists remains to be seen and depends on the model.

As in this thesis, renormalised entropies in other models might be formulated along a similar way, i.e. by defining it with respect to a reference entropy or geometry. Consequently, the Page curve obtained from such an entropy is more naturally related to actual measurements.

As one can imagine, this area of research gained considerable attention and remains like Piccadilly Circus. One can only hope this thesis aroused some curiosity in these fascinating concepts.

Appendix A

The Holographic Dual: SYK

In this appendix we briefly discuss the holographic dual of JT gravity: the SYK model [130–134, 190, 191].

This model resembles an ensemble theory of finite-dimensional QM models described by their Hamiltonians

$$H = \sum_{ijkl=1}^{N} J_{ijkl}\psi_i\psi_j\psi_k\psi_l \tag{A.1}$$

It contains all-to-all couplings J_{ijkl} picked at random from a Gaussian distribution with $\mu = 0,\ \sigma = \sqrt{3!}J/N^{3/2}$ with J a fixed parameter of the ensemble. The constituents are Majorana fermions; in this case, fermionic representations of the Lorentz group or rather the orthogonal group since we work in Euclidean space. They obey the usual Clifford algebra relation

$$\{\psi_i, \psi_j\} = \delta_{ij} \tag{A.2}$$

with reality condition $\psi_i = \psi_i^\dagger$.

Some interesting features of this model are [134]

- It is solvable in the classical limit for $N \to \infty$ in terms of two master fields in two dimensions;
- In the classical limit, a time reparametrisation symmetry $t \mapsto f(t)$ emerges in the low energy sector which gets spontaneously broken to $\mathrm{SL}(2,\mathbb{R})$. The Goldstone modes acquire a nontrivial action when moving away from the IR. Note the similarly with JT gravity;
- The spectrum has a long tail towards low energies: there are a lot of states just above the ground state and

  $$\lim_{\beta\to\infty}\lim_{N\to\infty} S(\beta) \propto N \tag{A.3}$$

  These two limits do not commute. For finite N the model has only a couple of ground states, resulting in a small entropy;
- This ensemble interpretation plays an important role in replica wormholes and the interpretation of the GPI as an ensemble average [19, 20, 122, 189].

Appendix B

The Time Reparametrisation

B.I Properties of the Modified Bessel Functions

When doing calculations with $f(t)$ (5.69) containing the modified Bessel functions of the first and second kind, we will need some of its properties. We list them below.

For large arguments z, the modified Bessel functions can be expanded as follows

$$I_\nu[z] = \frac{e^z}{\sqrt{2\pi z}}\left(1 - \frac{4\nu^2 - 1}{8z}\right) + \mathcal{O}(z^{-2}) \tag{B.1a}$$

$$K_\nu[z] = \sqrt{\frac{\pi}{2z}}e^{-z}\left(1 + \frac{4\nu^2 - 1}{8z}\right) + \mathcal{O}(z^{-2}) \tag{B.1b}$$

leading to the ratio [14]

$$\frac{K_\nu[z]}{I_\nu[z]} = \pi e^{-2z}\left[1 + \frac{4\nu^2 - 1}{4z} + \mathcal{O}(z^{-2})\right] \tag{B.2}$$

Their derivative is a linear combination of the function itself, but at different orders

$$\frac{\mathrm{d}}{\mathrm{d}z}I_\nu[z] = \frac{1}{2}\left(I_{\nu-1}[z] + I_{\nu+1}[z]\right) \tag{B.3a}$$

$$\frac{\mathrm{d}}{\mathrm{d}z}K_\nu[z] = -\frac{1}{2}\left(K_{\nu-1}[z] + K_{\nu+1}[z]\right) \tag{B.3b}$$

For the special case $\nu = 0$, we can make use of the following property

$$I_{-\nu}[z] = I_\nu, \qquad K_{-\nu}[z] = K_\nu \tag{B.4}$$

to obtain

$$\frac{\mathrm{d}}{\mathrm{d}z}I_0[z] = I_1[z], \qquad \frac{\mathrm{d}}{\mathrm{d}z}K_0[z] = -K_1[z] \tag{B.5}$$

Furthermore, the following result proves useful when we have terms proportional to $z^\nu I_\nu[z]$ or $z^\nu K_\nu[z]$

$$\frac{\mathrm{d}}{\mathrm{d}z}\left(z^\nu I_\nu[z]\right) = z^\nu I_{\nu-1}[z], \qquad \frac{\mathrm{d}}{\mathrm{d}z}\left(z^\nu K_\nu[z]\right) = -z^\nu K_{\nu-1}[z] \tag{B.6}$$

In our calculations, the only orders we will encounter are $\nu = 0, 1$, so it is worth noting their limits for $z \to 0$

$$\lim_{z\to 0} I_0[z] = 1, \qquad \lim_{z\to 0} K_0[z] = +\infty \tag{B.7a}$$

$$\lim_{z\to 0} I_1[z] = 0, \qquad \lim_{z\to 0} K_1[z] = +\infty \tag{B.7b}$$

B.II Taking Derivatives

In the analysis of the island, we will need to make use of the derivatives of the time reparametrisation (5.69). These calculations are not hard and exploit the properties of the modified Bessel function set out above. However, they are not very illuminating.

We first start by rewriting the time reparametrisation (5.69) as

$$\begin{aligned} f(t) &= \frac{1}{\pi T}\frac{I_0[\alpha]K_0[\alpha e^{-\frac{k}{2}t}] - K_0[\alpha]I_0[\alpha e^{-\frac{k}{2}t}]}{K_1[\alpha]I_0[\alpha e^{-\frac{k}{2}t}] + I_1[\alpha]K_0[\alpha e^{-\frac{k}{2}t}]} \\ &= \frac{1}{\pi T}\frac{A(t)}{N(t)} \end{aligned} \tag{B.8a}$$

$$\alpha = \frac{2\pi T}{k} \tag{B.8b}$$

This reparametrisation was originally expressed as an integral [141, 148], the first derivative can be easily read off as

$$f'(t) = \frac{1}{[\alpha N(t)]^2} \tag{B.9}$$

and satisfies $f(0) = 1$ by making use of some properties of the modified Bessel functions.

Its second derivative is therefore

$$f''(t) = -2f'(t)\frac{\partial_t N(t)}{N(t)} \tag{B.10}$$

Next, make use of (B.5)

$$\partial_t N(t) = -\alpha\frac{k}{2}e^{-\frac{k}{2}t}(K_1[\alpha]I_1[\alpha e^{-\frac{k}{2}t}] - I_1[\alpha]K_1[\alpha e^{-\frac{k}{2}t}]) \tag{B.11}$$

to end up with

$$\begin{aligned} f''(t) &= 2\pi T e^{-\frac{k}{2}t}f'(t)\frac{K_1[\alpha]I_1[\alpha e^{-\frac{k}{2}t}] - I_1[\alpha]K_1[\alpha e^{-\frac{k}{2}t}]}{N(t)} \\ &= 2\pi T e^{-\frac{k}{2}t}f'(t)\frac{B(t)}{N(t)} \end{aligned} \tag{B.12}$$

It has the correct initial condition $f''(0) = 0$.

From the general expression of the dilaton (5.82), we will need to calculate the derivative of the ratio $f''(v)/f'(v)$. Luckily, this work is somewhat simplified because $f''(t) \propto f'(t)$ and we can make use of the Schwarzian (5.68a)

$$\{f(t), t\} = -2(\pi T)^2 e^{-kt} \tag{B.13}$$

The result is quick and simple to obtain:

$$\begin{aligned} \partial_t\frac{f''(t)}{f'(t)} &= \frac{1}{2}\left(\frac{f''(t)}{f'(t)}\right)^2 + 2(\pi T)^2 e^{-kt} \\ &= 2(\pi T)^2 e^{-kt}\left[-1 + \left(\frac{B(t)}{N(t)}\right)^2\right] \end{aligned} \tag{B.14}$$

B.III An Approximation for the Reparametrisation

Making use of the expansions (B.1a, B.1b), there is an easier expression for the time reparametrisation (5.69) when $\frac{k}{T}$ is small while keeping kt fixed such that the argument remains large. The result was first written down in [157].

We start by rewriting the reparametrisation as (5.70)

$$f(t) = f_\infty \left(-\frac{K_0[\alpha]}{I_0[\alpha]} I_0[\alpha e^{-\frac{k}{2}t}] + K_0[\alpha e^{-\frac{k}{2}t}]\right) \left(\frac{K_1[\alpha]}{I_1[\alpha]} I_0[\alpha e^{-\frac{k}{2}t}] + K_0[\alpha e^{-\frac{k}{2}t}]\right)^{-1} \tag{B.15}$$

We can now expand each factor separately, starting with

$$\begin{aligned} -\frac{K_0[\alpha]}{I_0[\alpha]} I_0[\alpha e^{-\frac{k}{2}t}] + K_0[\alpha e^{-\frac{k}{2}t}] &\approx -\pi e^{-2\alpha} \left(1 - \frac{1}{4\alpha}\right) \frac{e^{\alpha e^{-\frac{k}{2}t}}}{\sqrt{2\pi\alpha e^{-\frac{k}{2}t}}} \left(1 + \frac{1}{8\alpha e^{-\frac{k}{2}t}}\right) \\ &\quad + \sqrt{\frac{\pi}{2\alpha e^{-\frac{k}{2}t}}} e^{-\alpha e^{-\frac{k}{2}t}} \left(1 - \frac{1}{8\alpha e^{-\frac{k}{2}t}}\right) \\ &\approx \sqrt{\frac{\pi}{2\alpha e^{-\frac{k}{2}t}}} e^{-\alpha} \left(-e^{-\alpha(1-e^{-\frac{k}{2}t})} + e^{\alpha(1-e^{-\frac{k}{2}t})}\right) \\ &= \sqrt{\frac{2\pi}{\alpha e^{-\frac{k}{2}t}}} e^{-\alpha} \sinh\left(\alpha[1 - e^{-\frac{k}{2}t}]\right) \end{aligned} \tag{B.16}$$

and completely similar

$$\frac{K_1[\alpha]}{I_1[\alpha]} I_0[\alpha e^{-\frac{k}{2}t}] + K_0[\alpha e^{-\frac{k}{2}t}] \approx \sqrt{\frac{2\pi}{\alpha e^{-\frac{k}{2}t}}} e^{-\alpha} \cosh\left(\alpha[1 - e^{-\frac{k}{2}t}]\right) \tag{B.17}$$

such that we obtain the easier expression

$$f(t) \approx f_\infty \tanh\left(\frac{2\pi T}{k}[1 - e^{-\frac{k}{2}t}]\right) \tag{B.18}$$

It satisfies the correct initial condition $f(0) = 0$. Moreover, it even satisfies $f(t \to +\infty) = f_\infty$ and remains a good approximation for all t.

It is also quite easy to calculate its derivatives

$$\begin{aligned} f'(t) &= \pi T f_\infty \frac{e^{-\frac{k}{2}t}}{\cosh^2\left(\alpha[1 - e^{-\frac{k}{2}t}]\right)} \\ &= \pi T f_\infty e^{-\frac{k}{2}t} \left[1 - \left(\frac{f(t)}{f_\infty}\right)^2\right] \end{aligned} \tag{B.19}$$

and

$$\begin{aligned} f''(t) &= -\frac{k}{2} f'(t) - 2f'(t) \tanh\left(\alpha[1 - e^{-\frac{k}{2}t}]\right) \alpha \frac{k}{2} e^{-\frac{k}{2}t} \\ &= -\frac{k}{2} f'(t) \left[1 + \frac{4\pi T}{k f_\infty} e^{-\frac{k}{2}t} f(t)\right] \end{aligned} \tag{B.20}$$

where both initial conditions are only approximately satisfied $f'(0) = \pi T f_\infty \approx 1, f''(0) = -\frac{\pi T}{2} k f_\infty \approx -\frac{k}{2}$. But they remain good approximations for kt up to $\mathcal{O}(1)$.

The following expression is necessary for the dilaton

$$\begin{aligned}\frac{f''(t)}{f'(t)} &= -\frac{k}{2}\left[1+\frac{4\pi T}{kf_\infty}e^{-\frac{k}{2}t}f(t)\right]\\ \Rightarrow \partial_t\frac{f''(t)}{f'(t)} &= -\frac{k}{2}\left[-\frac{k}{2}\frac{4\pi T}{kf_\infty}e^{-\frac{k}{2}t}f(t)+\frac{4\pi T}{kf_\infty}e^{-\frac{k}{2}t}f'(t)\right]\\ &= -\frac{2\pi T}{f_\infty}e^{-\frac{k}{2}t}\left[f'(t)-\frac{k}{2}f(t)\right]\end{aligned} \tag{B.21}$$

B.IV Early Time Approximation

We will encounter quite intricate expressions for the entropy associated to an island. Since the Page time requires us to equate these expressions, an exact analytical result is impracticable. For small k we can rely on the results above and approximate them further for small values of kt, or times of order $\mathcal{O}(k^{-1})$. Equivalently, this means an expansion in the argument of (B.18) $\left(1-e^{-\frac{k}{2}t}\right)$ which is close to zero for $kt \ll 1$

$$f(t) = \alpha f_\infty\left(1-e^{-\frac{k}{2}t}\right)\left[1-\frac{1}{3}\alpha^2\left(1-e^{-\frac{k}{2}t}\right)^2+\mathcal{O}^4\right] \tag{B.22}$$

where higher order terms are denoted by $\mathcal{O}^n \equiv \mathcal{O}\left[\left(1-e^{-\frac{k}{2}t}\right)^n\right]$.

Similarly, for its derivative (B.19) we acquire

$$\begin{aligned}f'(t) &= \pi T f_\infty e^{-\frac{k}{2}t}\left[1-\alpha^2(1-e^{-\frac{k}{2}t})^2+\mathcal{O}^4\right]\\ &= \pi T f_\infty\left[1-\left(1-e^{-\frac{k}{2}t}\right)-\alpha^2\left(1-e^{-\frac{k}{2}t}\right)^2+\mathcal{O}^3\right]\end{aligned} \tag{B.23}$$

The remaining expressions (B.20, B.21) solely depend on the reparametrisation and its derivative. This leads to

$$\begin{aligned}f''(t) &= -\frac{\pi Tk}{2}f_\infty e^{-\frac{k}{2}t}\left[1+2\alpha^2\left(1-e^{-\frac{k}{2}t}\right)-3\alpha^2\left(1-e^{-\frac{k}{2}t}\right)^2+\mathcal{O}^3\right]\\ &= -\frac{\pi Tk}{2}f_\infty\left[1+(2\alpha^2-1)\left(1-e^{-\frac{k}{2}t}\right)-5\alpha^2\left(1-e^{-\frac{k}{2}t}\right)^2+\mathcal{O}^3\right]\end{aligned} \tag{B.24a}$$

$$\begin{aligned}\partial_t\frac{f''(t)}{f'(t)} &= -2(\pi T)^2e^{-\frac{k}{2}t}\left[1-2\left(1-e^{-\frac{k}{2}t}\right)-\alpha^2\left(1-e^{-\frac{k}{2}t}\right)^2+\mathcal{O}^3\right]\\ &= -2(\pi T)^2\left[1-3\left(1-e^{-\frac{k}{2}t}\right)+(2-\alpha^2)\left(1-e^{-\frac{k}{2}t}\right)^2+\mathcal{O}^3\right]\end{aligned} \tag{B.24b}$$

We currently keep the expressions in terms of the variable $e^{-\frac{k}{2}t}$, this can proof useful when taking the logarithm for the entropy. When needed, we can approximate this further down by expanding this exponential. This amount to setting $1-e^{-\frac{k}{2}t} = \frac{k}{2}t$ leading to the same expansion but in this new parameter instead. Also the reparametrisation can then easily be written as $f(t) = \pi T f_\infty t$.

This approach was applied on (6.59) resulting in

$$0 = a(t) + b(t)y(v) \tag{B.25a}$$

$$a(t) = f_\infty^2 - f(t)^2 - \frac{5}{2}\frac{kf_\infty f(t)}{\pi T} \tag{B.25b}$$

$$b(t) = [f_\infty^2 - f(t)^2]\left[4\frac{\pi T f_\infty}{kf(t)} - 7\right] \tag{B.25c}$$

with expansion variable $y(t) = \left(1 - e^{-\frac{k}{2}t}\right)$. We discarded terms quadratic in k since we are working for small k anyway.

Moreover, we applied the same procedure to (7.35a, 7.35b) which led to

$$0 = -\frac{1 - \frac{k}{2}(u+v)}{(u-v)^2} + k\left(\frac{1}{t-u} - \frac{1}{t} - \frac{u}{t^2}\right) \tag{B.26a}$$

$$0 = -(\pi T)^2\left(1 - \frac{3}{2}kv\right) - \frac{k}{2}\frac{1}{u-v} + \frac{1-kv}{(u-v)^2} + k\left(\frac{1}{t-v} - \frac{1}{t} - \frac{v}{t^2}\right) \tag{B.26b}$$

But solving this system resulted in a set of solutions which amounted to nothing.

Since the Page time is not that small when rewritten in terms of island time, we suspected that following this road would not amount to a sensible formula or new information. This can also be seen from Fig. 5.6 in which the reparametrisation quickly deviates from linear behaviour already for small times. Consequently, we did not follow this approach completely through.

Appendix C

Mathematica Code

The system of nonlinear equations (7.35a, 7.35b) in Ch. 7 is most easily solved via Wolfram Mathematica. Of course, other programming languages are fine as well. Down below, we provide the code for the program used to solve these equations. The other numerical results were obtained in a likewise fashion, but mostly via Python. To avoid cluttering the appendix, we restricted us to the most important one.

```
In[•]:= k = 1 / 100
        T = 1 / (2 * Pi)
        a = 2 * Pi * T / k
        F = BesselI[0, a] / (Pi T BesselI[1, a])
        $PreRead = (# /. s_String /; StringMatchQ[s, NumberString] && Precision@ToExpression@s == MachinePrecision :> s <> "`80." &);

In[•]:= A[t_] := -BesselK[0, a] * BesselI[0, a * Exp[- k * 0.5 * t]] + BesselI[0, a] * BesselK[0, a * Exp[- k * 0.5 * t]]
        Nu[t_] := BesselK[1, a] * BesselI[0, a * Exp[- k * 0.5 * t]] + BesselI[1, a] * BesselK[0, a * Exp[- k * 0.5 * t]]
        f[t_] := SetPrecision[(1 / (T * Pi)) * A[t] / Nu[t], 100]
        fRatio[t_] := f''[t] / f'[t]

        entropyPost[u_, v_, t_] := 0.5 * f''[v] / f'[v] + f'[v] / (f[u] - f[v]) + 0.5 * k Log[(f[t] - f[u])^2 / (f'[u] * (t - u)^2)] +
          0.5 * k Log[(f[t] - f[v])^2 / (f'[v] (t - v)^2)] - k Log[f'[t]]
        conditionPost1[u_, v_, t_] := -f'[u] × f'[v] / ((f[u] - f[v])^2) + k * (-f'[u] / (f[t] - f[u])) + 1 / (t - u) - 0.5 * f''[u] / f'[u])
        conditionPost2[u_, v_, t_] := 0.5 * fRatio'[v] + f''[v] / (f[u] - f[v]) + (f'[v] / (f[u] - f[v]))^2 +
           k * (-f'[v] / (f[t] - f[v])) + 1 / (t - v) - 0.5 * f''[v] / f'[v])

In[•]:= solveEntropyPost[t_] := NMinimize[{entropyPost[u, v, t], 0 ≤ v ≤ t ≤ u}, {u, v}]
        solveEntropyPost[10]

Out[•]= {0.487102, {u → 15.3837, v → 9.27765}}

In[•]:= rootCondition[t_] := FindRoot[{conditionPost1[u, v, t] == 0, conditionPost2[u, v, t] == 0}, {{u, t + 5.2}, {v, t - 0.7}}, WorkingPrecision → 120]
        rootCondition[10]

Out[•]= {u → 15.383727981278147820638298446821680330392671393578100192231717122380224421500291724091813304608776368345950353798349120 6,
         v → 9.277654615821403536130129095717777895045257167060228441025741457263374750809032640643328508092518263625229555631184014 61}

        sols[t_] = {u, v} /. rootCondition[t]
        dataTest = Table[{t, sols[t]}, {t, 0.702461, 300, .5}]
        Export["IslandSolutions.txt", dataTest, "Table"]
```

Note how minimising the entropy and solving the island equations lead to the same solution. The initial input for all boundary times is best found after some iterations. The initial time was first obtained via the expressions in Subsect. 7.IV.a.

Appendix D

Acronyms

ADM Arnowitt–Deser–Misner

(A)dS (Anti-)de Sitter

AMPS Almheiri–Marolf–Polchinski–Sully

BC Boundary Conditions

BH Black Hole or Bekenstein–Hawking

BMS Bondi–Metzner–Sachs

BTZ Bañados–Teitelboim–Zanelli

CFT Conformal Field Theory

CHSH Clauser–Horne–Shimony–Holt

EBH Evaporating Black Hole

EE Entanglement Entropy

eom Equations of Motion

EPR Einstein–Podolsky–Rosen

ER Einstein–Rosen

EW Entanglement Wedge

FLM Faulkner–Lewkowycz–Maldacena

FTL Faster-than-light

GPI Gravitational Path Integral

GR General Relativity

HEE Holographic Entanglement Entropy

HRT Hubeny–Rangamani–Takayanagi

IP Island Parameter $\frac{k}{T}$

JT Gravity Jackiw–Teitelboim Gravity

LM Lewkowycz–Maldacena

OPE Operator Product Expansion

PI Path Integral

QES Quantum Extremal Surface

QFT Quantum Field Theory

QG Quantum Gravity

QM Quantum Mechanics/Mechanical

RT Ryu–Takayanagi

SYK Sachdev–Ye–Kitaev

vN von Neumann

Bibliography

[1] J. M. Bardeen, B. Carter, and S. W. Hawking. The four laws of black hole thermodynamics. 161-170, 24 January 1973.

[2] J. D. Bekenstein. Black holes and the second law. 4, 737-740, 1972. doi: https://doi.org/10.1007/BF02757029.

[3] S. W. Hawking. Particle creation by black holes. 199-220, 12 April 1975.

[4] J.D. Bekenstein. Black holes and entropy. Volume 7, Number 8, 15 April 1973.

[5] Juan Martin Maldacena. The Large N limit of superconformal field theories and supergravity. *Adv. Theor. Math. Phys.*, 2:231–252, 1998. doi: 10.1023/A:1026654312961. URL https://arxiv.org/abs/hep-th/9711200.

[6] Gerard 't Hooft. Dimensional reduction in quantum gravity. *Conf. Proc. C*, 930308: 284–296, 1993. URL https://arxiv.org/abs/gr-qc/9310026.

[7] Gerard 't Hooft. The Holographic principle: Opening lecture. *Subnucl. Ser.*, 37:72–100, 2001. doi: 10.1142/9789812811585_0005. URL https://arxiv.org/abs/hep-th/0003004.

[8] Leonard Susskind. The World as a hologram. *J. Math. Phys.*, 36:6377–6396, 1995. doi: 10.1063/1.531249. URL https://arxiv.org/abs/hep-th/9409089.

[9] Raphael Bousso. The holographic principle. *Reviews of Modern Physics*, 74(3):825–874, August 2002. doi: 10.1103/RevModPhys.74.825. URL https://arxiv.org/abs/hep-th/0203101.

[10] Shinsei Ryu and Tadashi Takayanagi. Holographic derivation of entanglement entropy from AdS/CFT. *Phys. Rev. Lett.*, 96:181602, 2006. doi: 10.1103/PhysRevLett.96.181602. URL https://arxiv.org/abs/hep-th/0603001.

[11] Don N. Page. Information in black hole radiation. *Phys. Rev. Lett.*, 71:3743–3746, 1993. doi: 10.1103/PhysRevLett.71.3743. URL https://arxiv.org/abs/hep-th/9306083v2.

[12] Don N. Page. Time Dependence of Hawking Radiation Entropy. *JCAP*, 09:028, 2013. doi: 10.1088/1475-7516/2013/09/028. URL https://arxiv.org/abs/1301.4995.

[13] Daniel Harlow. Jerusalem Lectures on Black Holes and Quantum Information. *Rev. Mod. Phys.*, 88:015002, 2016. doi: 10.1103/RevModPhys.88.015002. URL https://arxiv.org/pdf/1409.1231.pdf.

[14] Ahmed Almheiri, Netta Engelhardt, Donald Marolf, and Henry Maxfield. The entropy of bulk quantum fields and the entanglement wedge of an evaporating black hole. *JHEP*, 12:063, 2019. doi: 10.1007/JHEP12(2019)063. URL https://arxiv.org/abs/1905.08762.

[15] Geoffrey Penington. Entanglement Wedge Reconstruction and the Information Paradox. *JHEP*, 09:002, 2020. doi: 10.1007/JHEP09(2020)002. URL https://arxiv.org/abs/1905.08255.

[16] Roman Jackiw. Lower dimensional gravity. *Nuclear Physics B*, 252:343 – 356, 1985. ISSN 0550-3213. doi: https://doi.org/10.1016/0550-3213(85)90448-1. URL http://www.sciencedirect.com/science/article/pii/0550321385904481.

[17] Claudio Teitelboim. Gravitation and hamiltonian structure in two space-time dimensions. *Physical Review Letters D **126** (1983) 41*.

[18] Ahmed Almheiri, Raghu Mahajan, Juan Maldacena, and Ying Zhao. The Page curve of Hawking radiation from semiclassical geometry. *Journal of High Energy Physics*, 2020 (3):149, March 2020. doi: 10.1007/JHEP03(2020)149. URL https://arxiv.org/abs/1908.10996.

[19] Geoff Penington, Stephen H. Shenker, Douglas Stanford, and Zhenbin Yang. Replica wormholes and the black hole interior. 11 2019. URL https://arxiv.org/abs/1911.11977.

[20] Ahmed Almheiri, Thomas Hartman, Juan Maldacena, Edgar Shaghoulian, and Amirhossein Tajdini. Replica Wormholes and the Entropy of Hawking Radiation. *JHEP*, 05:013, 2020. doi: 10.1007/JHEP05(2020)013. URL https://arxiv.org/abs/1911.12333.

[21] Sabrina Pasterski and Herman Verlinde. HPS meets AMPS: How Soft Hair Dissolves the Firewall. 12 2020. URL https://arxiv.org/abs/2012.03850.

[22] Yasunori Nomura. From the Black Hole Conundrum to the Structure of Quantum Gravity. *Mod. Phys. Lett. A*, 36(08):2130007, 2021. doi: 10.1142/S021773232130007X. URL https://arxiv.org/abs/2011.08707.

[23] Alok Laddha, Siddharth G. Prabhu, Suvrat Raju, and Pushkal Shrivastava. The Holographic Nature of Null Infinity. *SciPost Phys.*, 10:041, 2021. doi: 10.21468/SciPostPhys.10.2.041. URL https://arxiv.org/abs/2002.02448.

[24] Suvrat Raju. Lessons from the Information Paradox. 12 2020. URL https://arxiv.org/abs/2012.05770.

[25] Gerard 't Hooft. On the Quantum Structure of a Black Hole. *Nucl. Phys. B*, 256:727–745, 1985. doi: 10.1016/0550-3213(85)90418-3.

[26] John Preskill. Do black holes destroy information? In *International Symposium on Black holes, Membranes, Wormholes and Superstrings*, 1 1992. URL https://arxiv.org/abs/hep-th/9209058.

[27] Andrew Strominger. Les Houches lectures on black holes. In *NATO Advanced Study Institute: Les Houches Summer School, Session 62: Fluctuating Geometries in Statistical Mechanics and Field Theory*, 8 1994. URL https://arxiv.org/abs/hep-th/9501071.

[28] Leonard Susskind. Trouble for remnants. 1 1995. URL https://arxiv.org/abs/hep-th/9501106.

[29] Steven B. Giddings. Why aren't black holes infinitely produced? *Phys. Rev. D*, 51:6860–6869, 1995. doi: 10.1103/PhysRevD.51.6860.

[30] W. G. Unruh. Sonic analog of black holes and the effects of high frequencies on black hole evaporation. *Phys. Rev. D*, 51:2827–2838, 1995. doi: 10.1103/PhysRevD.51.2827. URL https://arxiv.org/abs/gr-qc/9409008.

[31] Steven Corley and Ted Jacobson. Hawking spectrum and high frequency dispersion. *Phys. Rev. D*, 54:1568–1586, 1996. doi: 10.1103/PhysRevD.54.1568. URL https://arxiv.org/abs/hep-th/9601073.

[32] Leonard Susskind. Twenty years of debate with Stephen. In *Workshop on Conference on the Future of Theoretical Physics and Cosmology in Honor of Steven Hawking's 60th Birthday*, 4 2002. URL https://arxiv.org/abs/hep-th/0204027.

[33] Leonard Susskind. The Anthropic landscape of string theory. 2 2003. URL https://arxiv.org/abs/hep-th/0302219.

[34] Ahmed Almheiri, Donald Marolf, Joseph Polchinski, and James Sully. Black Holes: Complementarity or Firewalls? *JHEP*, 02:062, 2013. doi: 10.1007/JHEP02(2013)062. URL https://arxiv.org/abs/1207.3123.

[35] S. Carroll. *Something Deeply Hidden: Quantum Worlds and the Emergence of Spacetime*. Oneworld Publications, 2019. ISBN 9781786076342.

[36] T. Hartman. Lectures on quantum gravity and black holes, 2015. URL http://www.hartmanhep.net/topics2015/gravity-lectures.pdf.

[37] S. S. Gubser, Igor R. Klebanov, and Alexander M. Polyakov. Gauge theory correlators from noncritical string theory. *Phys. Lett. B*, 428:105–114, 1998. doi: 10.1016/S0370-2693(98)00377-3. URL https://arxiv.org/abs/hep-th/9802109.

[38] Edward Witten. Anti-de Sitter space and holography. *Adv. Theor. Math. Phys.*, 2:253–291, 1998. doi: 10.4310/ATMP.1998.v2.n2.a2. URL https://arxiv.org/abs/hep-th/9802150.

[39] M. Rangamani and T. Takayanagi. *Holographic Entanglement Entropy*. Springer International Publishing, 1 edition, 26 Jan 2017. ISBN 978-3-319-52571-6. doi: 10.1007/978-3-319-52573-0.

[40] Daniel Z. Freedman and Antoine Van Proeyen. *Supergravity*. Cambridge Univ. Press, Cambridge, UK, 5 2012. ISBN 978-1-139-36806-3, 978-0-521-19401-3.

[41] J. Zaanen, Y. W. Sun, Y. Liu, and K. Schalm. *Holographic Duality in Condensed Matter Physics*, volume 1. W. H. Cambridge University Press, 2015. ISBN 978-1-107-08008-9.

[42] Matthew Headrick. Lectures on entanglement entropy in field theory and holography. 7 2019. URL https://arxiv.org/abs/1907.08126.

[43] Christoph Holzhey, Finn Larsen, and Frank Wilczek. Geometric and renormalized entropy in conformal field theory. *Nucl. Phys. B*, 424:443–467, 1994. doi: 10.1016/0550-3213(94)90402-2. URL https://arxiv.org/abs/hep-th/9403108.

[44] Ahmed Almheiri, Thomas Hartman, Juan Maldacena, Edgar Shaghoulian, and Amirhossein Tajdini. The entropy of Hawking radiation. 6 2020. URL https://arxiv.org/abs/2006.06872.

[45] P. V. Buividovich and M. I. Polikarpov. Entanglement entropy in gauge theories and the holographic principle for electric strings. *Phys. Lett. B*, 670:141–145, 2008. doi: 10.1016/j.physletb.2008.10.032. URL https://arxiv.org/abs/0806.3376.

[46] Veronika E. Hubeny and Mukund Rangamani. Causal Holographic Information. *JHEP*, 06:114, 2012. doi: 10.1007/JHEP06(2012)114. URL https://arxiv.org/abs/1204.1698.

[47] Mark Srednicki. Entropy and area. *Phys. Rev. Lett.*, 71:666–669, 1993. doi: 10.1103/PhysRevLett.71.666. URL https://arxiv.org/abs/hep-th/9303048.

[48] Luca Bombelli, Rabinder K. Koul, Joohan Lee, and Rafael D. Sorkin. A Quantum Source of Entropy for Black Holes. *Phys. Rev. D*, 34:373–383, 1986. doi: 10.1103/PhysRevD.34.373.

[49] H. Casini and M. Huerta. A Finite entanglement entropy and the c-theorem. *Phys. Lett. B*, 600:142–150, 2004. doi: 10.1016/j.physletb.2004.08.072. URL https://arxiv.org/abs/hep-th/0405111.

[50] H. Araki and E. H. Lieb. Entropy inequalities. *Commun. Math. Phys.*, 18:160–170, 1970. doi: 10.1007/BF01646092.

[51] Elliott H. Lieb and Mary Beth Ruskai. A Fundamental Property of Quantum-Mechanical Entropy. *Phys. Rev. Lett.*, 30:434–436, 1973. doi: 10.1103/PhysRevLett.30.434.

[52] Elliott H. Lieb and Mary Beth Ruskai. Proof of the strong subadditivity of quantum-mechanical entropy. *Journal of Mathematical Physics*, 14(12):1938–1941, 1973. doi: 10.1063/1.1666274. URL https://doi.org/10.1063/1.1666274.

[53] Markus Hauru. Multiscale entanglement renormalisation ansatz. *Master's Thesis, University of Helsinki*, page 104, 2013. URL https://helda.helsinki.fi/bitstream/handle/10138/42005/Pro_gradu_M_Hauru.pdf.

[54] V. Vedral. The role of relative entropy in quantum information theory. *Rev. Mod. Phys.*, 74:197–234, 2002. doi: 10.1103/RevModPhys.74.197. URL https://arxiv.org/abs/quant-ph/0102094.

[55] F. Verstraete. *What Every Human Being should know about Quantum Information and Quantum Computing*. Ghent University, 2021.

[56] Suvrat Raju. A Toy Model of the Information Paradox in Empty Space. *SciPost Phys.*, 6(6):073, 2019. doi: 10.21468/SciPostPhys.6.6.073. URL https://arxiv.org/abs/1809.10154.

[57] J. S. Bell. On the Einstein-Podolsky-Rosen paradox. *Physics Physique Fizika*, 1:195–200, 1964. doi: 10.1103/PhysicsPhysiqueFizika.1.195.

[58] John F. Clauser, Michael A. Horne, Abner Shimony, and Richard A. Holt. Proposed experiment to test local hidden-variable theories. *Phys. Rev. Lett.*, 23:880–884, Oct 1969. doi: 10.1103/PhysRevLett.23.880. URL https://link.aps.org/doi/10.1103/PhysRevLett.23.880.

[59] B. S. Cirelson. QUANTUM GENERALIZATIONS OF BELL'S INEQUALITY. *Lett. Math. Phys.*, 4:93–100, 1980. doi: 10.1007/BF00417500.

[60] Benjamin Toner and Frank Verstraete. Monogamy of Bell correlations and Tsirelson's bound. *arXiv e-prints*, art. quant-ph/0611001, November 2006. URL https://arxiv.org/abs/quant-ph/0611001.

[61] Ben Toner. Monogamy of non-local quantum correlations. *Proceedings of the Royal Society of London Series A*, 465(2101):59–69, January 2009. doi: 10.1098/rspa.2008.0149. URL https://arxiv.org/abs/quant-ph/0601172.

[62] Pasquale Calabrese and John Cardy. Entanglement entropy and conformal field theory. *J. Phys. A*, 42:504005, 2009. doi: 10.1088/1751-8113/42/50/504005. URL https://arxiv.org/abs/0905.4013.

[63] Goran Lindblad. Brownian Motion of a Quantum Harmonic Oscillator. *Rept. Math. Phys.*, 10:393, 1976. doi: 10.1016/0034-4877(76)90029-X.

[64] L. V. Keldysh. Diagram technique for nonequilibrium processes. *Zh. Eksp. Teor. Fiz.*, 47:1515–1527, 1964.

[65] Felix M. Haehl, R. Loganayagam, and Mukund Rangamani. The Fluid Manifesto: Emergent symmetries, hydrodynamics, and black holes. *JHEP*, 01:184, 2016. doi: 10.1007/JHEP01(2016)184. URL https://arxiv.org/abs/1510.02494.

[66] Felix M. Haehl, R. Loganayagam, and Mukund Rangamani. Schwinger-Keldysh formalism. Part I: BRST symmetries and superspace. *JHEP*, 06:069, 2017. doi: 10.1007/JHEP06(2017)069. URL https://arxiv.org/abs/1610.01940.

[67] Samir D. Mathur. The Information paradox: A Pedagogical introduction. *Class. Quant. Grav.*, 26:224001, 2009. doi: 10.1088/0264-9381/26/22/224001. URL https://arxiv.org/abs/0909.1038.

[68] G. W. Gibbons and S. W. Hawking. Cosmological event horizons, thermodynamics, and particle creation. *Phys. Rev. D*, 15:2738–2751, May 1977. doi: 10.1103/PhysRevD.15.2738. URL https://link.aps.org/doi/10.1103/PhysRevD.15.2738.

[69] J. J Bisognano and E. H. Wichmann. On the Duality Condition for Quantum Fields. *J. Math. Phys.*, 17:303–321, 1976. doi: 10.1063/1.522898.

[70] E. Verlinde. Lectures on entanglement in quantum field theory and gravity, 2020.

[71] Michael E. Peskin and Daniel V. Schroeder. *An Introduction to quantum field theory*. Addison-Wesley, Reading, USA, 1995. ISBN 978-0-201-50397-5.

[72] Richard C. Tolman. On the weight of heat and thermal equilibrium in general relativity. *Phys. Rev.*, 35:904–924, Apr 1930. doi: 10.1103/PhysRev.35.904. URL https://link.aps.org/doi/10.1103/PhysRev.35.904.

[73] P. C. W. Davies. Scalar particle production in Schwarzschild and Rindler metrics. *J. Phys. A*, 8:609–616, 1975. doi: 10.1088/0305-4470/8/4/022.

[74] W. G. Unruh. Notes on black-hole evaporation. *Phys. Rev. D*, 14:870–892, Aug 1976. doi: 10.1103/PhysRevD.14.870. URL https://link.aps.org/doi/10.1103/PhysRevD.14.870.

[75] Steven B. Giddings. Hawking radiation, the Stefan–Boltzmann law, and unitarization. *Phys. Lett. B*, 754:39–42, 2016. doi: 10.1016/j.physletb.2015.12.076. URL https://arxiv.org/abs/1511.08221.

[76] Steven B. Giddings. (Non)perturbative gravity, nonlocality, and nice slices. *Phys. Rev. D*, 74:106009, 2006. doi: 10.1103/PhysRevD.74.106009. URL https://arxiv.org/abs/hep-th/0606146.

[77] S. Hossenfelder. Hawking radiation is not produced at the black hole horizon., 01 Dec 2015. URL http://backreaction.blogspot.com/2015/12/hawking-radiation-is-not-produced-at.html.

[78] G. W. Gibbons and S. W. Hawking. Action Integrals and Partition Functions in Quantum Gravity. *Phys. Rev. D*, 15:2752–2756, 1977. doi: 10.1103/PhysRevD.15.2752.

[79] Aitor Lewkowycz and Juan Maldacena. Generalized gravitational entropy. *JHEP*, 08: 090, 2013. doi: 10.1007/JHEP08(2013)090. URL https://arxiv.org/abs/1304.4926.

[80] S. W. Hawking and W. Israel. *General Relativity: An Einstein Centenary Survey*. Univ. Pr., Cambridge, UK, 1979. ISBN 978-0-521-29928-2.

[81] Leonard Susskind and John Uglum. Black hole entropy in canonical quantum gravity and superstring theory. *Phys. Rev. D*, 50:2700–2711, 1994. doi: 10.1103/PhysRevD.50.2700. URL https://arxiv.org/abs/hep-th/9401070.

[82] Jean-Guy Demers, Rene Lafrance, and Robert C. Myers. Black hole entropy without brick walls. *Phys. Rev. D*, 52:2245–2253, 1995. doi: 10.1103/PhysRevD.52.2245. URL https://arxiv.org/abs/gr-qc/9503003.

[83] Jacob D. Bekenstein. A Universal Upper Bound on the Entropy to Energy Ratio for Bounded Systems. *Phys. Rev. D*, 23:287, 1981. doi: 10.1103/PhysRevD.23.287.

[84] S. W. Hawking. Gravitational radiation from colliding black holes. *Phys. Rev. Lett.*, 26: 1344–1346, May 1971. doi: 10.1103/PhysRevLett.26.1344. URL https://link.aps.org/doi/10.1103/PhysRevLett.26.1344.

[85] Aron C. Wall. A proof of the generalized second law for rapidly changing fields and arbitrary horizon slices. *Phys. Rev. D*, 85:104049, 2012. doi: 10.1103/PhysRevD.85.104049. URL https://arxiv.org/abs/1105.3445. [Erratum: Phys.Rev.D 87, 069904 (2013)].

[86] Andrew Strominger and Cumrun Vafa. Microscopic origin of the Bekenstein-Hawking entropy. *Phys. Lett. B*, 379:99–104, 1996. doi: 10.1016/0370-2693(96)00345-0. URL https://arxiv.org/abs/hep-th/9601029.

[87] Don N. Page. Particle Emission Rates from a Black Hole: Massless Particles from an Uncharged, Nonrotating Hole. *Phys. Rev. D*, 13:198–206, 1976. doi: 10.1103/PhysRevD.13.198.

[88] R. Giles, Larry D. McLerran, and Charles B. Thorn. THE STRING REPRESENTATION FOR A FIELD THEORY WITH INTERNAL SYMMETRY. *Phys. Rev. D*, 17:2058–2073, 1978. doi: 10.1103/PhysRevD.17.2058.

[89] Leonard Susskind and Larus Thorlacius. Gedanken experiments involving black holes. *Phys. Rev. D*, 49:966–974, 1994. doi: 10.1103/PhysRevD.49.966. URL https://arxiv.org/abs/hep-th/9308100.

[90] Patrick Hayden and John Preskill. Black holes as mirrors: Quantum information in random subsystems. *JHEP*, 09:120, 2007. doi: 10.1088/1126-6708/2007/09/120. URL https://arxiv.org/abs/0708.4025.

[91] Yasuhiro Sekino and Leonard Susskind. Fast Scramblers. *JHEP*, 10:065, 2008. doi: 10.1088/1126-6708/2008/10/065. URL https://arxiv.org/abs/0808.2096.

[92] A. Einstein and N. Rosen. The particle problem in the general theory of relativity. *Phys. Rev.*, 48:73–77, Jul 1935. doi: 10.1103/PhysRev.48.73. URL https://link.aps.org/doi/10.1103/PhysRev.48.73.

[93] Albert Einstein, Boris Podolsky, and Nathan Rosen. Can quantum mechanical description of physical reality be considered complete? *Phys. Rev.*, 47:777–780, 1935. doi: 10.1103/PhysRev.47.777.

[94] Juan Maldacena and Leonard Susskind. Cool horizons for entangled black holes. *Fortsch. Phys.*, 61:781–811, 2013. doi: 10.1002/prop.201300020. URL https://arxiv.org/abs/1306.0533.

[95] D. Deutsch. It from qubit. 2004.

[96] Mark Van Raamsdonk. Building up spacetime with quantum entanglement. *Gen. Rel. Grav.*, 42:2323–2329, 2010. doi: 10.1142/S0218271810018529. URL https://arxiv.org/abs/1005.3035.

[97] G. W. Gibbons and N. P. Warner. Global structure of five-dimensional fuzzballs. *Class. Quant. Grav.*, 31:025016, 2014. doi: 10.1088/0264-9381/31/2/025016. URL https://arxiv.org/abs/1305.0957.

[98] Brian Swingle. Entanglement Renormalization and Holography. *Phys. Rev. D*, 86: 065007, 2012. doi: 10.1103/PhysRevD.86.065007. URL https://arxiv.org/abs/0905.1317.

[99] Mark Van Raamsdonk. Comments on quantum gravity and entanglement. 7 2009. URL https://arxiv.org/abs/0907.2939.

[100] Xi Dong. Holographic Entanglement Entropy for General Higher Derivative Gravity. *JHEP*, 01:044, 2014. doi: 10.1007/JHEP01(2014)044. URL https://arxiv.org/abs/1310.5713.

[101] Joan Camps. Generalized entropy and higher derivative Gravity. *JHEP*, 03:070, 2014. doi: 10.1007/JHEP03(2014)070. URL https://arxiv.org/abs/1310.6659.

[102] Veronika E. Hubeny, Mukund Rangamani, and Tadashi Takayanagi. A Covariant holographic entanglement entropy proposal. *JHEP*, 07:062, 2007. doi: 10.1088/1126-6708/2007/07/062. URL https://arxiv.org/abs/0705.0016.

[103] Matthew Headrick, Veronika E. Hubeny, Albion Lawrence, and Mukund Rangamani. Causality \& holographic entanglement entropy. *JHEP*, 12:162, 2014. doi: 10.1007/JHEP12(2014)162. URL https://arxiv.org/abs/1408.6300.

[104] Aron C. Wall. Maximin Surfaces, and the Strong Subadditivity of the Covariant Holographic Entanglement Entropy. *Class. Quant. Grav.*, 31(22):225007, 2014. doi: 10.1088/0264-9381/31/22/225007. URL https://arxiv.org/abs/1211.3494.

[105] Matthew Headrick and Tadashi Takayanagi. A Holographic proof of the strong subadditivity of entanglement entropy. *Phys. Rev. D*, 76:106013, 2007. doi: 10.1103/PhysRevD.76.106013. URL https://arxiv.org/abs/0704.3719.

[106] Matthew Headrick. General properties of holographic entanglement entropy. *JHEP*, 03:085, 2014. doi: 10.1007/JHEP03(2014)085. URL https://arxiv.org/abs/1312.6717.

[107] Patrick Hayden, Matthew Headrick, and Alexander Maloney. Holographic Mutual Information is Monogamous. *Phys. Rev. D*, 87(4):046003, 2013. doi: 10.1103/PhysRevD.87.046003. URL https://arxiv.org/abs/1107.2940.

[108] Matthew Headrick. Entanglement Renyi entropies in holographic theories. *Phys. Rev. D*, 82:126010, 2010. doi: 10.1103/PhysRevD.82.126010. URL https://arxiv.org/abs/1006.0047.

[109] Thomas Faulkner. The Entanglement Renyi Entropies of Disjoint Intervals in AdS/CFT. 3 2013. URL https://arxiv.org/abs/1303.7221.

[110] Felix M. Haehl, Thomas Hartman, Donald Marolf, Henry Maxfield, and Mukund Rangamani. Topological aspects of generalized gravitational entropy. *JHEP*, 05:023, 2015. doi: 10.1007/JHEP05(2015)023. URL https://arxiv.org/abs/1412.7561.

[111] Veronika E. Hubeny, Henry Maxfield, Mukund Rangamani, and Erik Tonni. Holographic entanglement plateaux. *JHEP*, 08:092, 2013. doi: 10.1007/JHEP08(2013)092. URL https://arxiv.org/abs/1306.4004.

[112] J. David Brown and M. Henneaux. Central Charges in the Canonical Realization of Asymptotic Symmetries: An Example from Three-Dimensional Gravity. *Commun. Math. Phys.*, 104:207–226, 1986. doi: 10.1007/BF01211590. URL http://srv2.fis.puc.cl/~mbanados/Cursos/TopicosRelatividadAvanzada/BrownHenneaux.pdf.

[113] Thomas Faulkner, Aitor Lewkowycz, and Juan Maldacena. Quantum corrections to holographic entanglement entropy. *JHEP*, 11:074, 2013. doi: 10.1007/JHEP11(2013)074. URL https://arxiv.org/abs/1307.2892.

[114] Taylor Barrella, Xi Dong, Sean A. Hartnoll, and Victoria L. Martin. Holographic entanglement beyond classical gravity. *JHEP*, 09:109, 2013. doi: 10.1007/JHEP09(2013)109. URL https://arxiv.org/abs/1306.4682.

[115] Netta Engelhardt and Aron C. Wall. Quantum Extremal Surfaces: Holographic Entanglement Entropy beyond the Classical Regime. *JHEP*, 01:073, 2015. doi: 10.1007/JHEP01(2015)073. URL https://arxiv.org/abs/1408.3203.

[116] Chris Akers, Netta Engelhardt, Geoff Penington, and Mykhaylo Usatyuk. Quantum Maximin Surfaces. *JHEP*, 08:140, 2020. doi: 10.1007/JHEP08(2020)140. URL https://arxiv.org/abs/1912.02799.

[117] Xi Dong and Aitor Lewkowycz. Entropy, Extremality, Euclidean Variations, and the Equations of Motion. *JHEP*, 01:081, 2018. doi: 10.1007/JHEP01(2018)081. URL https://arxiv.org/abs/1705.08453.

[118] S. W. Hawking. Breakdown of predictability in gravitational collapse. *Phys. Rev. D*, 14: 2460–2473, Nov 1976. doi: 10.1103/PhysRevD.14.2460. URL https://link.aps.org/doi/10.1103/PhysRevD.14.2460.

[119] H. Casini, C. D. Fosco, and M. Huerta. Entanglement and alpha entropies for a massive Dirac field in two dimensions. *J. Stat. Mech.*, 0507:P07007, 2005. doi: 10.1088/1742-5468/2005/07/P07007. URL https://arxiv.org/abs/cond-mat/0505563.

[120] H. Casini and M. Huerta. Reduced density matrix and internal dynamics for multicomponent regions. *Class. Quant. Grav.*, 26:185005, 2009. doi: 10.1088/0264-9381/26/18/185005. URL https://arxiv.org/abs/0903.5284.

[121] Timothy J. Hollowood and S. Prem Kumar. Islands and Page Curves for Evaporating Black Holes in JT Gravity. *JHEP*, 08:094, 2020. doi: 10.1007/JHEP08(2020)094. URL https://arxiv.org/abs/2004.14944.

[122] Kanato Goto, Thomas Hartman, and Amirhossein Tajdini. Replica wormholes for an evaporating 2D black hole. 11 2020. URL https://arxiv.org/abs/2011.09043.

[123] Bartlomiej Czech, Joanna L. Karczmarek, Fernando Nogueira, and Mark Van Raamsdonk. The Gravity Dual of a Density Matrix. *Class. Quant. Grav.*, 29:155009, 2012. doi: 10.1088/0264-9381/29/15/155009. URL https://arxiv.org/abs/1204.1330.

[124] M. Ohya and D. Petz. *Quantum Entropy and Its Use*. Springer-Verlag Berlin Heidelberg, 1993. ISBN 978-3-540-20806-8.

[125] Jordan Cotler, Patrick Hayden, Geoffrey Penington, Grant Salton, Brian Swingle, and Michael Walter. Entanglement Wedge Reconstruction via Universal Recovery Channels. *Phys. Rev. X*, 9(3):031011, 2019. doi: 10.1103/PhysRevX.9.031011. URL https://arxiv.org/abs/1704.05839.

[126] Ahmed Almheiri, Xi Dong, and Daniel Harlow. Bulk Locality and Quantum Error Correction in AdS/CFT. *JHEP*, 04:163, 2015. doi: 10.1007/JHEP04(2015)163. URL https://arxiv.org/abs/1411.7041.

[127] Ahmed Almheiri. Holographic Quantum Error Correction and the Projected Black Hole Interior. 10 2018. URL https://arxiv.org/abs/1810.02055.

[128] Bruce S. DeWitt and Raymond Stora, editors. *Relativity, groups and topology: Proceedings, 40th Summer School of Theoretical Physics - Session 40: Les Houches, France, June 27 - August 4, 1983, vol. 2*, Amsterdam, 1984. North-holland.

[129] P. Hayden. Spacetime, entropy, and quantum information, 08 May 2015. URL https://simons.berkeley.edu/talks/patrick-hayden-2015-05-08.

[130] Subir Sachdev and Jinwu Ye. Gapless spin fluid ground state in a random, quantum Heisenberg magnet. *Phys. Rev. Lett.*, 70:3339, 1993. doi: 10.1103/PhysRevLett.70.3339. URL https://arxiv.org/abs/cond-mat/9212030.

[131] Subir Sachdev. Bekenstein-Hawking Entropy and Strange Metals. *Phys. Rev. X*, 5 (4):041025, 2015. doi: 10.1103/PhysRevX.5.041025. URL https://arxiv.org/abs/1506.05111.

[132] A. Kitaev. A simple model of quantum holography (part 1), 07 Apr 2015. URL https://online.kitp.ucsb.edu/online/entangled15/kitaev/.

[133] A. Kitaev. A simple model of quantum holography (part 2), 27 May 2015. URL https://online.kitp.ucsb.edu/online/entangled15/kitaev2/.

[134] Gábor Sárosi. AdS_2 holography and the SYK model. *PoS*, Modave2017:001, 2018. doi: 10.22323/1.323.0001. URL https://arxiv.org/abs/1711.08482.

[135] A. Fabbri and J. Navarro-Salas. *Modeling black hole evaporation*. Imperial College Press, 26 Jan 2005. ISBN 978-1860945274.

[136] Sean M. Carroll. *Spacetime and Geometry*. Cambridge University Press, July 2019. ISBN 978-0-8053-8732-2, 978-1-108-48839-6, 978-1-108-77555-7.

[137] M. Headrick. Compendium of Useful Formulas. pages 1–67. URL http://people.brandeis.edu/~headrick/HeadrickCompendium.pdf.

[138] Ahmed Almheiri and Joseph Polchinski. Models of AdS_2 backreaction and holography. *JHEP*, 11:014, 2015. doi: 10.1007/JHEP11(2015)014. URL https://arxiv.org/abs/1402.6334.

[139] Kristan Jensen. Chaos in AdS_2 Holography. *Phys. Rev. Lett.*, 117(11):111601, 2016. doi: 10.1103/PhysRevLett.117.111601. URL https://arxiv.org/abs/1605.06098.

[140] Juan Maldacena, Douglas Stanford, and Zhenbin Yang. Conformal symmetry and its breaking in two dimensional Nearly Anti-de-Sitter space. *PTEP*, 2016(12):12C104, 2016. doi: 10.1093/ptep/ptw124. URL https://arxiv.org/abs/1606.01857.

[141] Julius Engelsöy, Thomas G. Mertens, and Herman Verlinde. An investigation of AdS_2 backreaction and holography. *JHEP*, 07:139, 2016. doi: 10.1007/JHEP07(2016)139. URL https://arxiv.org/abs/1606.03438.

[142] Andreas Blommaert, Thomas G. Mertens, and Henri Verschelde. Clocks and Rods in Jackiw-Teitelboim Quantum Gravity. *JHEP*, 09:060, 2019. doi: 10.1007/JHEP09(2019)060. URL https://arxiv.org/abs/1902.11194.

[143] Nele Callebaut. The gravitational dynamics of kinematic space. *JHEP*, 02:153, 2019. doi: 10.1007/JHEP02(2019)153. URL https://arxiv.org/abs/1808.10431.

[144] R. Jackiw. Weyl symmetry and the Liouville theory. *Theor. Math. Phys.*, 148:941–947, 2006. doi: 10.1007/s11232-006-0090-9. URL https://arxiv.org/abs/hep-th/0511065.

[145] Daniel Grumiller and Roman Jackiw. Liouville gravity from Einstein gravity. 12 2007. URL https://arxiv.org/abs/0712.3775.

[146] Jan de Boer, Felix M. Haehl, Michal P. Heller, and Robert C. Myers. Entanglement, holography and causal diamonds. *JHEP*, 08:162, 2016. doi: 10.1007/JHEP08(2016)162. URL https://arxiv.org/abs/1606.03307.

[147] Upamanyu Moitra, Sunil Kumar Sake, Sandip P. Trivedi, and V. Vishal. Jackiw-Teitelboim Model Coupled to Conformal Matter in the Semi-Classical Limit. *JHEP*, 04:199, 2020. doi: 10.1007/JHEP04(2020)199. URL https://arxiv.org/abs/1908.08523.

[148] Thomas G. Mertens. Towards Black Hole Evaporation in Jackiw-Teitelboim Gravity. *JHEP*, 07:097, 2019. doi: 10.1007/JHEP07(2019)097. URL https://arxiv.org/abs/1903.10485.

[149] Philipp A. Hoehn, Maximilian P. E. Lock, Shadi Ali Ahmad, Alexander R. H. Smith, and Thomas D. Galley. Quantum Relativity of Subsystems. 3 2021. URL https://arxiv.org/abs/2103.01232.

[150] Vijay Balasubramanian and Per Kraus. A Stress tensor for Anti-de Sitter gravity. *Commun. Math. Phys.*, 208:413–428, 1999. doi: 10.1007/s002200050764. URL https://arxiv.org/abs/hep-th/9902121.

[151] Tze Dan Chung and Herman L. Verlinde. Dynamical moving mirrors and black holes. *Nucl. Phys. B*, 418:305–336, 1994. doi: 10.1016/0550-3213(94)90249-6. URL https://arxiv.org/abs/hep-th/9311007.

[152] Ahmed Almheiri and James Sully. An Uneventful Horizon in Two Dimensions. *JHEP*, 02:108, 2014. doi: 10.1007/JHEP02(2014)108. URL https://arxiv.org/abs/1307.8149.

[153] Ibrahim Akal, Yuya Kusuki, Noburo Shiba, Tadashi Takayanagi, and Zixia Wei. Entanglement Entropy in a Holographic Moving Mirror and the Page Curve. *Phys. Rev. Lett.*, 126(6):061604, 2021. doi: 10.1103/PhysRevLett.126.061604. URL https://arxiv.org/abs/2011.12005.

[154] T. Mertens. Jt gravity - a review; part 2: Quantum matter and quantum gravity, 26 Mar 2021.

[155] Ahmed Almheiri, Raghu Mahajan, and Juan Maldacena. Islands outside the horizon. 10 2019. URL https://arxiv.org/abs/1910.11077.

[156] Hong Zhe Chen, Zachary Fisher, Juan Hernandez, Robert C. Myers, and Shan-Ming Ruan. Information Flow in Black Hole Evaporation. *JHEP*, 03:152, 2020. doi: 10.1007/JHEP03(2020)152. URL https://arxiv.org/abs/1911.03402.

[157] Hong Zhe Chen, Zachary Fisher, Juan Hernandez, Robert C. Myers, and Shan-Ming Ruan. Evaporating Black Holes Coupled to a Thermal Bath. *JHEP*, 01:065, 2021. doi: 10.1007/JHEP01(2021)065. URL https://arxiv.org/abs/2007.11658.

[158] Timothy J. Hollowood, S. Prem Kumar, and Andrea Legramandi. Hawking radiation correlations of evaporating black holes in JT gravity. *J. Phys. A*, 53(47):475401, 2020. doi: 10.1088/1751-8121/abbc51. URL https://arxiv.org/abs/2007.04877.

[159] Thomas M. Fiola, John Preskill, Andrew Strominger, and Sandip P. Trivedi. Black hole thermodynamics and information loss in two-dimensions. *Phys. Rev. D*, 50:3987–4014, 1994. doi: 10.1103/PhysRevD.50.3987. URL https://arxiv.org/abs/hep-th/9403137.

[160] I. Affleck and A. W. W. Ludwig. The Fermi edge singularity and boundary condition changing operators. *Journal of Physics A Mathematical General*, 27(16):5375–5392, August 1994. doi: 10.1088/0305-4470/27/16/007. URL https://arxiv.org/abs/cond-mat/9405057.

[161] Raphael Bousso, Zachary Fisher, Stefan Leichenauer, and Aron C. Wall. Quantum focusing conjecture. *Phys. Rev. D*, 93(6):064044, 2016. doi: 10.1103/PhysRevD.93.064044. URL https://arxiv.org/abs/1506.02669.

[162] Hong Zhe Chen, Robert C. Myers, Dominik Neuenfeld, Ignacio A. Reyes, and Joshua Sandor. Quantum Extremal Islands Made Easy, Part II: Black Holes on the Brane. *JHEP*, 12:025, 2020. doi: 10.1007/JHEP12(2020)025. URL https://arxiv.org/abs/2010.00018.

[163] Moshe Rozali, James Sully, Mark Van Raamsdonk, Christopher Waddell, and David Wakeham. Information radiation in BCFT models of black holes. *JHEP*, 05:004, 2020. doi: 10.1007/JHEP05(2020)004. URL https://arxiv.org/abs/1910.12836.

[164] Friðrik Freyr Gautason, Lukas Schneiderbauer, Watse Sybesma, and Lárus Thorlacius. Page Curve for an Evaporating Black Hole. *JHEP*, 05:091, 2020. doi: 10.1007/JHEP05(2020)091. URL https://arxiv.org/abs/2004.00598.

[165] Thomas Hartman, Edgar Shaghoulian, and Andrew Strominger. Islands in Asymptotically Flat 2D Gravity. *JHEP*, 07:022, 2020. doi: 10.1007/JHEP07(2020)022. URL https://arxiv.org/abs/2004.13857.

[166] Koji Hashimoto, Norihiro Iizuka, and Yoshinori Matsuo. Islands in Schwarzschild black holes. *JHEP*, 06:085, 2020. doi: 10.1007/JHEP06(2020)085. URL https://arxiv.org/abs/2004.05863.

[167] Leonard Susskind, Larus Thorlacius, and John Uglum. The Stretched horizon and black hole complementarity. *Phys. Rev. D*, 48:3743–3761, 1993. doi: 10.1103/PhysRevD.48.3743. URL https://arxiv.org/abs/hep-th/9306069.

[168] Hong Zhe Chen, Robert C. Myers, Dominik Neuenfeld, Ignacio A. Reyes, and Joshua Sandor. Quantum Extremal Islands Made Easy, Part I: Entanglement on the Brane. *JHEP*, 10:166, 2020. doi: 10.1007/JHEP10(2020)166. URL https://arxiv.org/abs/2006.04851.

[169] W. H. Zurek. Entropy evaporated by a black hole. *Phys. Rev. Lett.*, 49:1683–1686, Dec 1982. doi: 10.1103/PhysRevLett.49.1683. URL https://link.aps.org/doi/10.1103/PhysRevLett.49.1683.

[170] Watse Sybesma. Pure de Sitter space and the island moving back in time. 8 2020. URL https://arxiv.org/abs/2008.07994.

[171] Yasunori Nomura. Black Hole Interior in Unitary Gauge Construction. *Phys. Rev. D*, 103 (6):066011, 2021. doi: 10.1103/PhysRevD.103.066011. URL https://arxiv.org/abs/2010.15827.

[172] Yasunori Nomura. From the Black Hole Conundrum to the Structure of Quantum Gravity. *Mod. Phys. Lett. A*, 36(08):2130007, 2021. doi: 10.1142/S021773232130007X. URL https://arxiv.org/abs/2011.08707.

[173] Stephen W. Hawking, Malcolm J. Perry, and Andrew Strominger. Soft Hair on Black Holes. *Phys. Rev. Lett.*, 116(23):231301, 2016. doi: 10.1103/PhysRevLett.116.231301. URL https://arxiv.org/abs/1601.00921.

[174] Peng Cheng and Yang An. Soft BHIP: Page curve from Maxwell soft hair of black hole. 12 2020. URL https://arxiv.org/abs/2012.14864.

[175] Nava Gaddam and Nico Groenenboom. Soft graviton exchange and the information paradox. 12 2020. URL https://arxiv.org/abs/2012.02355.

[176] Hao Geng, Andreas Karch, Carlos Perez-Pardavila, Suvrat Raju, Lisa Randall, Marcos Riojas, and Sanjit Shashi. Information Transfer with a Gravitating Bath. *SciPost Phys.*, 10(5):103, 2021. doi: 10.21468/SciPostPhys.10.5.103. URL https://arxiv.org/abs/2012.04671.

[177] Hao Geng and Andreas Karch. Massive islands. *JHEP*, 09:121, 2020. doi: 10.1007/JHEP09(2020)121. URL https://arxiv.org/abs/2006.02438.

[178] Ben Freivogel, Yasuhiro Sekino, Leonard Susskind, and Chen-Pin Yeh. A Holographic framework for eternal inflation. *Phys. Rev. D*, 74:086003, 2006. doi: 10.1103/PhysRevD.74.086003. URL https://arxiv.org/abs/hep-th/0606204.

[179] Yiming Chen, Victor Gorbenko, and Juan Maldacena. Bra-ket wormholes in gravitationally prepared states. *JHEP*, 02:009, 2021. doi: 10.1007/JHEP02(2021)009. URL https://arxiv.org/abs/2007.16091.

[180] Vijay Balasubramanian, Arjun Kar, and Tomonori Ugajin. Islands in de Sitter space. *JHEP*, 02:072, 2021. doi: 10.1007/JHEP02(2021)072. URL https://arxiv.org/abs/2008.05275.

[181] Donald Marolf and Henry Maxfield. Observations of Hawking radiation: the Page curve and baby universes. *JHEP*, 04:272, 2021. doi: 10.1007/JHEP04(2021)272. URL https://arxiv.org/abs/2010.06602.

[182] Steven B. Giddings and Gustavo J. Turiaci. Wormhole calculus, replicas, and entropies. *JHEP*, 09:194, 2020. doi: 10.1007/JHEP09(2020)194. URL https://arxiv.org/abs/2004.02900.

[183] Mark Van Raamsdonk. Comments on wormholes, ensembles, and cosmology. 8 2020. URL https://arxiv.org/abs/2008.02259.

[184] Thomas Hartman, Yikun Jiang, and Edgar Shaghoulian. Islands in cosmology. *JHEP*, 11:111, 2020. doi: 10.1007/JHEP11(2020)111. URL https://arxiv.org/abs/2008.01022.

[185] Lars Aalsma and Watse Sybesma. The Price of Curiosity: Information Recovery in de Sitter Space. *JHEP*, 05:291, 2021. doi: 10.1007/JHEP05(2021)291. URL https://arxiv.org/abs/2104.00006.

[186] Hao Geng, Yasunori Nomura, and Hao-Yu Sun. Information paradox and its resolution in de Sitter holography. *Phys. Rev. D*, 103(12):126004, 2021. doi: 10.1103/PhysRevD.103.126004. URL https://arxiv.org/abs/2103.07477.

[187] A. Manu, K. Narayan, and Partha Paul. Cosmological singularities, entanglement and quantum extremal surfaces. *JHEP*, 04:200, 2021. doi: 10.1007/JHEP04(2021)200. URL https://arxiv.org/abs/2012.07351.

[188] Kevin Langhoff, Chitraang Murdia, and Yasunori Nomura. The multiverse in an inverted island, 2021. URL https://arxiv.org/abs/2106.05271.

[189] Netta Engelhardt, Sebastian Fischetti, and Alexander Maloney. Free energy from replica wormholes. *Phys. Rev. D*, 103(4):046021, 2021. doi: 10.1103/PhysRevD.103.046021. URL https://arxiv.org/abs/2007.07444.

[190] Juan Maldacena and Douglas Stanford. Remarks on the Sachdev-Ye-Kitaev model. *Phys. Rev. D*, 94(10):106002, 2016. doi: 10.1103/PhysRevD.94.106002. URL https://arxiv.org/abs/1604.07818.

[191] Joseph Polchinski and Vladimir Rosenhaus. The Spectrum in the Sachdev-Ye-Kitaev Model. *JHEP*, 04:001, 2016. doi: 10.1007/JHEP04(2016)001. URL https://arxiv.org/abs/1601.06768.